

Publication 814

August 1987

CLAMP-ON ACOUSTIC PRODUCTION MEASUREMENT

by

A.S. van Heel

Reviewed by: Prof. J.M. Smith M. Sc. (TUD)
Dr. R.G. Smeenk (KSEPL)

Graduation Project, Department of Applied Physics
Technical University Delft

Carried out at the Royal/Shell Exploration and
Production Laboratories, Rijswijk over the period
November 1986 - August 1987.

The author is free to use all or part of this
report for future external publication.

Reproduction of this document in whole or in part is allowed if due acknowledgement is made to Shell Research B.V.

Neither Royal Dutch Petroleum Company nor The "SHELL" Transport and Trading Company p.l.c. nor any company of the Royal Dutch/Shell Group will accept any liability for loss or damage originating from the use of the information contained therein.

Although **SHELL** companies have their own separate identities the expressions "**SHELL**" and "**GROUP**" are used for convenience to refer to companies of the Royal Dutch/Shell Group in general, or to one or more such companies as the context may require.

© Shell Internationale Research Maatschappij B.V. 1987

KONINKLIJKE/SHELL EXPLORATIE EN PRODUKTIE LABORATORIUM

RIJSWIJK, THE NETHERLANDS

(Shell Research B.V.)

ABSTRACT

A feasibility study has been done on the measurement of noise generated by a gas-liquid flow as an indicator for the flowrate.

Usually the production of several oil-gas wells is fed through a bulk separator and the gas and liquid phases are measured separately. About once a month each well is tested individually with a test separator. To monitor the well-production between two well tests a production surveillance monitor, (PSM) is commercially available. Its operation is based on the relation between the pressure fluctuation in the gas-liquid flow and the liquid flowrate. The purpose of the present study was to carry out a feasibility study on a clamp-on version of the PSM.

Tests have been done with two-phase flow test loops to investigate the relation between the flow variables and the flow-noise acquired with a clamp-on accelerometer.

In gas-liquid flow, bubbles act as sound scatterers of the turbulent pressure fluctuations in a wide frequency band (up to 25kHz). Therefore the pressure fluctuations related to the flowrate can be detected by a clamp-on accelerometer.

It has been found that under certain conditions the average Root Mean Square (RMS) value of the flow noise gives a good indication of the liquid flowrate. Unfortunately the mechanical structure of the test-loop and the line pressure regulation were found to be of influence as well. It was found to be possible to determine slug speeds and slug frequencies with the clamp-on accelerometer. In general the flow-noise is found to be related only to a limited volume of gas-liquid flow. Because the flow-noise is generated locally the signals are similar to signals obtained with intrusive transducers such as differential pressure signals. As those signals are reported in literature to be used for flow-pattern recognition and possibly in the near future as flowrate indicator as well, this resemblance encourages further efforts on the statistical processing of the RMS value of clamp-on acquired gas-liquid flow-noise.

<u>CONTENTS</u>	page
1. INTRODUCTION	1
2. OBJECTIVE	3
3. THE PRODUCTION SURVEILLANCE MONITOR	7
4. TEST FACILITIES	11
4.1. test-loop Wolga	11
4.2. test-loop Donau	13
5. EXPERIMENTAL RESULTS	21
5.1. introductory tests with the Wolga	21
5.1.1. stethoscope	21
5.1.2. accelerometer	21
5.1.3. filtering by steel pipe	23
5.1.4. pipe vibrations	23
5.1.5. low frequency signals	27
5.1.6. high frequency signals	27
5.2. Wolga test series	31
5.3. Donau test series	39
5.4. statistical processing	63
5.4.1. slug frequency	63
5.4.2. slug velocity	65
5.4.3. other signal processing	70
6. THEORETICAL BACKGROUND	73
6.1. a bubble as sound scatterer, single bubble	73
6.2. a bubble as sound scatterer, dispersed bubbles	77
6.3. turbulent eddies	79
6.4. bubble formation	81
6.5. theory: concluding remarks	87
7. CONCLUSIONS AND RECOMMENDATIONS	89
8. LITERATURE	93
9. SYMBOLS	105
ACKNOWLEDGEMENTS	109

1. INTRODUCTION

As a graduation project for a degree in applied physics (Technical University Delft) a feasibility study has been done on the clamp-on measurement of noise generated by a gas-liquid flow as an indicator of the flow-rate. The project lasted ten months and was conducted at the Royal/Shell Exploration and Production Laboratory in Rijswijk in the Section Measurement and Control. The laboratory with its ca 700 employees covers most of the Shell Group's research on exploration and production. Most of the projects are carried out for Group Operating Companies, usually coordinated by the Central Office in The Hague.

The initial purpose of the project was to study and improve the operation of the PSM (Production Surveillance Monitor). This instrument is basically a pressure transducer and it derives the liquid volume flowrate in a liquid-gas mixture in a pipe-line from a measurement of the pressure fluctuations. One of the aims of the present study was to investigate the possibility to measure these pressure fluctuations outside the pipe with a clamp-on transducer. As the clamp-on approach soon proved to be hopeful, this was given priority.

In this report the use of production surveillance and a comparison with the existing multi-phase flow-meters is explained. After the explanation of the principle of operation of the PSM, the test facilities are described. In chapter five the development of the idea behind clamp-on flow-noise measurement is related, followed by a selection of the results of the many tests and a paragraph on the statistical analysis of the flow-noise. Chapter six gives the theoretical background of flow-noise generation. The report finally deals with the conclusions and suggestions for further work on clamp-on two-phase flow-noise analysis.

2. OBJECTIVE

In the oil industry a major problem in measuring the production of a well is the fact that one often encounters two-phase flow systems. Even if the reservoir is free of gas, the well will produce a gas-oil mixture, because gas comes out of solution at the lower pressure at the surface. As accurate measurements in gas-liquid flow are extremely difficult, the liquid and the gas phase are separated and measured individually. The importance of multi-phase flow measurement in the oil-producing industry is discussed in detail by Jamieson et al (2).

In general the production of several wells is combined and fed into a bulk separator. In this way the gas and oil production of the total field can be measured. To obtain information about an individual well, that well can be produced over a second separator, the test separator. This procedure is called a well test. As such a well test usually takes a day and as there may be thirty wells producing through one production separator, the period between two well tests of a single well can be a month. The behaviour of the well in the interval time remains uncertain. When the production of a single well changes drastically, the change in the output of the production separator will be minor due to the dilution with the production of all the other wells. So when a small change in the total production is noticed it is unknown whether the total field or only one of the wells has changed its production. This uncertainty is an incentive for the development of an instrument monitoring each individual well. As a separator for each well is much too expensive such an instrument has to cope with two-phase flow. The required accuracy has to be something between a flow/no-flow detector and a normal flowmeter. In other words it has to be able to detect more than marginal production changes (say 10-20%) to give warning that some action has to be taken

As there are many wells to monitor the device has to be cheap, free of maintenance, easy to install, preferably clamp-on so there is no need to stop production while installing the instrument. Besides that it should be safe and it should not protrude into the flow.

SYSTEM	PHYSICAL QUANTITY	FLOW VAR	LIT	PROBLEMS
separators	single-phase liquid and gas	U_{sl}, U_{sg}		E, L, F
β -, γ -, X-ray absorption	absorption coeff.	a, c	89	R
capacitance	spec. capacitance	a, c	42, 52	L, F
conductance	spec. conductance	a, c	52	L, F
hot wire anemometry	heat transfer	a, c	12	L, F, S
optical fibres	refractive index	a, c	121	L, F, S
acoustic sounding	sound scatter	a, c	99	L, F, A
tracers	time delay	c		R, L
vibrating tube	coriolis force	ϕ_{mass}	122	L, A
orifice	pressure drop	U_{mix}	124	L, F, A
venturi	pressure drop	U_{mix}	125	L, F, A
Production Surveillance Monitor	pressure fluct.	U_{mix}, c	8	L

Table 2.1. Gas-liquid measurement techniques. For a full explanation see the introduction.

Symbols:

- a gas fraction
- c correlation for determination of $U_{mixture}$ possible
- ϕ_{mass} mass flow
- U_{mix} velocity of the gas-liquid mixture
- U_{sg} superficial gas velocity
- U_{sl} superficial liquid velocity

- A inaccurate
- E expensive
- F intruding in the flow
- L to be installed in-line
- R radiation
- S not strong enough

In table 2.1. a list of measurement techniques suitable to determine certain parameters of a gas-liquid flow are listed. The second column of the table lists the physical quantity which is measured and the third column lists the flow variable determined from this quantity. In the column "problems" the disadvantages of the technique are specified. In the last column a literature reference to the particular system is given. When a "c" is stated for a system it is suitable for transit time correlations using two transducers. From this correlation the velocity of the gas-liquid mixture can be derived, using techniques described by Peters ea (100) and Kipphan ea (104). A combination of two or more of these techniques is not unusual as for instance a combination of a separating device and a γ -absorption system as described by Arnaudeau (37). More elaborate and complete reviews of multi-phase measurement techniques have been published by Hewitt (88), Jones (93), and Banerjee ea (69).

As a test-separator per well is too expensive, the R marked instruments are not preferred in many operations, and the α -marked systems need two probes plus a correlation algorithm while some of them intrude in the flow as well, the two instruments left are the vibrating-tube and the PSM (Production Surveillance Monitor). The vibrating tube instrument is still too inaccurate for gas-liquid flow, so the most suitable instrument at the moment is the PSM. This system is based on the relation between pressure fluctuations and liquid velocity and is commercially available since 1978 . In chapter 3 its principle of operation will be explained.

The purpose of the present study is to investigate the feasibility of a clamp-on version of the PSM.

3. THE PRODUCTION SURVEILLANCE MONITOR

Since 1971 work has been done on the Production-Surveillance-Monitor (PSM) at the various Shell research centres. The most important aspects of the PSM are published by Alford e.a. (8). As the principles of operation are of primary importance to the Clamp-On-Production-Surveillance-monitor (COPS), they will be discussed here.

Consider a single-phase turbulent flow through a pipe-line with an instantaneous velocity U , an average velocity U_a , and an instantaneous variation of velocity from the average, u , such that

$$U = U_a + u \tag{3.1}$$

A measure for the velocity fluctuation is u' , defined by

$$u' = \sqrt{(u^2)} \tag{3.2}$$

For the instantaneous pressure P , the average pressure P_a , and the instantaneous variation of pressure from the average p , a similar equation exists:

$$P = P_a + p \tag{3.3}$$

A measure for the pressure fluctuation is p' , defined by

$$p' = \sqrt{(p^2)} \tag{3.4}$$

Hinze (28) empirically found that for $0.01 \text{ m/s} \leq U_a \leq 10 \text{ m/s}$:

$$u' = 0.1 U_a \tag{3.5}$$

Although the Bernoulli relation between hydrodynamic pressure and kinetic energy is not valid in this turbulent flow, Hinze found an empirical relation between the pressure fluctuation and the velocity fluctuation:

$$p' = 0.7 \rho (u')^2 \tag{3.6}$$

Combining equations 3.3. to 3.6. results in

$$\sqrt{(P-P_a)^2} = 0.007 \rho U_a^2 \tag{3.7}$$

In other words the root-mean-square (RMS) value of the dynamic pressure is proportional to the density of the fluid times the square of the fluid velocity.

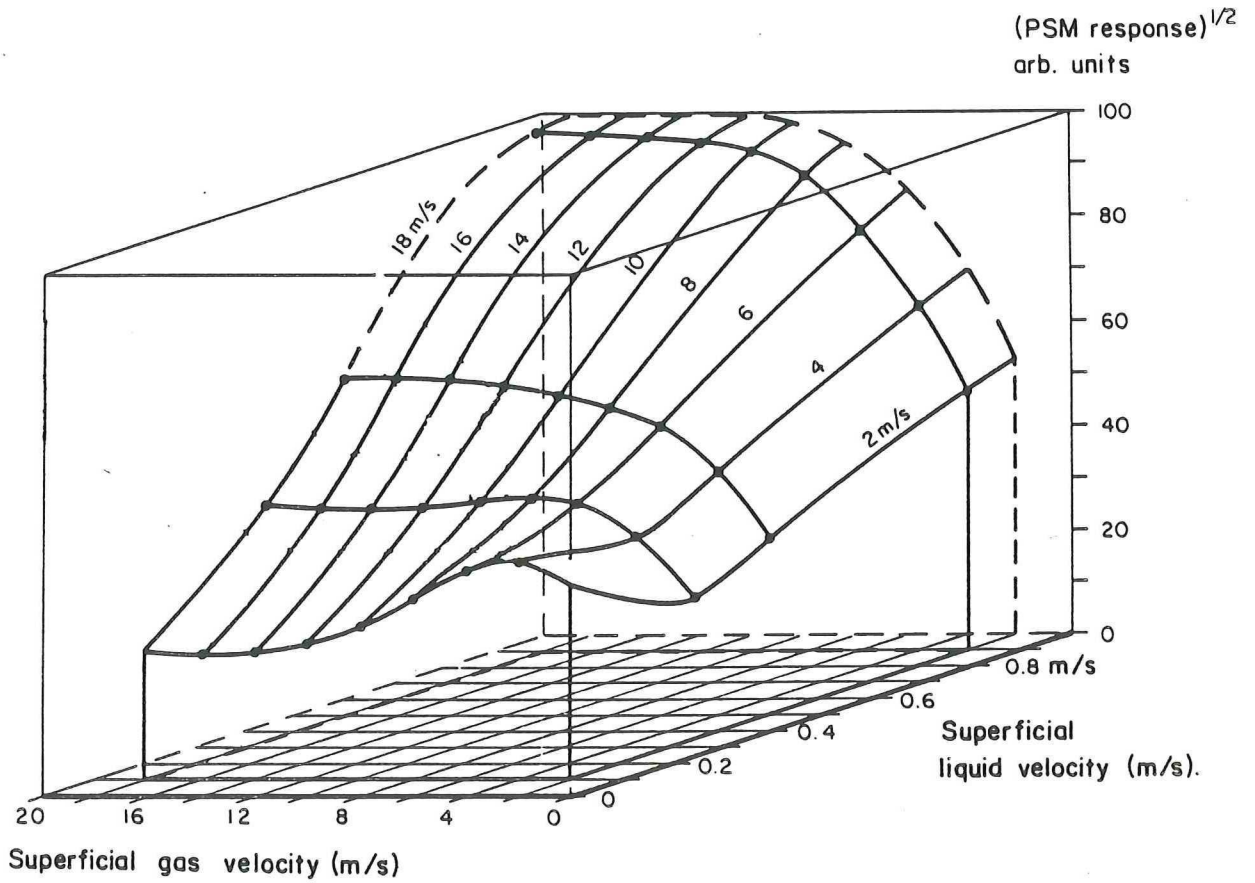


Figure 3.1. The square root of the average RMS value of the pressure fluctuations as a function of the superficial air and water velocity as determined by the Production Surveillance Monitor.

In gas-liquid flow the liquid density has to be replaced by the mixture density ρ_{mix} and the average fluid velocity by the average mixture velocity $U_{mix,a}$. As in the last two parameters the averaging is with respect to time the space specifications will have to be given as well. Sami (34) uses the overall time average mixture density and the time averaged centreline mixture velocity.

In low-pressure gas-liquid flow the pressure fluctuations will be mainly caused by the velocity fluctuations of the liquid because the density of the gas is much less than the density of the liquid. So the pressure fluctuations are mainly related to the liquid production. The relationship between the pressure fluctuation intensity and the liquid production is then calibrated per well. Because the gas-liquid ratio is usually more stable than flowrate of the well this proved to be a useful approach.

The commercially available PSM as manufactured by Sundstrand Data Corporation has been tested in the KSEPL test-loop DONAU (described in chapter 4.2.) in 1984. The piezoelectric crystal of the PSM measures the dynamic pressure. The signal is passed through a low-pass filter with a cut-off frequency of 1kHz and converted into a RMS value which is then averaged for 200 seconds. A second model with a supposedly better performance has a low-pass cut-off frequency of 30 Hz.

In Fig.3.1. the square root of this RMS value is plotted against the superficial liquid and gas velocity. It is clear that the signal is not independent of the gas flow. This influence is introduced by replacing the real mixture velocity by the superficial velocity. An increase in the superficial gas velocity with a constant superficial liquid velocity will result in a higher void fraction which means that the real liquid velocity goes up while the cross-section of the liquid flow gets smaller. This results in a more turbulent flow (higher Reynolds numbers). One is tempted to try to calculate a correction using e.g. a Lockhart-Martinelli void fraction prediction. The problem is that the field of operation of the PSM is mainly slug-flow, in which case calculation of slug speed has to be involved as well. So after all it appears much more practical to calibrate the PSM for superficial liquid and gas velocity.

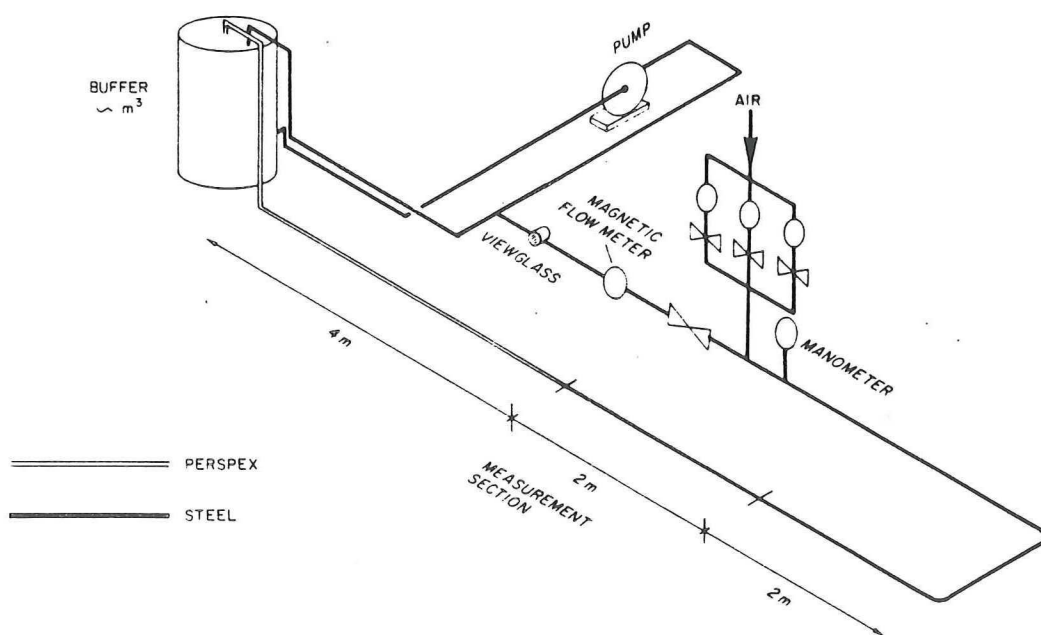


figure 4.1. The two-phase test-loop Wolga.

4. TEST-FACILITIES

For any study concerning two-phase flow, well defined flow conditions are of primary importance. Essential is the separate measurement of the individual phases before they are mixed. For this study two such multi-phase test-loops, Wolga and Donau were available.

4.1. TEST-LOOP WOLGA

The Wolga is a flexible and easy to handle water-air test loop. For one test series the viscosity of the water was increased with CMC (Carboxy Methyl Cellulose). The set-up of the WOLGA test-loop is drawn in figure 4.1. It consists of a 1 m^3 tank from which water is circulated through a steel pipe (internal diameter $D_i=7.0 \text{ cm}$) by a centrifugal pump. The water volume flow can be adjusted by two valves, one in the test-loop and another in a by-pass line. After the liquid flow has been measured by a magnetic flowmeter, air from a 8-Bar pressure-line is introduced through a T-junction. Before its introduction the air volume flow is measured by one of the three parallel rotameters. Downstream of the T-junction the line pressure is measured by a manometer. The last 4 meters of the horizontal section and the 2 meters rising to the top of the tank are made of perspex to be able to see the two-phase flow pattern. This perspex section cannot withstand high pressures so no restriction has been built in the outlet.

A 2-meter measurement section with pressure transducer mountings has been inserted just upstream of the perspex section and ca 100 diameters downstream of the mixing point.

The maximum water volume flowrate of the pump is 8 l/s. The maximum air flow is $32 \text{ sm}^3/\text{s}$ (standard cubic meters: 0°C , 101.3 kN/m^2).

In multi-phase systems flow is usually expressed in terms of superficial velocities. This is the velocity the fluid would have in the absence of the another fluid. So the superficial liquid velocity, U_{sl} is the liquid volume rate divided by the area of the cross-section of the pipe. The superficial gas velocity, U_{sg} is the gas volume rate divided by the same area. As the gas volume rate is measured in standard cubic meters, one has to divide by the absolute line pressure, p_1 as well. The temperature may be as high as 35°C , resulting in a systematic error of ca 11%. As the temperature fluctuations during a measurement series are much smaller, no corrections

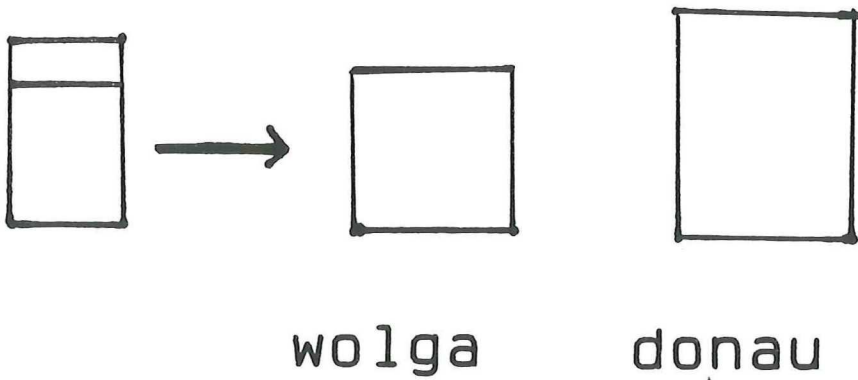
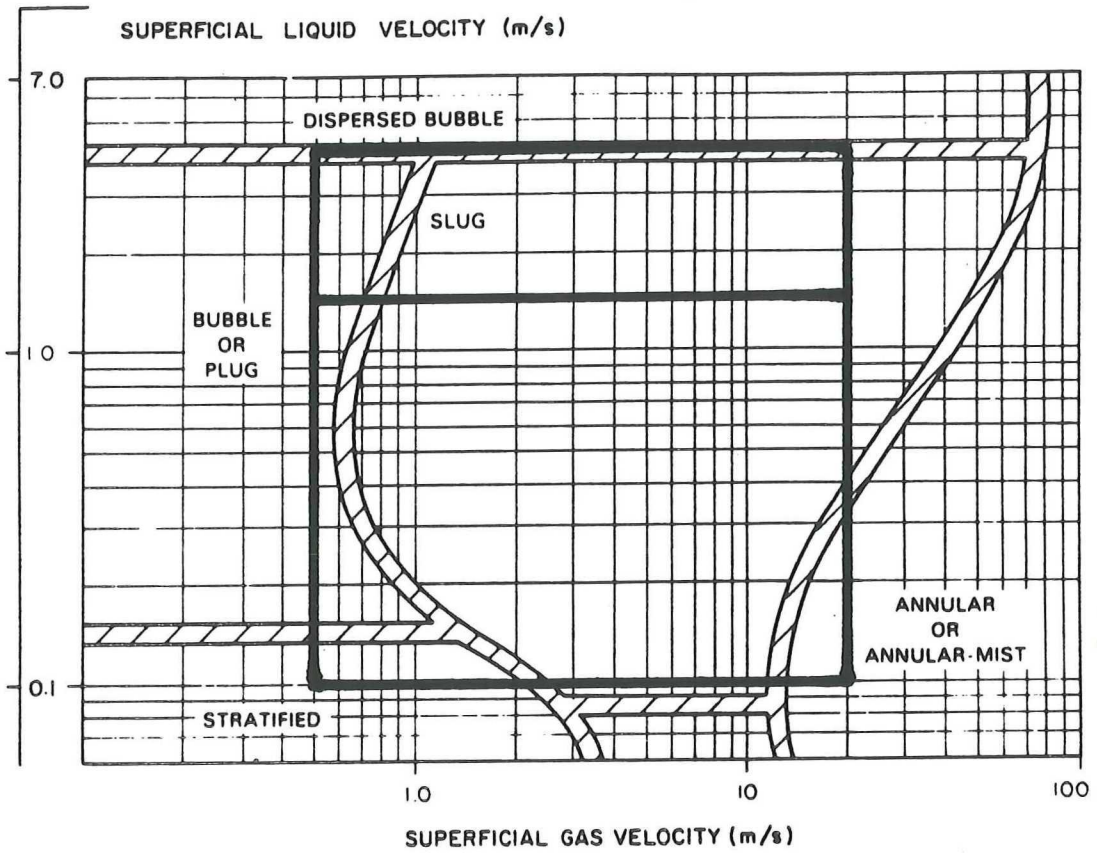


figure 4.2. The limits of the flowrates of the test-loop Wolga and Donau drawn in the Mandhane (23) two-phase flow-pattern map.

are made for the temperature. The minimum and maximum superficial velocities for water and air are drawn in the Mandhane (23) flow-pattern map (fig4.2.). Visual observations of the flow patterns in the Wolga coincided reasonably well with this map.

In order to prevent pump vibrations to reach the measurement section, it was decided after some initial tests to modify the WOLGA into a static-head-loop (fig 4.3.). A 1 m³ tank was bolted to the wall and the by-pass line was replaced by an overflow from the higher tank to the lower. The higher tank was put up on such level that the maximum water volume flow is the same for both configurations. The level in the upper tank remains at overflow level for any flow-rate in the test-loop. As the overflow level is 4.5 meters above the test-loop level, the pressure in the test-loop can never exceed the ambient pressure by 0.45 atmosphere. Both tanks are fed by free outflowing streams so the vibration of the pump cannot reach the test-loop through the steel or the fluid. The third advantage is that the upper tank is designed as a separator as well, so the air introduced by the pump doesn't reach the test-loop.

4.2. TEST-LOOP DONAU

In figure 4.4. a schematic plan of the Donau test-loop is drawn. The basic lay-out (separator, pumps, single-phase measurements, and recirculation through the test-loop) is similar to that of the WOLGA. The loop is suitable for oil, water, and air. Most of the tests were done with water and air. To test for the influence of viscosity one measurement series has been conducted with air and an emulsion of water and Tellus oil.

The maximum flowrates have been drawn in the same Mandhane flow pattern map as the WOLGA maxima (figure 4.2.). By using the water and oil pump simultaneously for water a very high superficial water velocity in the three inch line can be obtained for low air velocities.

The main advantage of the DONAU test-loop is its very good instrumentation. Turbine flow meters and vibrating tube density meters measure volume flow and density of the liquid flow. Air flow is measured by orifice plates. Pressure and temperature are measured in various places of

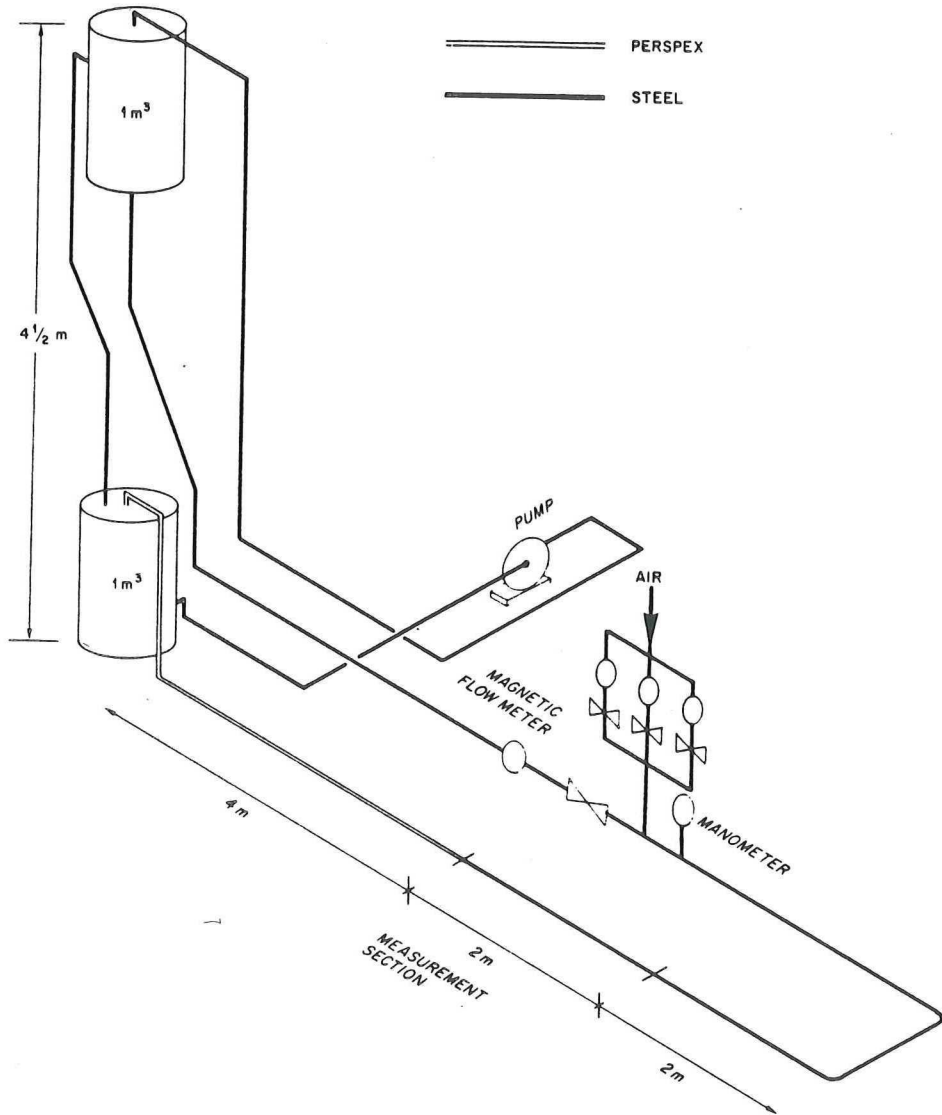


figure 4.3. The two-phase test-loop Wolga in the static-head configuration.

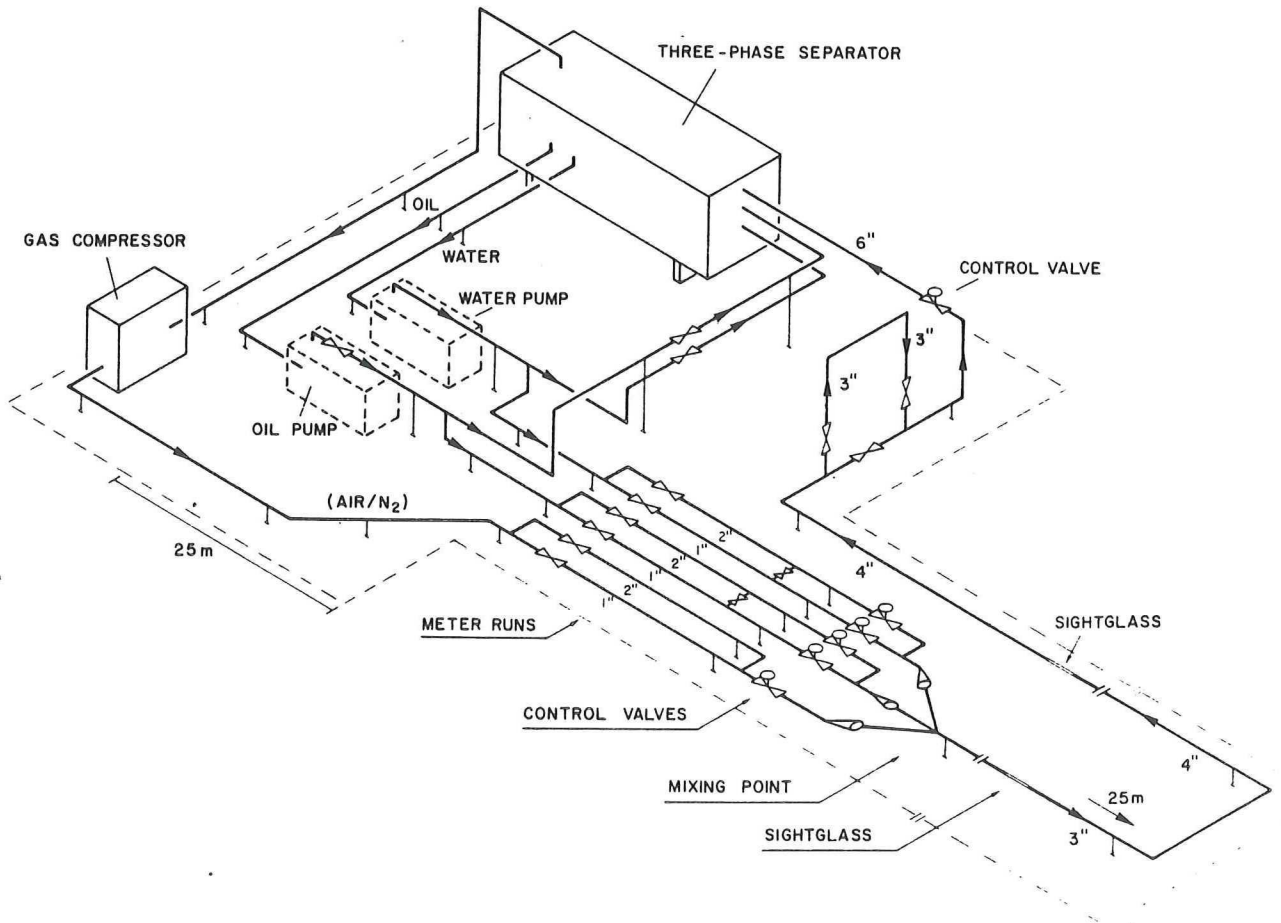


figure 4.4. The multi-phase test-loop Donau.

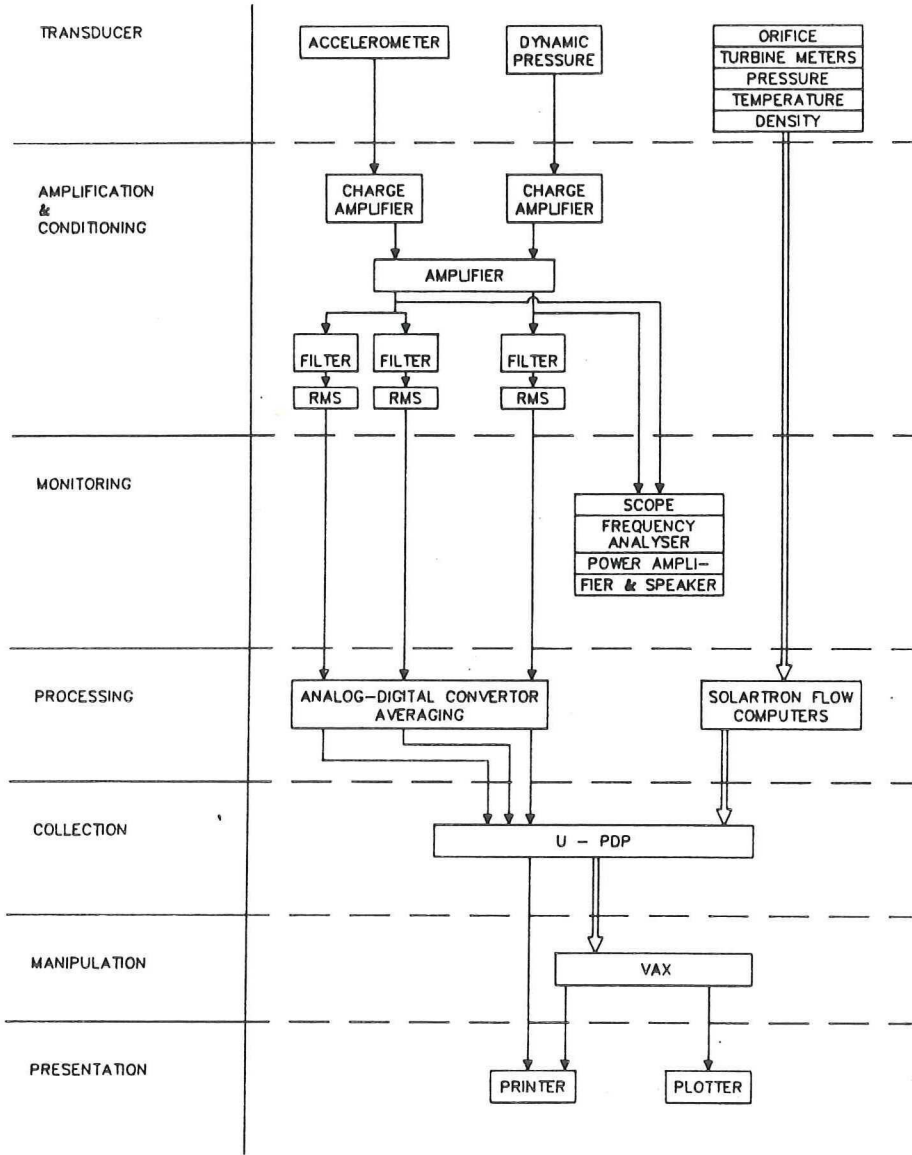


figure 4.5. Schematic representation of the data processing of the multi-phase test-loop Donau.

the system. The signals from these transducers are collected and processed by three flow computers (Solartron 7910). The superficial air velocity is calculated by one of the flow computers using the air volume flow from the orifice-plate, the cross-sectional area of the pipe and the line pressure from the pressure transducer in the elbow of the loop between the 3 and 4 inch line.

Similar to the WOLGA set-up the accelerometer and dynamic pressure transducer charge-signals are converted into a voltage, amplified, filtered and put through a RMS-circuit. The RMS-signals are sampled, digitized, and processed by a multi channel AD-converter (type μ Mac 5000). Together with the test-loop signals processed by the Solartron flow-computer, the flow-noise results are sampled and stored by a PDP 11/23 computer. In this way the relevant information about one flow-condition is presented in one screen of data. In figure 4.5. the layout of the data processing is schematically presented and an example of the lay-out of such a screen of data is shown in figure 4.6.

After a measurement series the data fields can be converted into a standardised print file to be printed locally or plot file to be sent to the VAX cluster for further editing and plotting.

Date: 14-APR-87		Time: 10:29:02			
SOLARTRON CHANNEL		OIL	WATER	O/W	GAS
Large turbine	Hz	+0.000	+109.442	+0.000	N/C
Small turbine	Hz	+0.000	+0.000	+0.000	N/C
Line density	kg/m3	+926.417	+909.041	+995.642	N/C
Base density	kg/m3	+914.676	+903.868	+988.193	N/C
Volume flow	m3/h	+0.000	+24.625	+0.000	N/C
Mass flow	kg/h	+0.000	+22384.701	+0.000	N/C
Watercut	%	+5.39560E+01	+4.71002E+01	+9.67389E+01	N/C
Temperature	oC	+10.449	+24.854	+8.691	N/C
DONAU P(bar) & T(oC)		A/D VALUES (Volts)			FUTURE OPTIONS
Plab	+7.595	ADC0	.0199		N/C
Pbeg	+2.628	ADC1	.0185		N/C
Pelb	+2.190	ADC2	.0826		N/C
Pend	+1.28544E+00	ADC3			N/C
Qair	+63.608	ADC4			N/C
Qair	-4.89600E-03	ADC5			N/C
Vsl	+7.41040E-01	ADC6			N/C
Vsg	+8.77550E-01	ADC7	128		N/C

figure 4.6. An example of a screen of data from the test-loop Donau as gathered by the PDP 11/23 computer. The values marked A/D are copied from the μ -Mac computer, the others from the Solartron flow-computers.

REF LEVEL /DIV
0.000dB 5.000dB

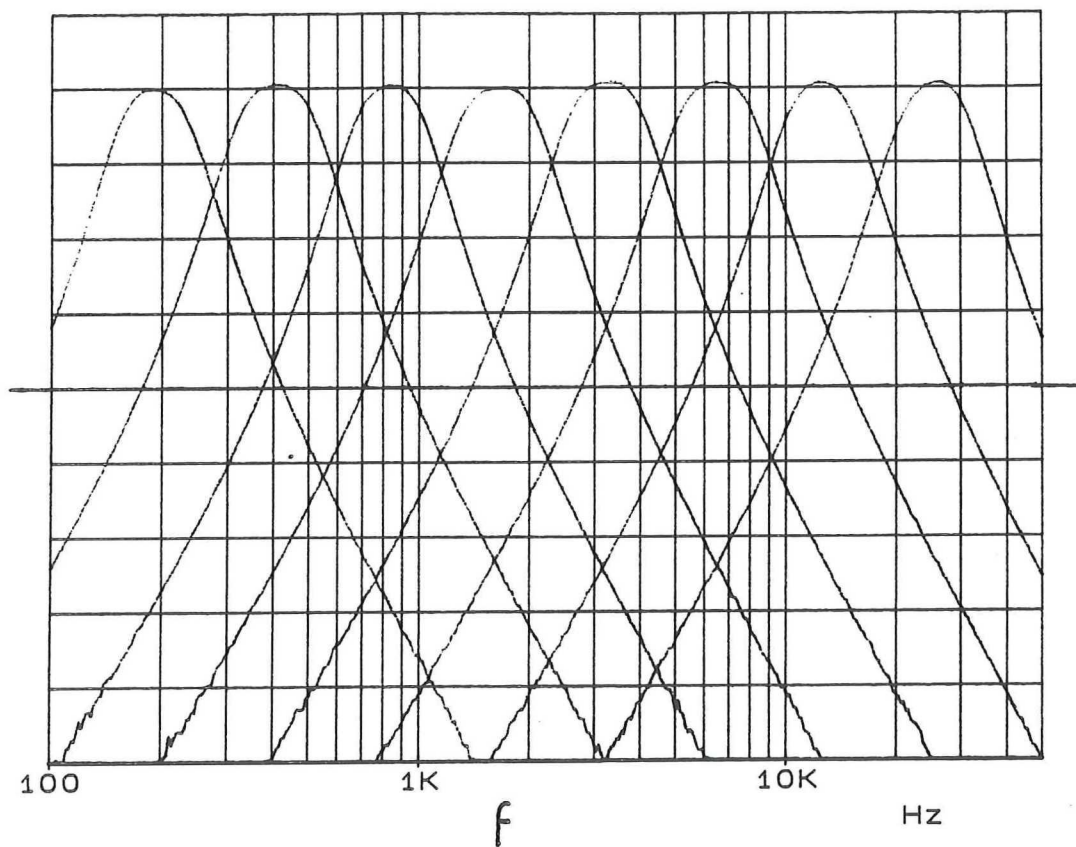


Figure 4.7. The filter characteristics of the 8-band RMS-meter.

In a later stage a specially designed 8-band RMS meter replaced the individual filters and RMS converters for the processing of the accelerometer signal. This device splits one signal into eight frequency bands which are put through eight separate RMS circuits. The eight filter characteristics are shown in figure 4.7. The time constant of the RMS converters is three seconds. This time constant is as small as possible for time resolution but larger than the time constant of the sampling μ -Mac.

Like the PSM-signal processing the wildly (especially for slug flow) varying flow-noise has to be converted into a reasonably stable indication of the flow. Therefore the μ -Mac program samples and averages the RMS-signals. Initially three RMS-signals were sampled sequentially with a sampling time of 0.1 s. Later sampling the eight channels of the 8-band RMS meter the sampling time was changed into .01 s. The program in the μ -Mac consists of the main averaging program with an interrupt procedure taking care of the communication with the μ -pdp.

After a pre-averaging routine the averaging is continuous:

$$\text{Average} = ((T-1) \times \text{Average} + \text{sample}) / T \quad 4.1.$$

with T the numerical time constant. The real time constant depends on the sampling time and unfortunately on the execution time as well. Changing the number of statements in the program as in case of sampling eight instead of three channels is always compensated by adjusting the numerical constant T. In this way the averaging time constant was kept in the order of 30 s.

For the Donau results the averaged RMS-signal is plotted as a function of the superficial water velocity without taking the square root. As the electronic configuration was changed a few times the amplification is not the same for all the tests. So the absolute RMS-value is of no interest, and one should focus the attention on the change in the RMS-signal as a function of varying certain flow parameters.

5. EXPERIMENTAL RESULTS

5.1. INTRODUCTORY TESTS WITH THE WOLGA

This chapter describes the introductory tests necessary for the understanding of gas-liquid flow induced noise. These tests have been conducted using the test-loop Wolga either in the straight configuration (fig 4.1.) or the static-head pressure configuration (fig 4.3.).

5.1.1. STETHOSCOPE

The first exploration in the field of flow-noise has been done with a stethoscope pressed on the steel of the measurement section. The first days a lot of time has been spent listening to the noise of the water-air mixture flowing through the WOLGA. After some practice comparing the flow-noise with visual observations of the flow in the perspex section, one can easily identify the various flow-regimes just by listening to the flow-noise. This means that flow-related information is passed through the steel pipe. So it might be possible that this information contains more than just an indication of the flow-regime.

5.1.2. ACCELEROMETER

To convert the flow noise into an electronic signal a piezoelectric accelerometer was mounted on the pipe with a magnet and some "Weimaplast" coupling compound. The accelerometer produces a charge proportional to acceleration which is converted into a voltage by a charge amplifier. As we are trying to adapt the PSM-principle of operation to a clamp-on version, a comparison with a PSM-like signal is necessary. Therefore a piezoelectric pressure transducer has been placed on the measurement section. A charge amplifier converts the charge into a voltage. For extra flow-noise recognition training, electronic circuit check, and for demonstration purpose the accelerometer signal was fed through a power amplifier to a loudspeaker. Besides that the signals are visualised with an oscilloscope. By varying the superficial air and water velocities, one tries to get an idea from loudspeaker and scope which frequency band has the most flow-related signal. To become more quantitative a frequency analyser (Data 6000) has been used to sample and process the signals.

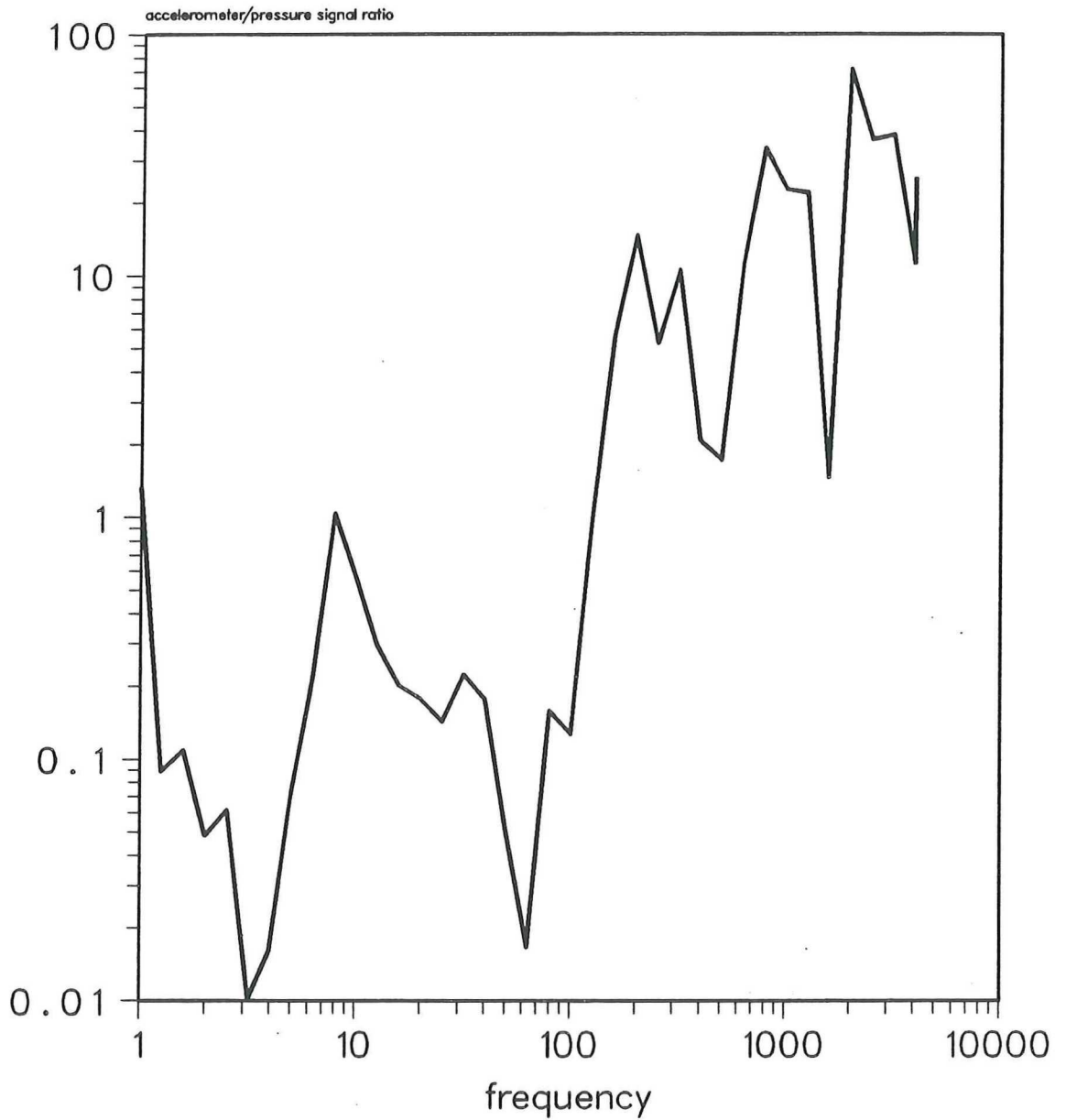


Figure 5.1. The ratio of the accelerometer and the pressure transducer signal as a function of frequency. The transducers were mounted on the measurement section of the Wolga test-loop and the water in the pipe was put to motion through a membrane by an exitator.

5.1.3. FILTERING BY STEEL PIPE

As one suspects that the low frequency pressure fluctuations will not pass the steel of the pipe, a test has been set up to compare the pressure-signal with the acceleration signal as a function of the frequency with the test-loop completely filled with water. A membrane fitted to a pressure mounting, so in direct contact with the water, is put to motion by an exitator fed by a lock-in amplifier. Sweeping from 1 Hz to 4 kHz the ratio of the signals of the accelerometer and the pressure transducer is determined by the lock-in amplifier. The results are shown in figure 5.1. Apart from mechanically determined resonance peaks there is an up-going trend in the ratio as a function of the frequency.

5.1.4. PIPE VIBRATIONS

To distinguish between vibrations of the pipe and flow-noise a second accelerometer has been positioned opposite the first one and later on next to the first one. Both signals are filtered by a variable electronic filter and fed into the oscilloscope, the first to the X-channel and the second to the Y-channel. The superficial velocities were $U_{sl} = 2$ m/s, and $U_{sg} = 1.4$ m/s, resulting in slug flow. The results have been schematically drawn in figure 5.2. The first configuration (accelerometers opposite each other) and a 100 Hz or 200 Hz low-pass filter for both channels results in the line $Y = -X$ on the scope. This means that for frequencies below 200 Hz the acceleration is caused by vibration of the pipe. This vibration is determined by the mechanical structure of the pipe and the supports, and therefore not a reliable source of information about the flow-system. The second configuration (accelerometers next to each other) and a 100 Hz low pass filter result in a narrow elliptical figure around the line $Y = X$. The same configuration but with a 200 Hz low-pass filter produces a slightly wilder movement around the line $Y = X$. This also implicates a vibration of the tube. In this case however the separation of the accelerometers create a phase-shift. For both configurations high pass (200 Hz) filtering results in spirals, and ellipses in all directions, indicating signals only different in phase. The variation of the phase-shift proves that these signals are not caused by vibrations of the pipe and implicates randomly located sources of sound.

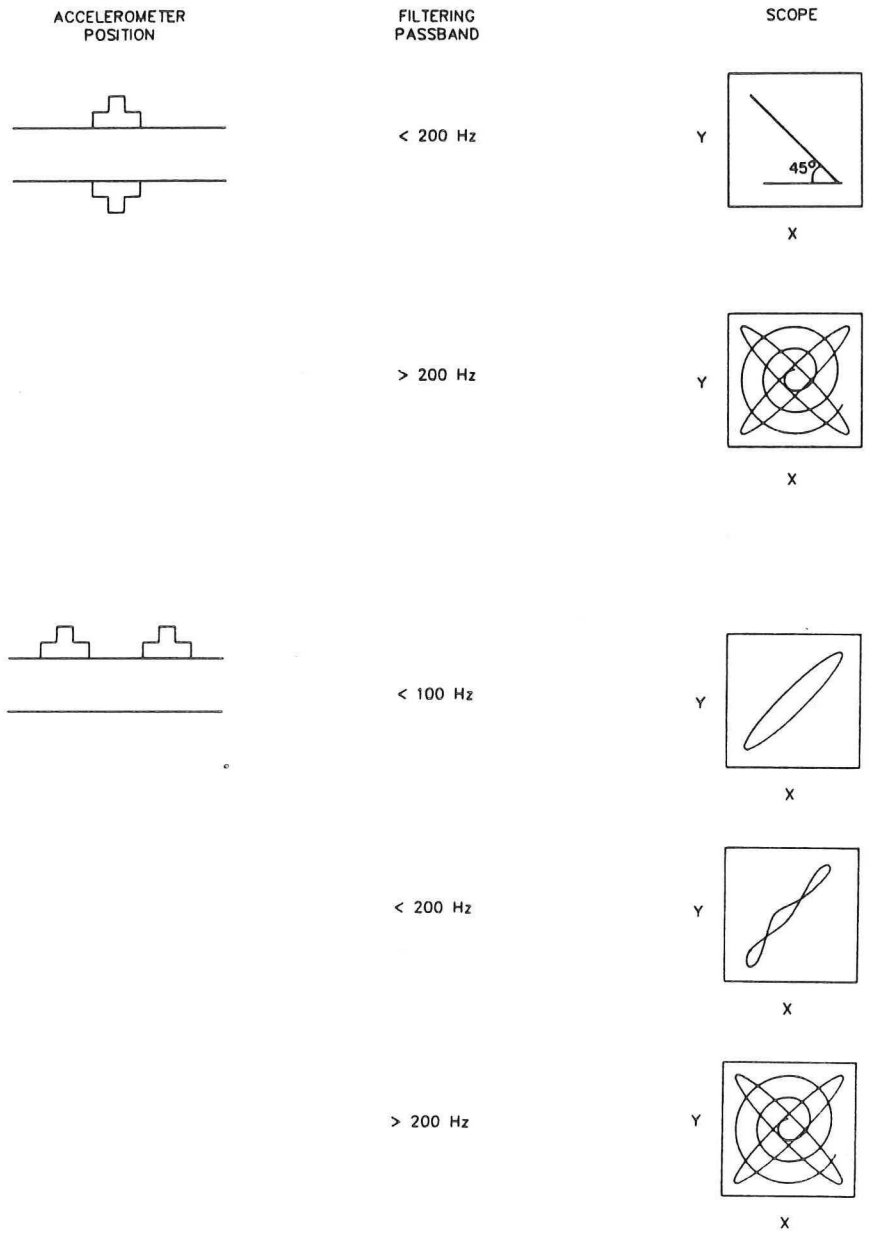


Figure 5.2. Schematic copies of the scope-display with one accelerometer fed to the X channel and another to the Y channel, for different accelerometer positions and various filtering.

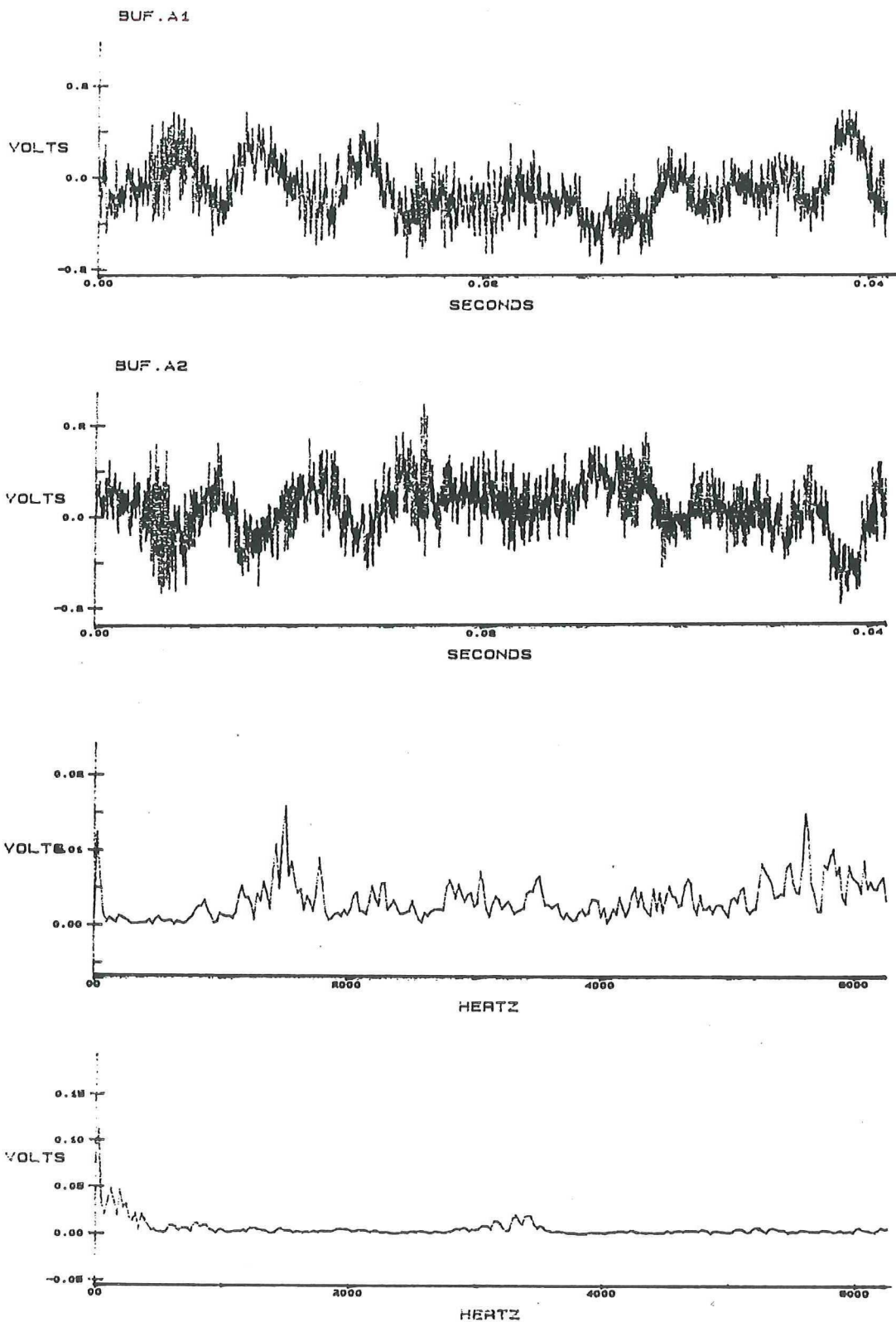


Figure 5.3. The signals of two accelerometers positioned opposite each other, for $U_{sl}=2$ m/s and $V_{sg}=1.4$ m/s. The PSD is given for the sum of the signals (first PSD) and for the difference (second PSD).

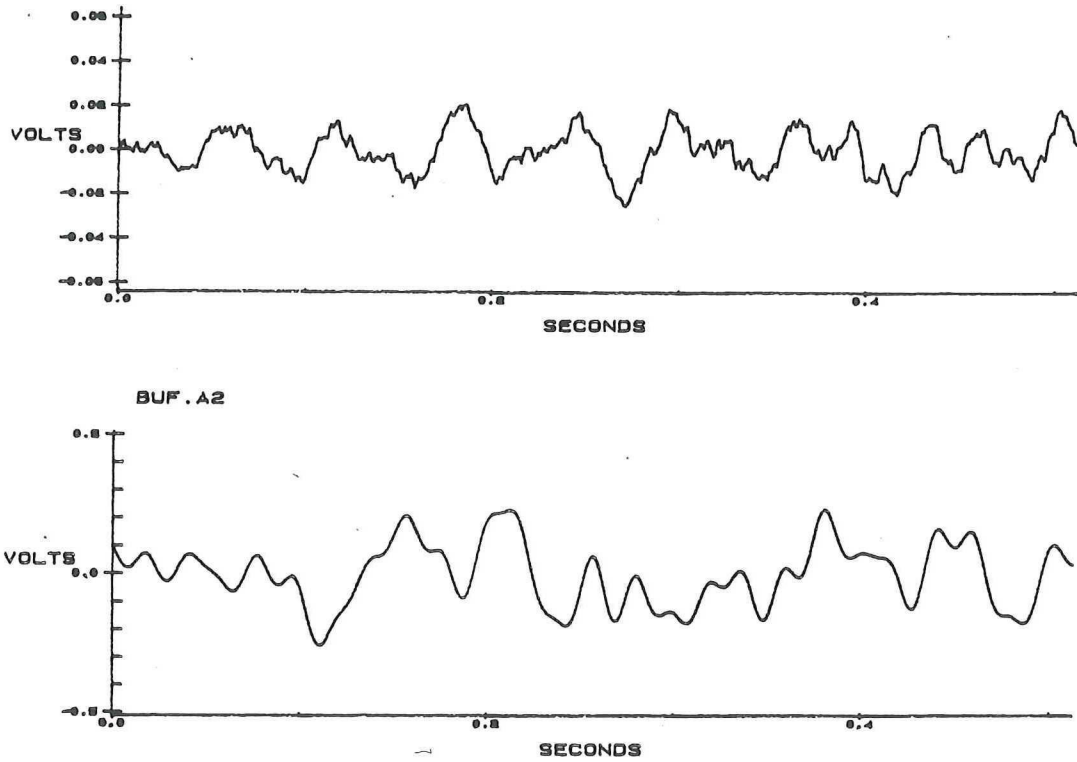


Figure 5.4. Low pass (30Hz) filtered accelerometer signal (top) and dynamic pressure transducer signal (bottom) for single-phase flow ($U_{s1}=1.45$ m/s).

This explains Wolga test-results where the signals from two opposite accelerometers are added and subtracted (see figure 5.3.). By adding the signals the low frequency signal disappears and the high frequency noise has information about the flow. In the Power Spectral Densities of the added and the subtracted signals the filtering effect of adding the signals is clearly seen. So discerning flow-related noise from vibration induced signals can be attained by a high-pass filter and by a combination of two opposite transducers. As long as the vibrations do not cause the electronics to overflow, the filtering method is much easier to use.

5.1.5. LOW-FREQUENCY SIGNALS

To make sure no flow-related information in the PSM frequency band is passed through the pipe, the accelerometer signal is amplified and passed through two low pass filters (30 Hz). The amplification is such that the amplitude of the accelerometer is of the same order of magnitude as the unfiltered pressure transducer. The signals simultaneously sampled during a single-phase water flow ($U_{s1}=1.45$ m/s) are shown in figure 5.4. From the absence of a clear correlation it is concluded that no future work should be done to try to obtain the low frequency pressure fluctuations by means of a clamp-on transducer.

5.1.6. HIGH-FREQUENCY SIGNALS

From the previous tests, listening to the flow-noise and watching the flow structure, the following idea has been born:

The two-phase flow pressure fluctuations related to the liquid flow are modulated by resonating bubbles. The resonance frequency of the bubbles is high enough to detect the modulated signal outside the steel pipe.

To check this idea the accelerometer signal has been sampled and processed into power-spectral-densities (PSD) for various superficial air and water velocities, while pictures of the flow were taken at the same time. To check for repeatability for each case six spectra are collected sampling 143 ms using 7168 points (for this purpose the limit of the frequency analyser). In figure 5.5 two out of six spectra are shown for four cases. The corresponding photo's are schematically copied (figure 5.6). In each case the superficial water velocity $U_{s1}=1.7$ m/s. The superficial

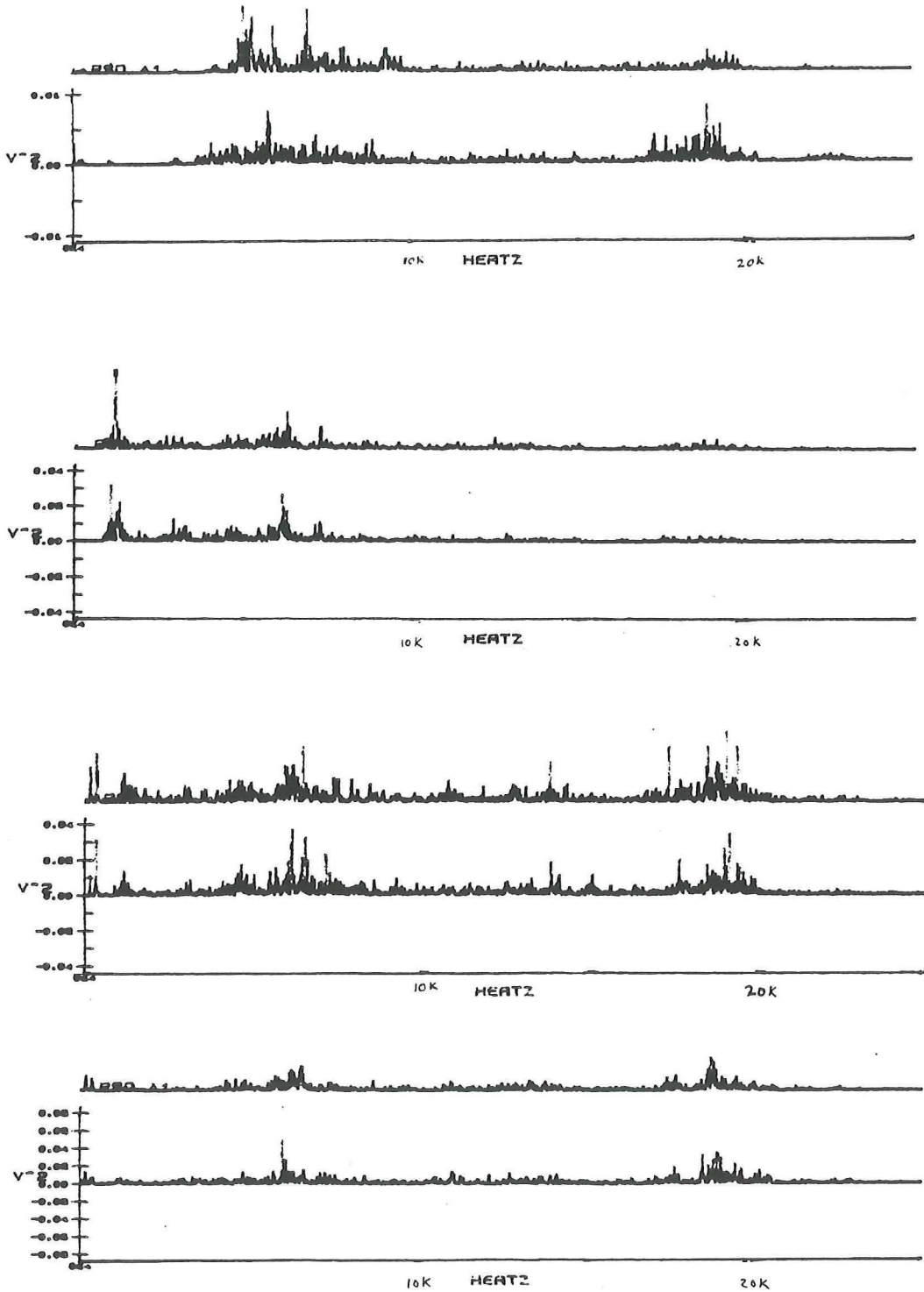


Figure 5.5. Two PSD's of the accelerometer signal for $U_{sl}=1.7$ m/s and four different air velocities, increasing from top to bottom. For the third PSD: $U_{sg}=2$ m/s and for the fourth: $U_{sg}=4$ m/s.

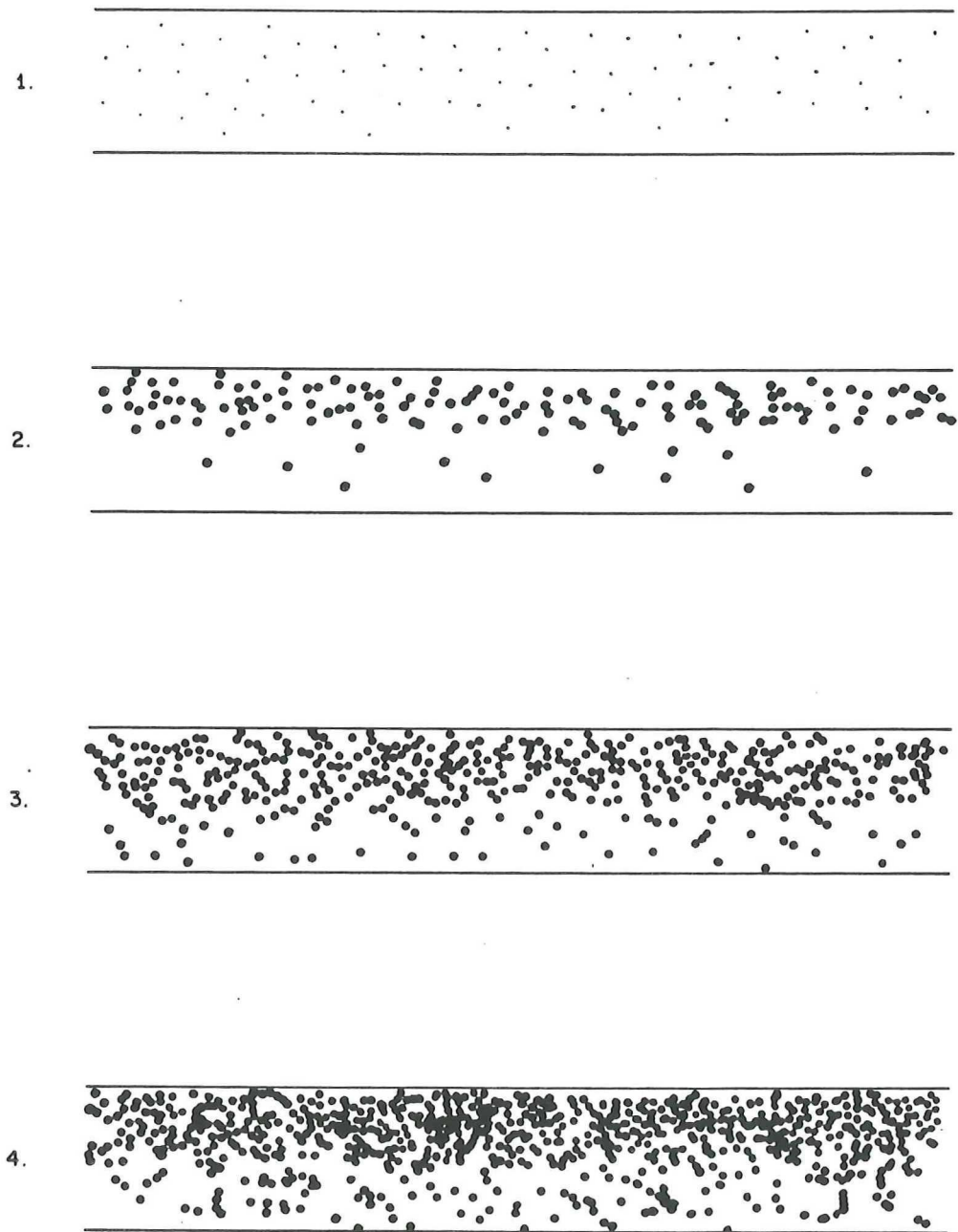


Figure 5.6. Schematic copies of pictures of gas-liquid flow in the test-loop Wolga. $U_{sl} = 1.7$ m/s. U_{sg} increasing from top to bottom. Third case: $U_{sg} = 2$ m/s and fourth case $U = 4$ m/s. First two: too small too measure.

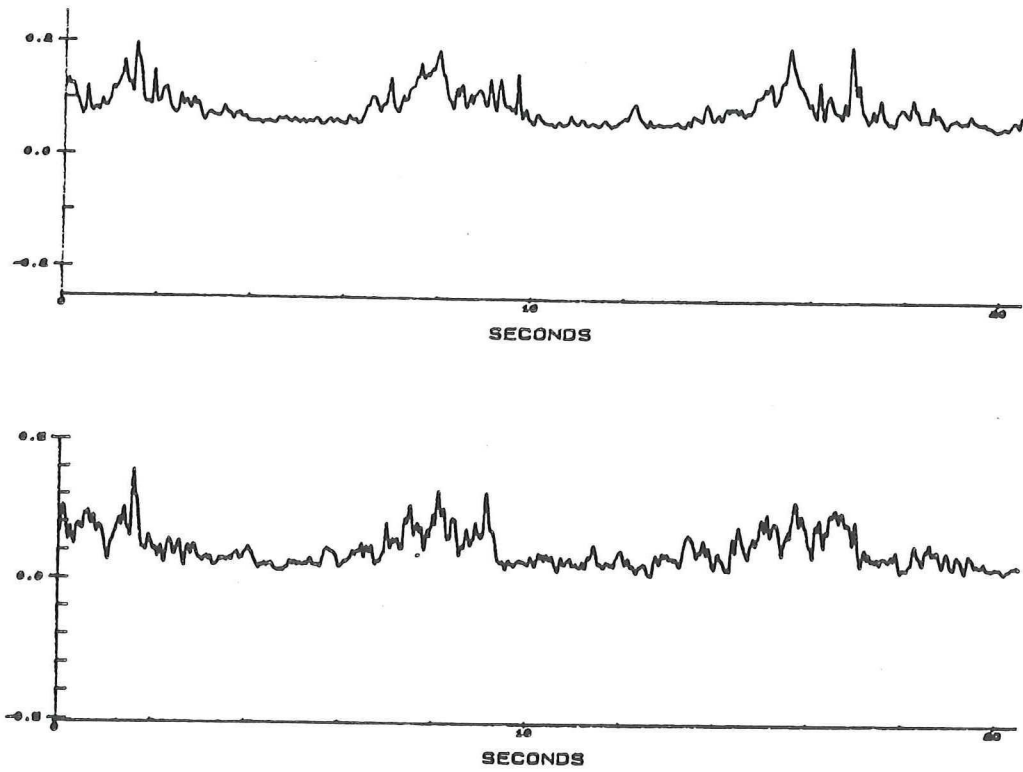


Figure 5.7. Square root of the RMS value of the accelerometer signal (top) and the dynamic pressure transducer (bottom) for slug flow ($U_{sl}=0.25$ m/s, $U_{sg}=3$ m/s).

air velocity U_{sg} is 2m/s in the fourth case and 1m/s in the third case. As the rotameters have a lower limit much higher than necessary to show the signal dependence on air flow, the air supply in the first two cases is caused by the pump introducing a little air into the system. This is caused by the low-pressure in the upstream line of the pump, resulting in cavitation. Not using the static-head pressure configuration, the air introduced by the pump flows directly into the measurement section. By putting a water-tap line on the upstream part of the pump the pressure is increased and the introduction of air is greatly reduced, as is shown in the first case.

From the spectra and the pictures it can be concluded that smaller bubbles create higher frequency sound (case one and two). And more bubbles result in a higher power spectral density. More bubbles than in the case of U_{sg} is 1m/s do not result in a higher power spectral density as is clear from case three and four. Even the spectra of the cases with U_{sg} is 4m/s or 8 m/s (not shown here) have a similar PSD as case three. One is tempted to believe that in those case the maximum turbulent energy is being converted already into high frequencies.

5.2. WOLGA TEST SERIES

In order to be able to compare the dynamic pressure transducer and accelerometer signal both transducers are put next (3 cm) to each other on the horizontal measurement section of the test-loop. For a few flow regimes the signals are sampled simultaneously and processed in accordance with the theory: The signals are put through a bandfilter (0-20 Hz for the pressure signal, and 100 Hz-10 kHz for the accelerometer) and fed through a RMS circuit (time constant 35 ms) and finally sampled by a Data 6000 frequency analyser (2048 points, 10 ms each). The Data 6000 takes the square root of the sampled RMS signal to comply with the theory (formula 5.8.).

Figure 5.7. shows the square root of the RMS value of both signals for a slug flow ($U_{sl}=0.25$ m/s, $U_{sg}=3$ m/s). The three slugs can be easily recognised in both signals. The time lag caused by the distance between the transducers is negligible for these flow speeds and the time scale of figure 5.7.

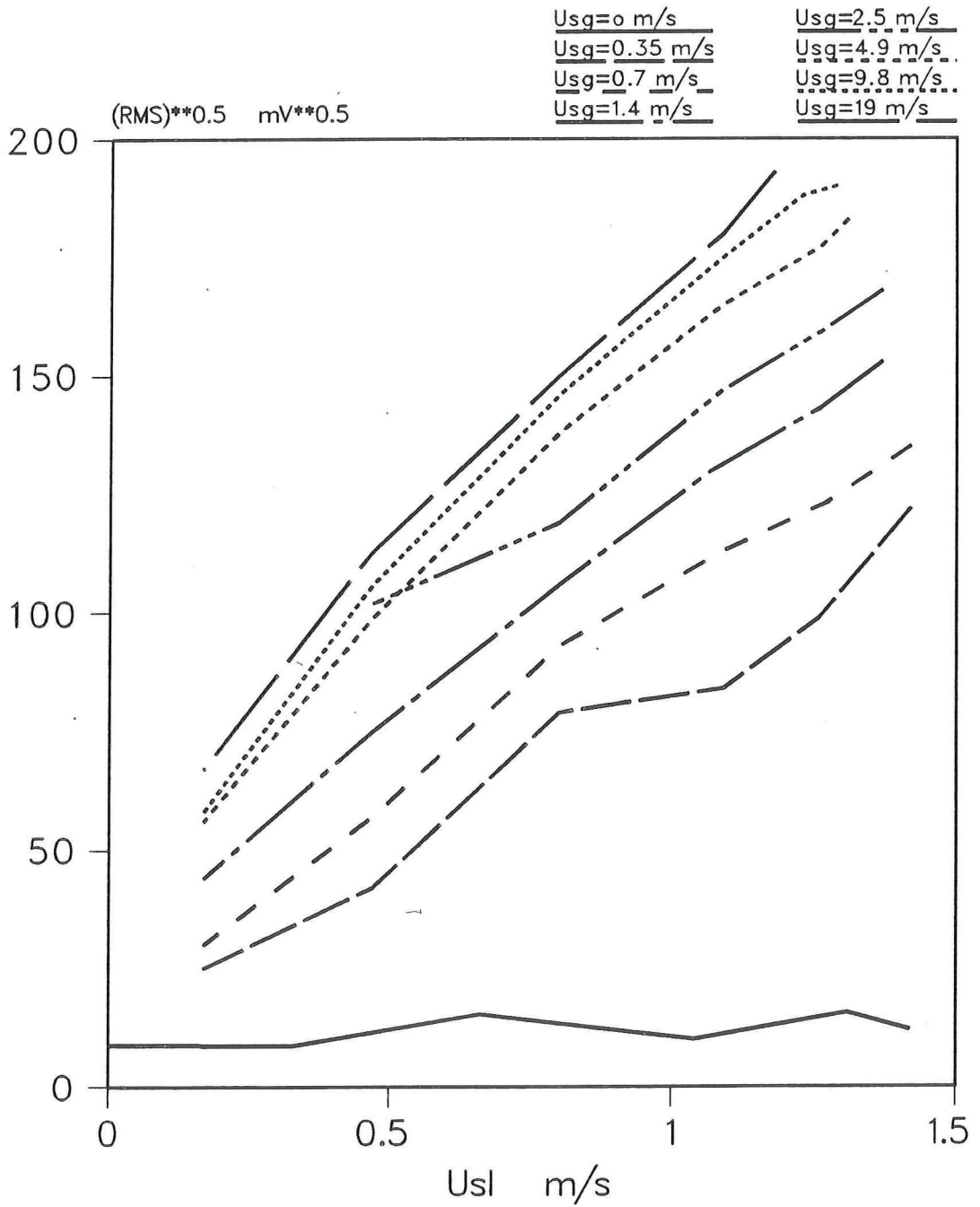


Figure 5.8. The average square root of the RMS of the accelerometer signal as a function of the superficial water velocity with the superficial air velocity as a parameter. Measured with the Wolga.

The structure of the signal during a slug is not the same for both signals. The pressure signal measures all the turbulent pressure fluctuations, while the accelerometer can only detect them when there are bubbles near the turbulence (cf. the theory in paragraph 6.1.). As the air bubbles are not homogeneously dispersed in the slug, the RMS value of the high frequency sound will not have the same structure as the RMS of the pressure fluctuations.

The front of the slug regularly engulfs an amount of air, which is broken up into bubbles by the turbulence in the slug. Some of the bubbles rise to the top of the pipe and because of the lower speed near the pipe-wall they are transported to the rear of the slug where they collect in the wake of the slug and finally coalesce with other bubbles and the air behind the slug. This bubble distribution is the reason that the accelerometer signal is high at the beginning of a slug and dies out slowly until the end of the slug. The third slug in figure 5.7. probably had a second slug-front with many bubbles. For higher slug speeds the bubbles will disperse better in the slug and the structure of the RMS signals will probably be more similar.

Similar to the PSM-test, measuring the relation between pressure fluctuations and the superficial gas and liquid velocities, (figure 3.1.) the time average of the square root of the RMS value of the accelerometer signal is recorded as a function of U_{sl} and U_{sg} . The filtering was changed into a 2kHz-10kHz band pass filter as signal under 2kHz showed to be less dependent on the flow. The Data 6000 sampled 2048 points of 10 ms and calculated the average of the square root of the RMS value of the signals. The results are shown in figure 5.8. Striking is the absolute independence of the signal on the superficial water velocity for $U_{sg}=0$. Using the static-head WOLGA configuration, the loop was absolutely free of visible air bubbles. As soon as a little air is introduced the dependence of the signal on U_{sl} becomes clear. Doubling the superficial air velocity increases the signal but the increase is less for higher superficial air velocity. Gregory et al (115) show that the air fraction in slugs increase with the mixture velocity. So an increase in superficial air velocity will increase the turbulence because of higher mixture velocities and will produce more bubbles in the slug.

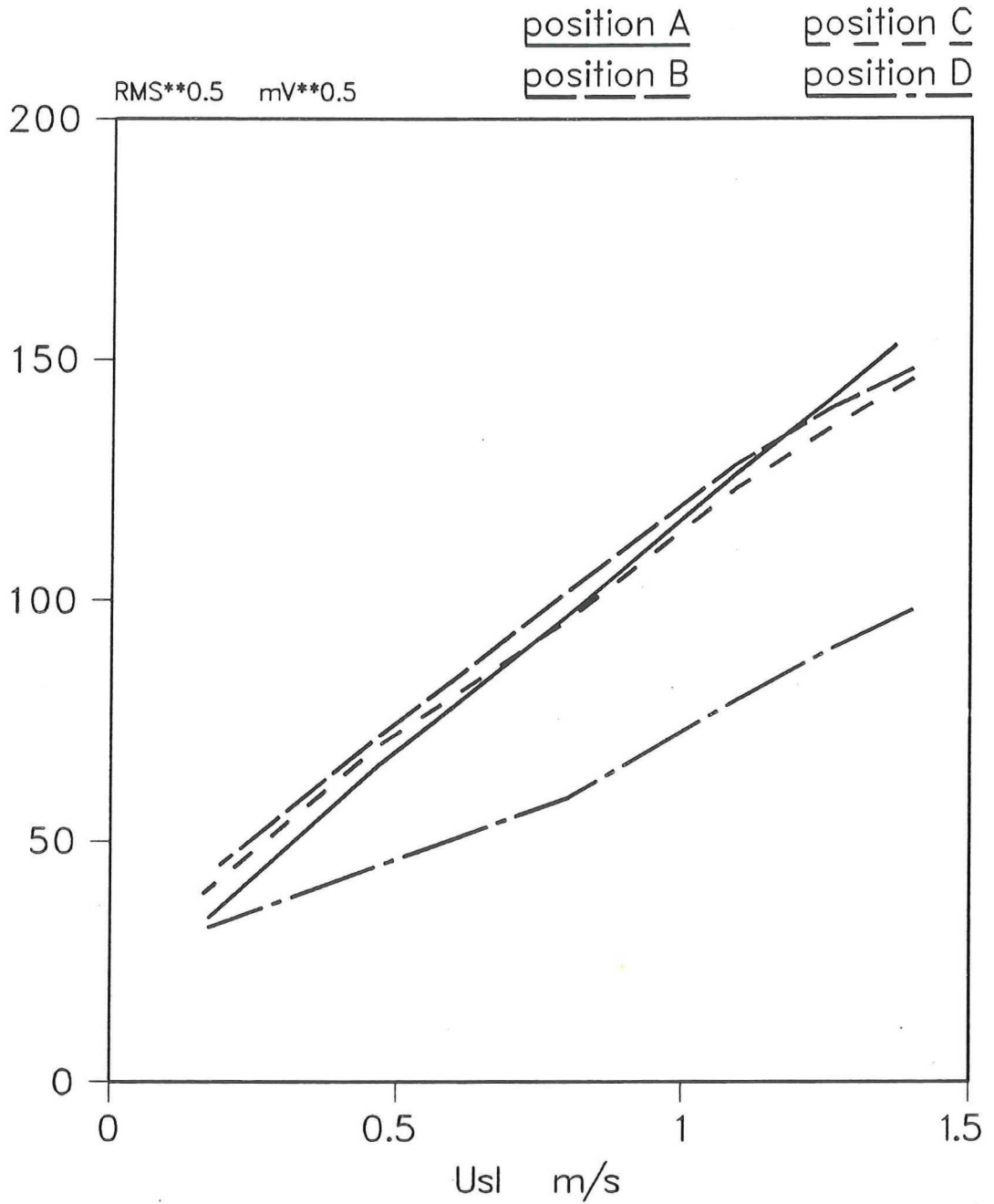


Figure 5.9. The average of the square root of the RMS value of the accelerometer signal as a function of the superficial water velocity with the position of the accelerometer as a parameter. Measured with the Wolga. A-on top of the pipe. B-on top of the pipe 15 cm further on. C-on the bottom of the pipe. D-on the flange.

According to the theory (chapter 6) this should increase the flow-noise level. The decrease of the superficial air velocities for higher rates was found as well in the PSM response (figure 3.1.).

Repeating the tests resulted in discrepancies less than 5%, which is the same order of magnitude as the accuracy of measuring U_{sl} and U_{sg} . For a well with a reasonable constant oil-gas production ratio a flow-noise behaviour like displayed in figure 5.8. would result in a production surveillance system well capable of determining the well production within 10%.

The influence of the position of the accelerometer on the flow-noise was also looked into. For one superficial air velocity $U_{sg} = 1.4$ m/s the signal dependency on U_{sl} was determined for four positions of the accelerometer. Two positions were on top of the pipe with a separation of 15 cm, one on the other side of the pipe and one on the flange. The results are shown in figure 5.9. Apart from the line for the position on the flange the lines are nearly the same. The discrepancies have the same order of magnitude as the accuracy of the measurement of the superficial velocities.

The method of attaching the accelerometer had little influence as well. In figure 5.10. the dependency of the signal on U_{sl} for four ways of attaching the accelerometer is shown. Using a magnet & Weimaplast (a coupling compound), a tie-wrap & Weimaplast, a tie-wrap & Weimaplast 3 meters upstream, or just a tie-wrap made no appreciable difference.

Because a (clamp-on) production surveillance monitor is calibrated with respect to the test separator, it can be concluded that the dependency of the RMS value on the superficial air and water velocities is sufficiently repeatable and independent of the position and the method of attachment to constitute a basis for a clamp-on acoustic production surveillance monitor.

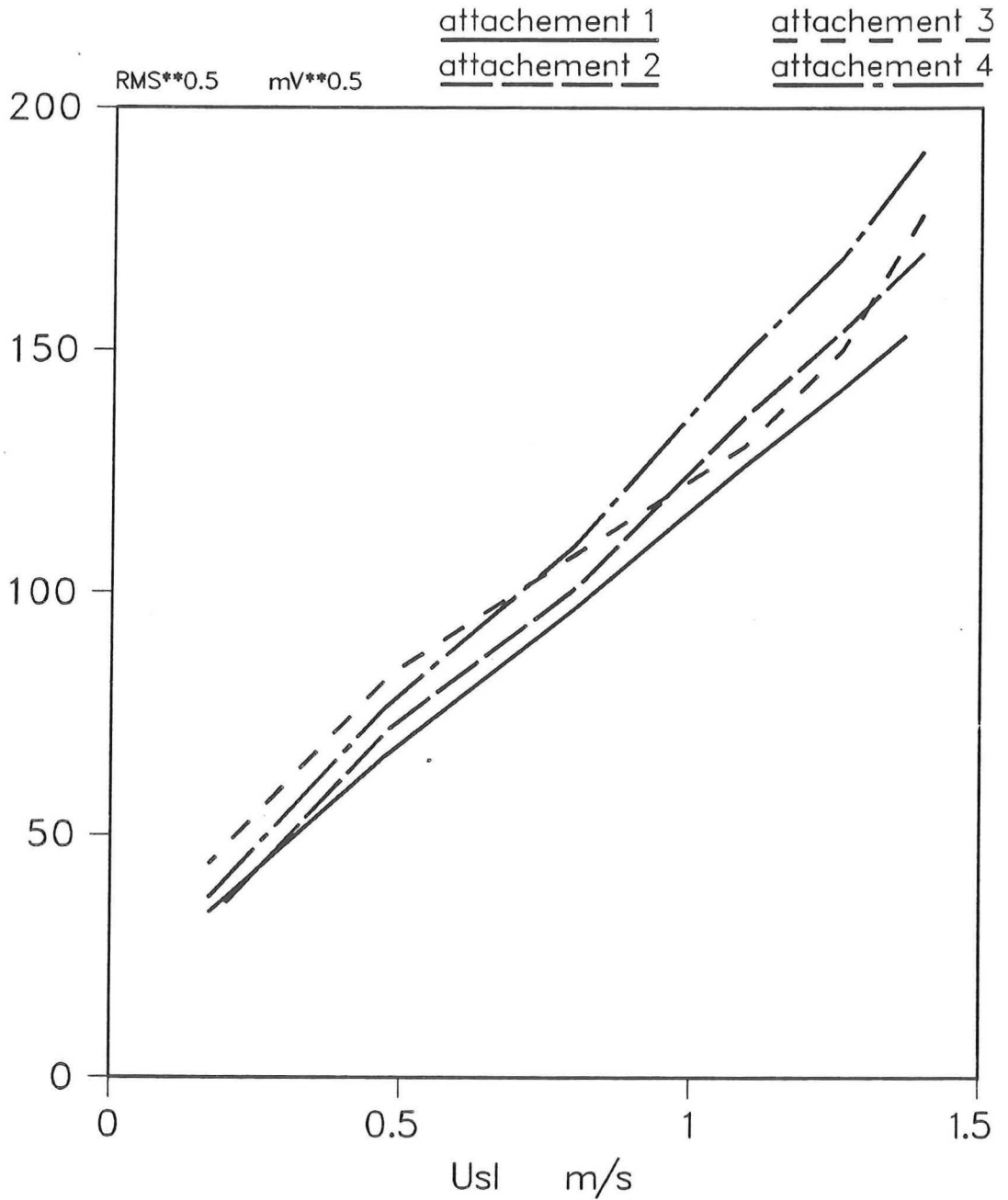


Figure 5.10. The average of the square root of the RMS value of the accelerometer signal as a function of the superficial water velocity with the way of attachment as a parameter. Measured with the Wolga. 1-magnet & Weimaplast. 2-tie-wrap & Weimaplast. 3-tie-wrap & Weimaplast 3 meters upstream. 4-just a tie-wrap.

figure	position	configur.	parameter	filter Hz	U_{sg} m/s	pressure Bar	various
5.11	4"	hor	filter	par	2.5	2.5	
5.12	4", 3"	?, 2"	U_{sg}	2k-10k	par	free	
5.13a	3"	vert, 2"	U_{sg}	2k-10k	par	free	3" upflow
5.13b	3"	vert, 2"	U_{sg}	2k-10k	par	free	3" downflow
5.14	4"	h&v, 2"	P_1	2k-10k	0.4	free	
5.15	4"	hor	U_{sg}	2k-10k	par	4	
5.16	3"	hor	U_{sg}	2k-10k	par	4	
5.17	4"	hor	filter	par	$5 \cdot U_{sl}$	4	
5.18	4"	par	config	4k2-8k5	5	par	
5.19	4"	hor	flow reg	2k1-4k2	par	4	
5.20	4"	?	U_{sg}	2k-10k	par	free	Tellusoil/water emulsion-air

Table 5.1. Test conditions of the various plots of measurements with the test-loop Donau. In the column "config.", "hor" means that the vertical section is by passed by a horizontal section, and "vert." that it is not. A "?" means that it is unknown whether the vertical section was bypassed or not. " 2" " means that 6 meters downstream of the accelerometer a 2-meter 2" section was inserted. "free" in the column "pressure" means that the pressure was not controlled (free outflow). The 3" up or down flow means that the accelerometer was mounted on the vertical section.

5.3. DONAU TEST SERIES

Of the numerous Donau tests, a selection of the plots has been made. Unfortunately they are not as convincing as the Wolga test results. In table 5.1. the flow conditions of the Donau-plots are specified. The plots are presented at the end of this paragraph. The position of the accelerometer can be on the four-inch pipe ($D_1=10.82$ cm) just upstream of the view-glass (see figure 4.4.) or on the three-inch pipe ($D_1=8.28$ cm). Three positions have been used on the three-inch pipe: on the three-inch line opposite the measurement section of the four-inch line, and the up and down pipe of the vertical section, ca two meters from the horizontal line level. In configuration the set-up of the loop is specified. If 'obstruction' is stated the test has been done with a two meter section of two-inch pipe (another flow-metering instrument) in the loop eight meters downstream of the four-inch measurement section. The horizontal configuration means that the flow is by-passing the vertical section. In the vertical configuration this horizontal bypass is closed and the vertical section is used.

The pressure in the loop can be regulated with a valve just before the outflow in the separator. When it is left open (free outflow) the superficial gas velocity must be kept constant by changing the air volume flow to compensate the change in pressure caused by varying the superficial water velocity. When closed partly the pressure can be controlled by an automatic feedback system. The feedback signal is derived from the pressure transducer in the beginning of the loop just downstream of the mixing point. In this way for moderate liquid flows even the pressure in the elbow (between the three and four inch pipe) is kept sufficiently constant to result in an unchanging superficial gas velocity.

In figure 5.11. the RMS-signal is plotted as a function of time for fixed flow conditions. As the real averaging time constant is about 30 seconds and the RMS-signal remains constant for more than an hour it can be concluded that the flow-noise remains constant for unchanging flow parameters.

From the use of the eight-band RMS converter it is found that the flow noise nearly has a white noise frequency distribution with an upper frequency limit of ca 25 kHz. Combined with the fact that from visual observations the bubble size distribution appears to be quite narrow, one

can conclude that the bubbles scatter the pressure waves of all the turbulent eddies instead of only the eddies with a frequency equal to the bubble resonance frequency. The advantage of the near white noise distribution is that specific acoustic disturbances can be filtered out without losing too much essential flow-noise. In this way lorries passing the test-loop within a few meters and seismic tests ca twenty meters away did not interfere with the measurement series. Kicking the pipe or hitting it with a wrench however produces too much high frequency sound to separate it from the essential flow-noise.

In figure 5.12. the average RMS-signal is given as a function of U_{s1} with U_{sg} as parameter. In fact there were only two measurement series but the response of accelerometer on the the horizontal 3" and 4" pipe were monitored simultaneously. The results resemble those of the Wolga quite reasonably.

For vertical flow fig 5.13. shows that the RMS-signal from the rising pipe has no information about the flow but the flow-noise from the downgoing pipe gives a clear relationship between the noise level and the superficial water velocity even for low air speeds. Like the previous case the signals from both vertical pipes were recorded simultaneously.

Closing the valve at the end of the loop but without switching to automatic pressure control results in a pressure higher than with an open outflow but still increasing with superficial water velocity. From figure 5.14. it is clear that the response increases slightly for higher pressure. Striking is the fact that the flow-noise decreases for increasing superficial water velocity above a certain critical water speed. This critical speed is less for lower air speed.

From 5.15. it can be concluded that the superficial air velocity should be more than 3 m/s to obtain a useful relationship between U_{s1} and the flow-noise. The four measurement series of this plot have been monitored by the horizontal 3" accelerometer as well. Those results are presented in figure 5.16. The dependency of the flow-noise on the water speed is much different from that in figure 5.15. The high noise level for low water speed is caused by the fact that the slug interval length is of such a length that the flow between the mixing point and the position of the accelerometer is

stratified. Consequently the loud noise from the air flowing into the loop is not attenuated by the two-phase flow. Even with a small number of slugs the attenuation is too small to consider the accelerometer signal as local. The difference between figure 5.16. and 5.12. is most likely to be caused by the pressure control because the other major change (the 2" section) is too far from the 3" accelerometer to be of any influence.

In figure 5.17. the results has been plotted for a constant U_{sl} , U_{sg} ratio ($U_{sg} = 5U_{sl}$). As we have seen in figure 5.15. near $U_{sg} = 2\text{m/s}$ an increase in air decreases the flow-noise. This effect has more influence than the increase in flow-noise caused by an increase in water velocity. This explains the dip in figure 5.17. Although locally the flow-noise level can be a good indication of the superficial water velocity, the absence of a monotonous increase in flow-noise as a function of U_{sl} means that with this signal processing there is no basis for a clamp-on production surveillance monitor for this U_{sl} , U_{sg} ratio.

The influence of the configuration of the loop and the pressure is shown in figure 5.18. The horizontal free outflowing configuration produces most flow-noise but for $U_{sg} = 5 \text{ m/s}$ the horizontal and vertical configuration both result in a monotonously increasing flow-noise level.

The flow-regime is of great importance to the flow-noise. In figure 5.19. the response to various flow-regimes is given. It can be concluded that only the slug regime can have a useful noise velocity relationship. This corresponds nicely with the conclusion that U_{sg} should be more than 3m/s.

Finally an exotic liquid has been tested in a two-phase flow with air. The liquid was a stable water/Tellus oil emulsion with a viscosity of 200 kg/ms and a interfacial tension of $55 \pm 15 \text{ N/m}$. The results are shown in figure 5.20. Surprisingly the relationship between the noise-level and the liquid velocity is a straight line. Together with the dependency on the air velocity it resembles the Wolga results very closely.

So the following three cases result in a monotonous increase with sufficient resolution of flow-noise level as a function of the superficial water velocity:

- $U_{sg} > 3$ m/s free outflowing horizontal 4" flow
- vertical downflowing 3" flow
- high viscosity liquid horizontal 4" flow

From these results no simple criterion can be derived for flow conditions that produce flow-noise that can be used as a liquid production indicator. More tests are necessary and more work will have to be done on the signal processing to ascertain under which flow conditions a clamp-on acoustic surveillance monitor can be applied.

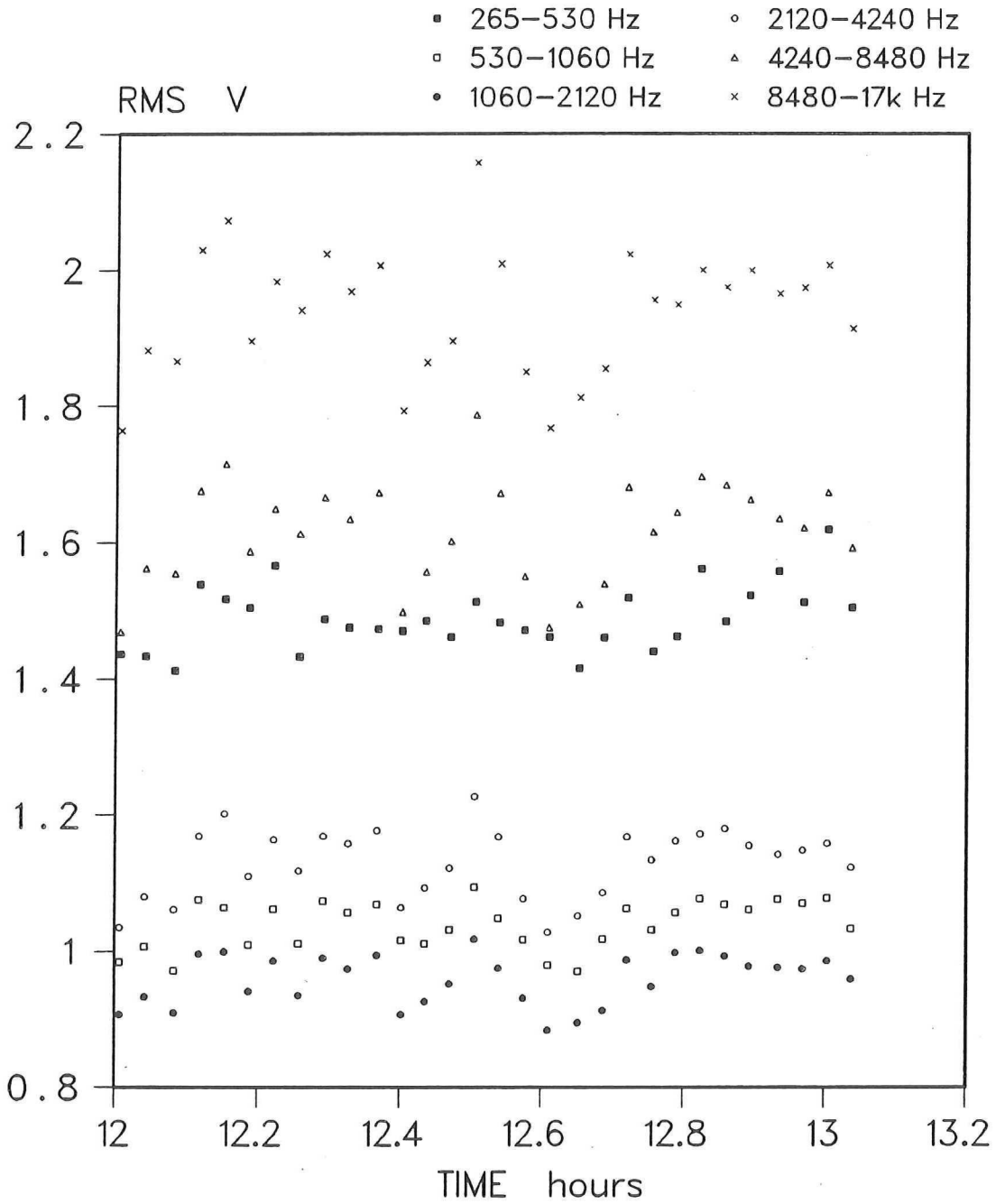


Figure 5.11. Accelerometer response to a 4 inch horizontal flow in the Donau test-loop with the filtering as a parameter. The vertical riser section was by-passed. $U_{sg}=2.5$ m/s and $p_1=2.5$ Bar.

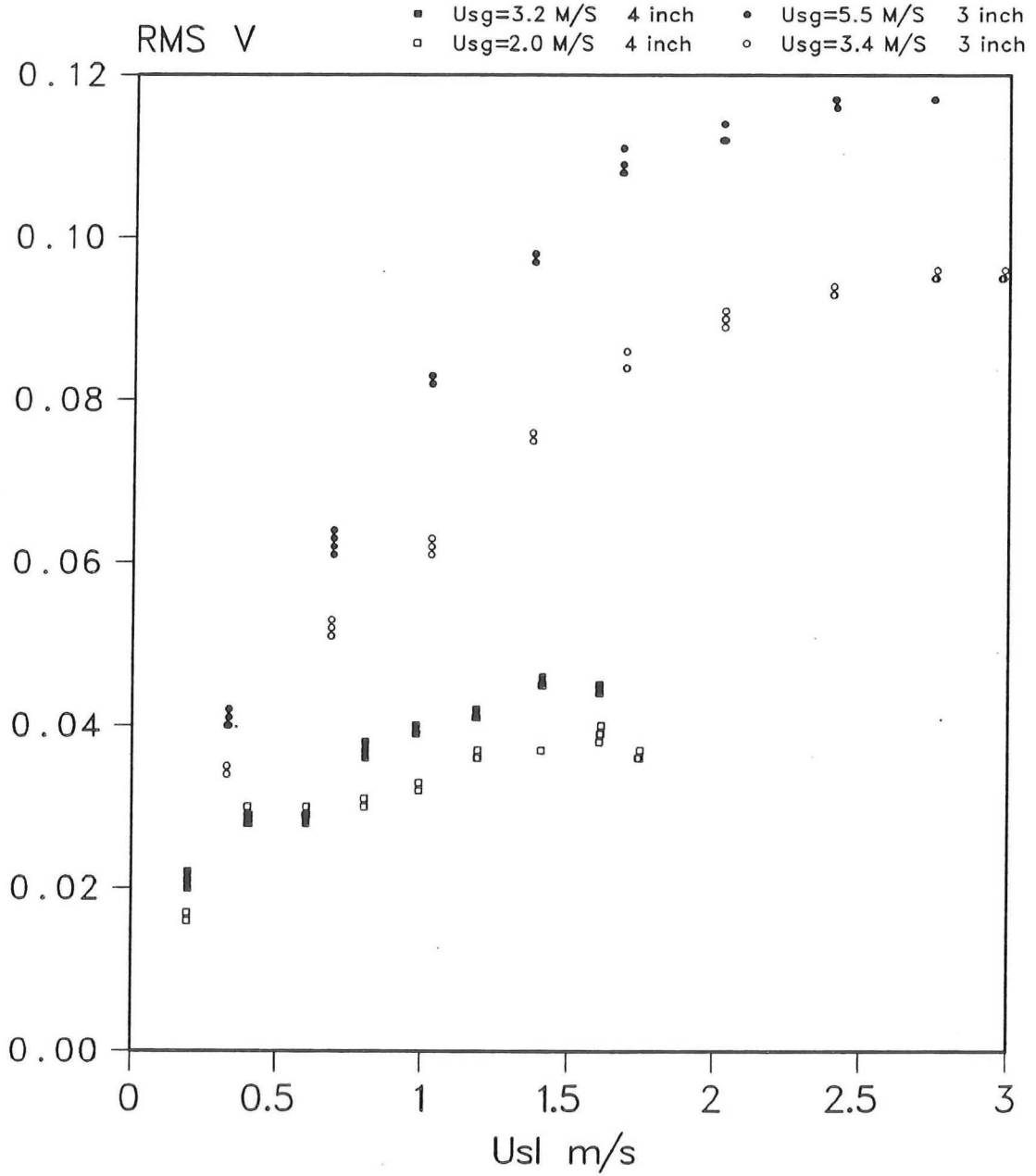


Figure 5.12. Accelerometer response to a 4 inch and 3 inch horizontal flow in the test-loop Donau with the superficial velocity is the parameter. 6 meters downstream a 2 meter 2 inch section was inserted. The filtering was 2k-10k Hz and the pressure was not controlled (free outflow).

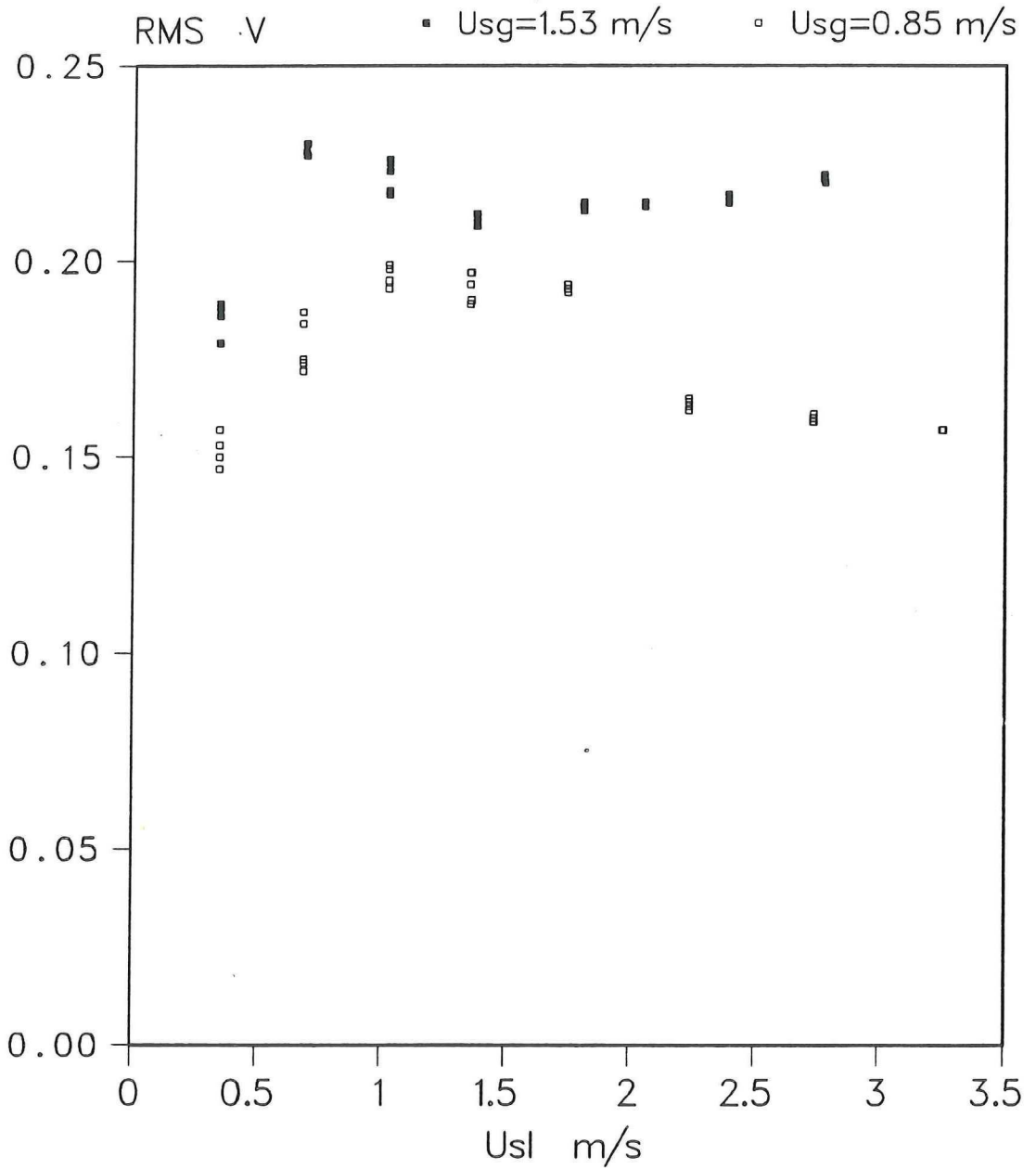


Figure 5.13a. Accelerometer response to a 3 inch upward flow in the test-loop Donau with the superficial air velocity as a parameter. 6 meters downstream of the 4 inch viewglass a 2 meter 2 inch section was inserted. The filtering was 2k-10k Hz and the pressure was uncontrolled (free outflow).

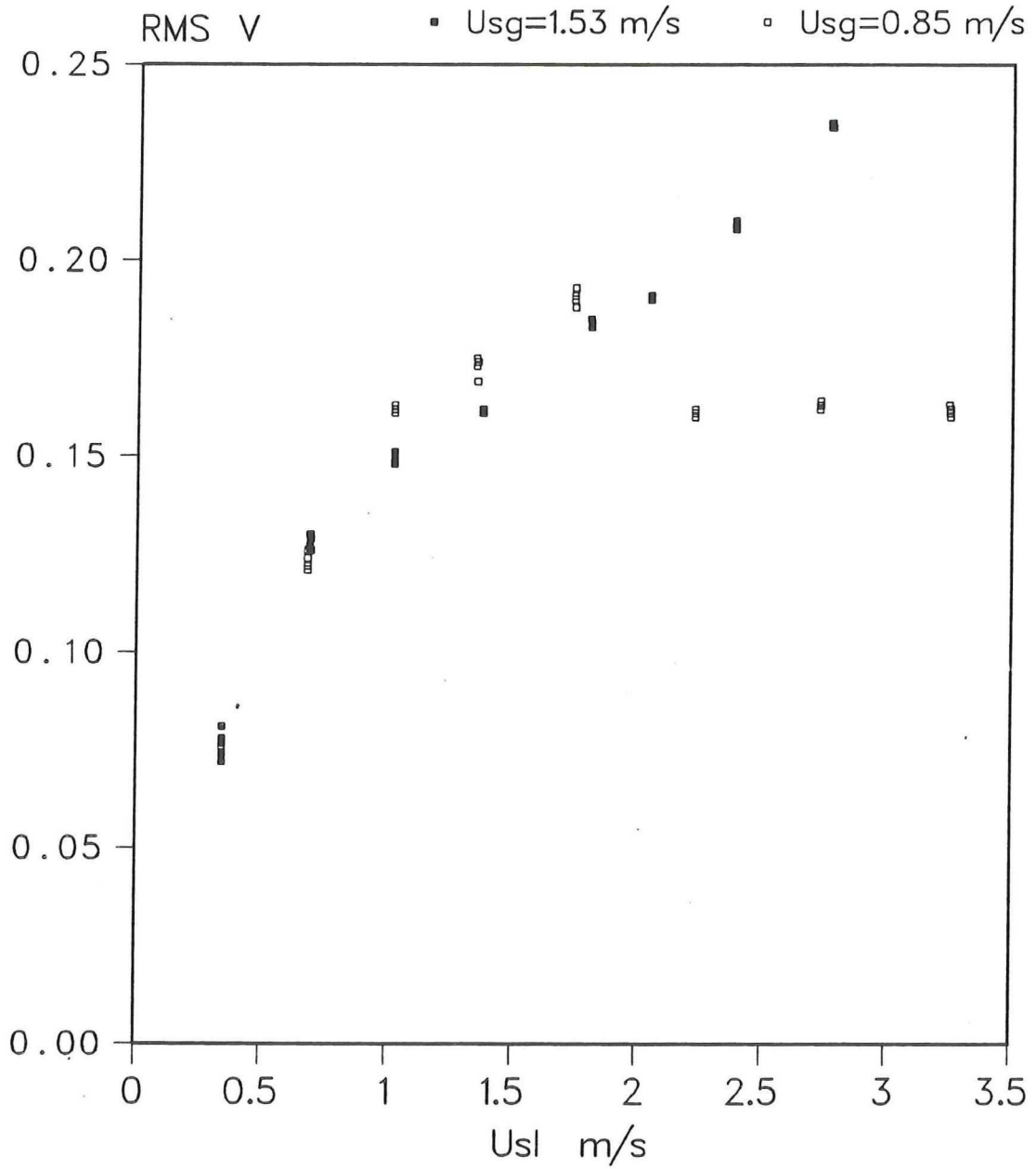


Figure 5.13b. Accelerometer response to a 3 inch downward flow in the test-loop Donau with the superficial air velocity as a parameter. 6 meters downstream of the viewglass a 2 meter 2 inch section was inserted. The filtering was 2k-10k Hz and the pressure was uncontrolled (free outflow).

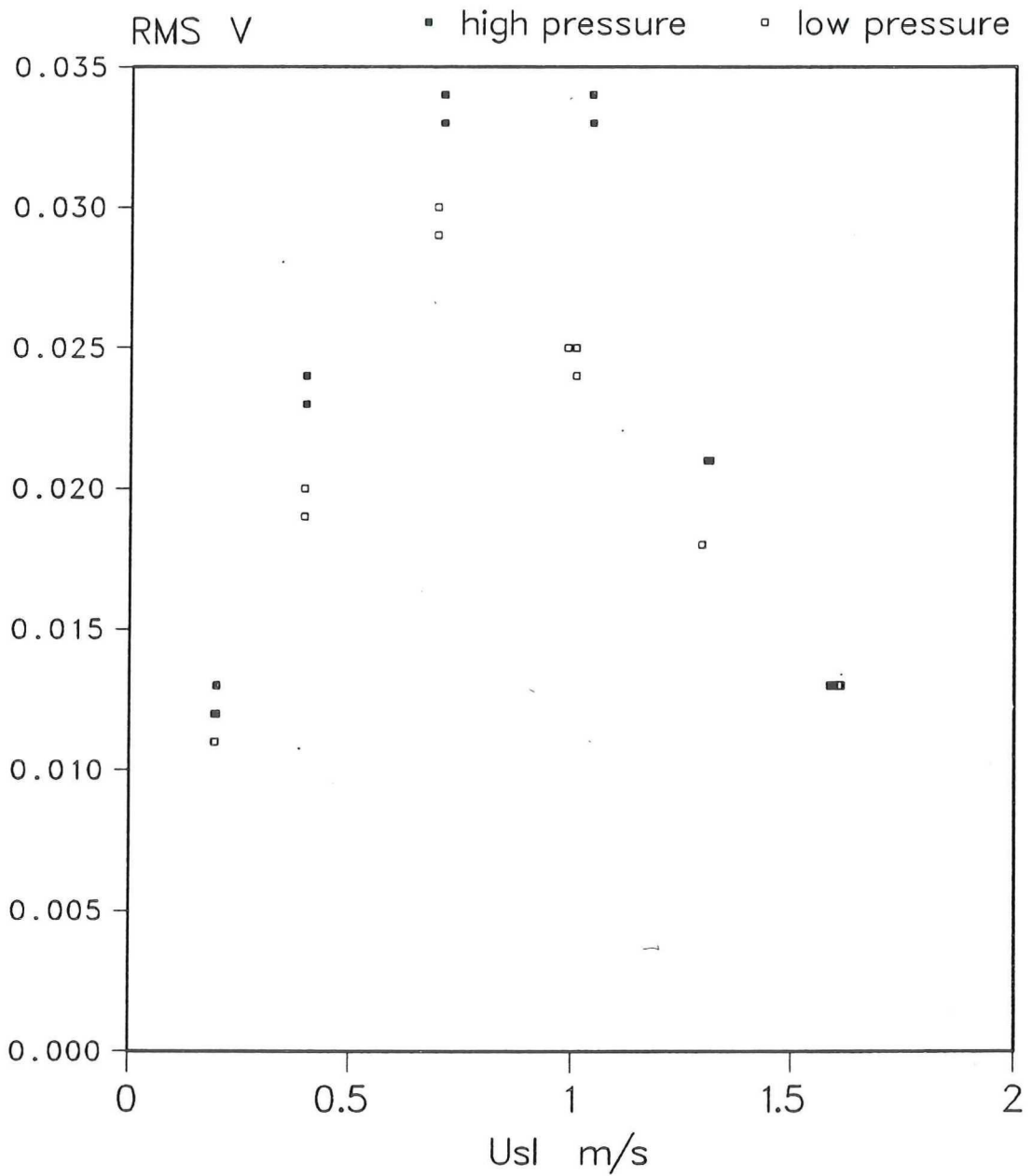


Figure 5.14. Accelerometer response to a 4 inch horizontal flow in the test-loop Donau with the line pressure as parameter. 6 meter downstream of the 4 inch viewglass a 2 meter 2 inch section was inserted. The riser section and the horizontal by-pass were both opened. The filtering was 2k-10k Hz, $U_{sg}=0.4$ m/s, and the pressure was uncontrolled (free outflow in the first case and the valve at the end of the loop partly closed in the second case).

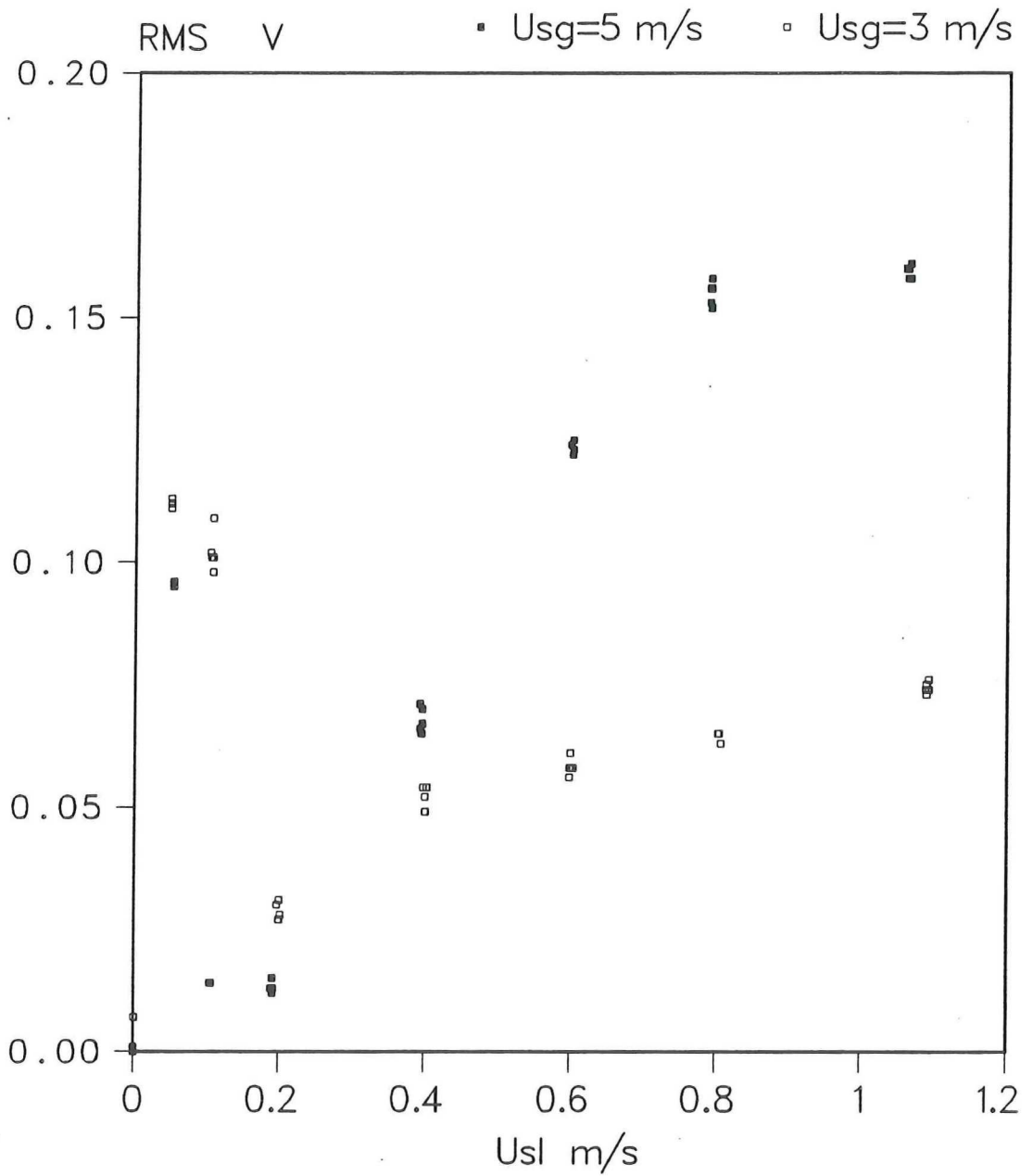


Figure 5.15a. Accelerometer response to a 4 inch horizontal flow in the test-loop Donau with the superficial air velocity as a parameter. The riser section was bypassed, the filtering was 2k-10k Hz, and the pressure was kept at 4 Bar.

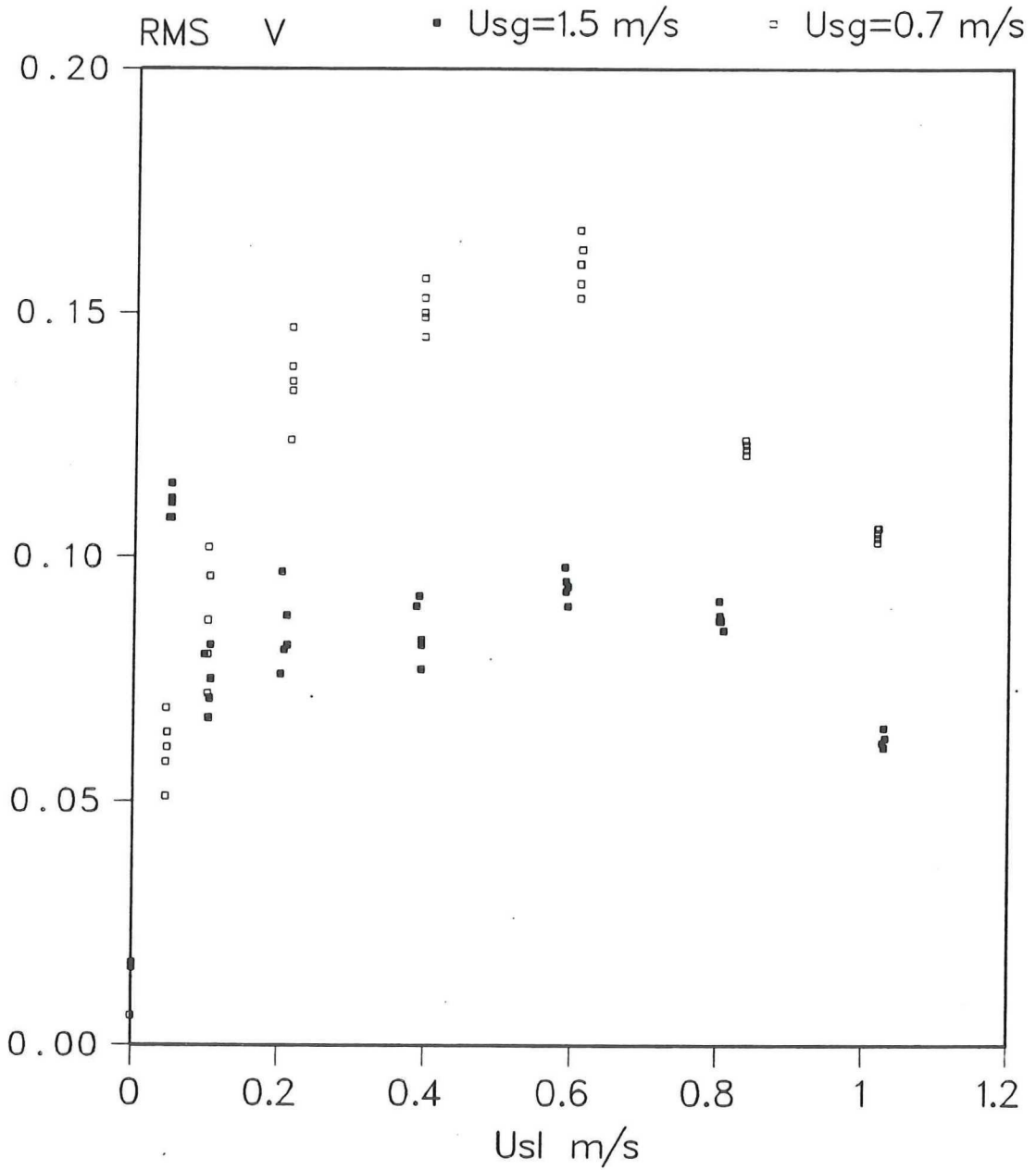


Figure 5.15b. Accelerometer response to a 4 inch horizontal flow in the test-loop Donau with the superficial air velocity as a parameter. The riser section was bypassed, the filtering was 2k-10k Hz, and the pressure was kept at 4 Bar.

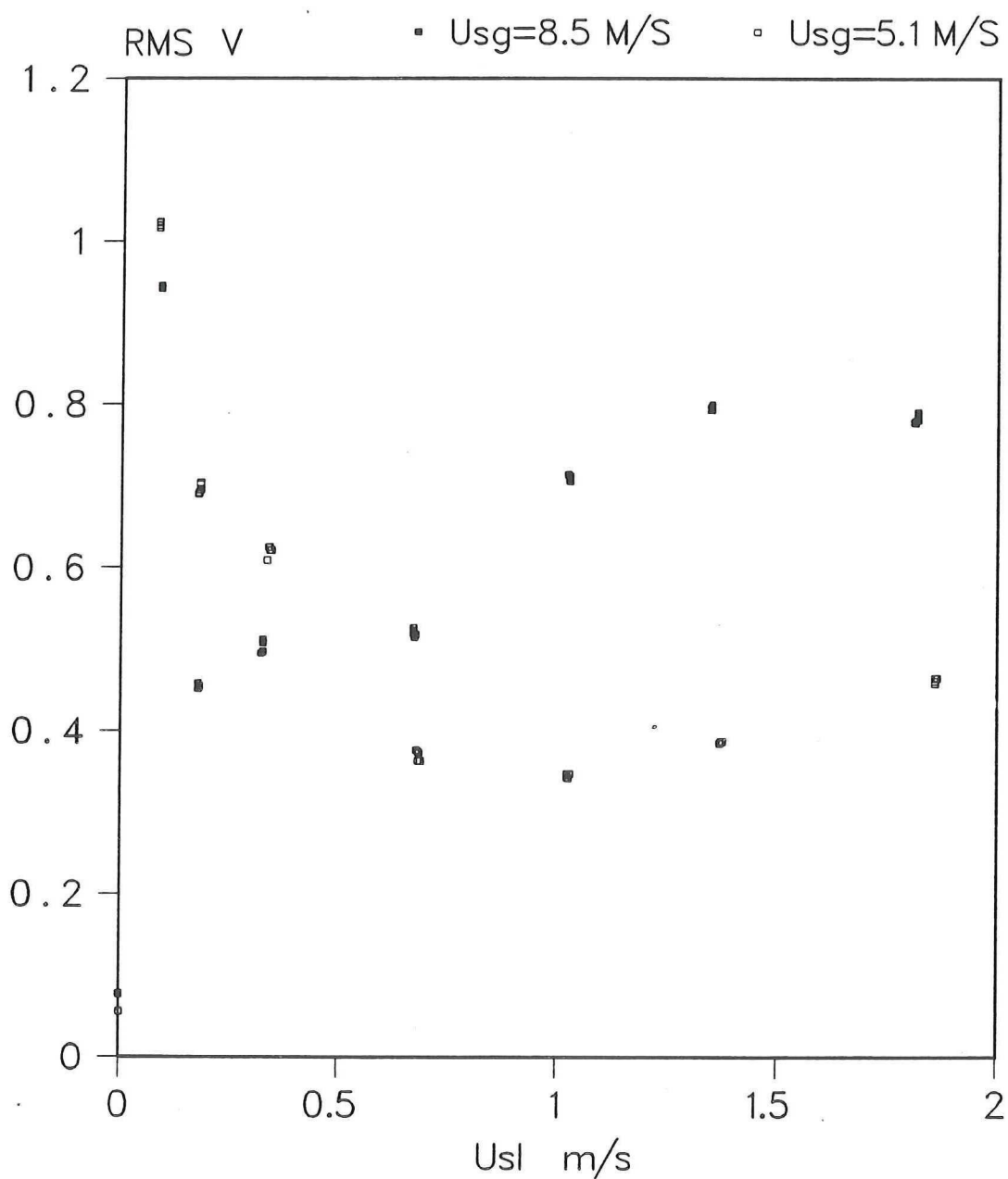


Figure 5.16a. Accelerometer response to a 3 inch horizontal flow in the test-loop Donau with the superficial air velocity as a parameter. The riser section was bypassed, the filtering was 2k-10k Hz, and the pressure was kept at 4 Bar.

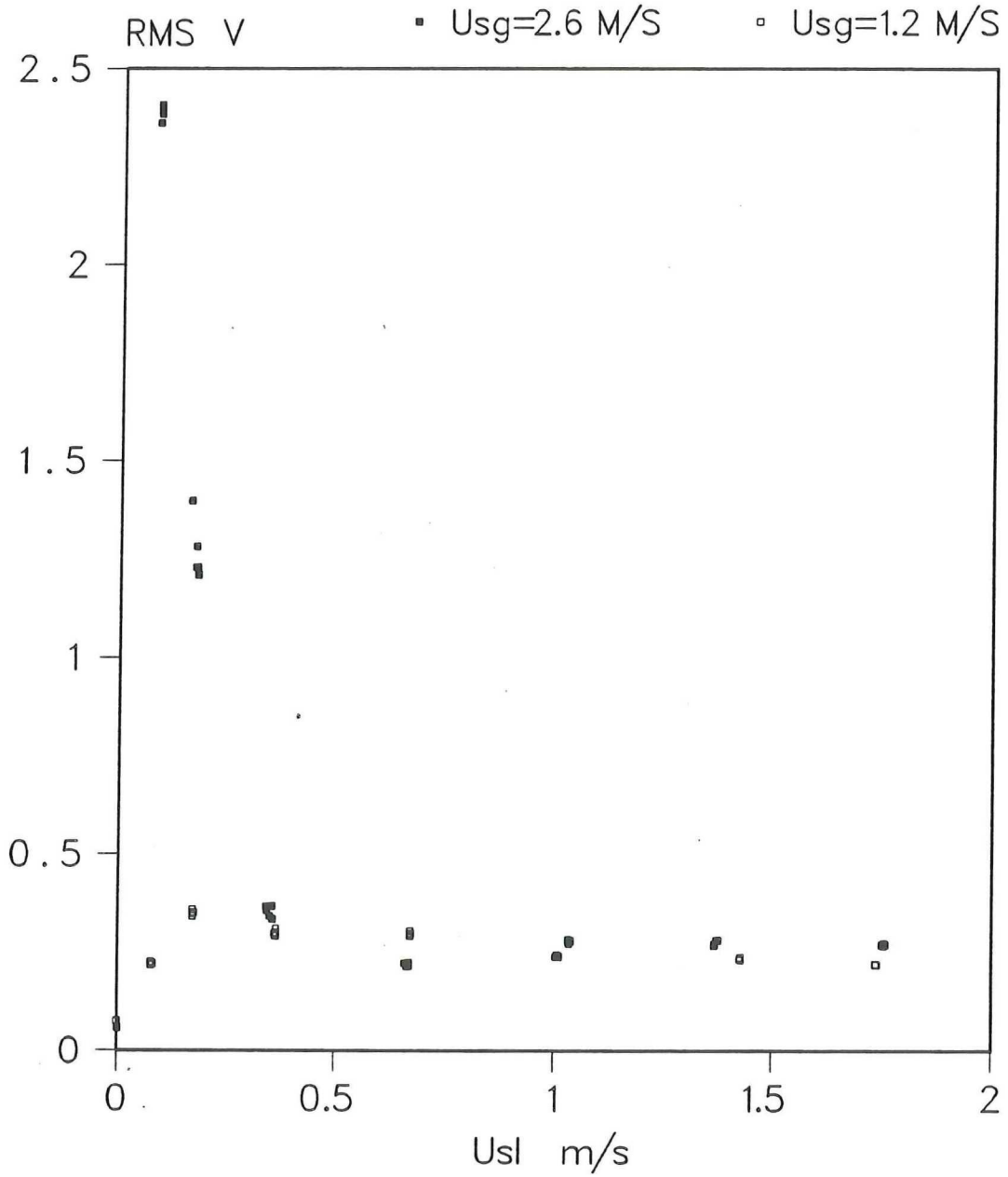


Figure 5.16b. Accelerometer response to a 3 inch horizontal flow in the test-loop Donau with the superficial air velocity as a parameter. The riser section was bypassed, the filtering was 2k-10k Hz, and the pressure was kept at 4 Bar.

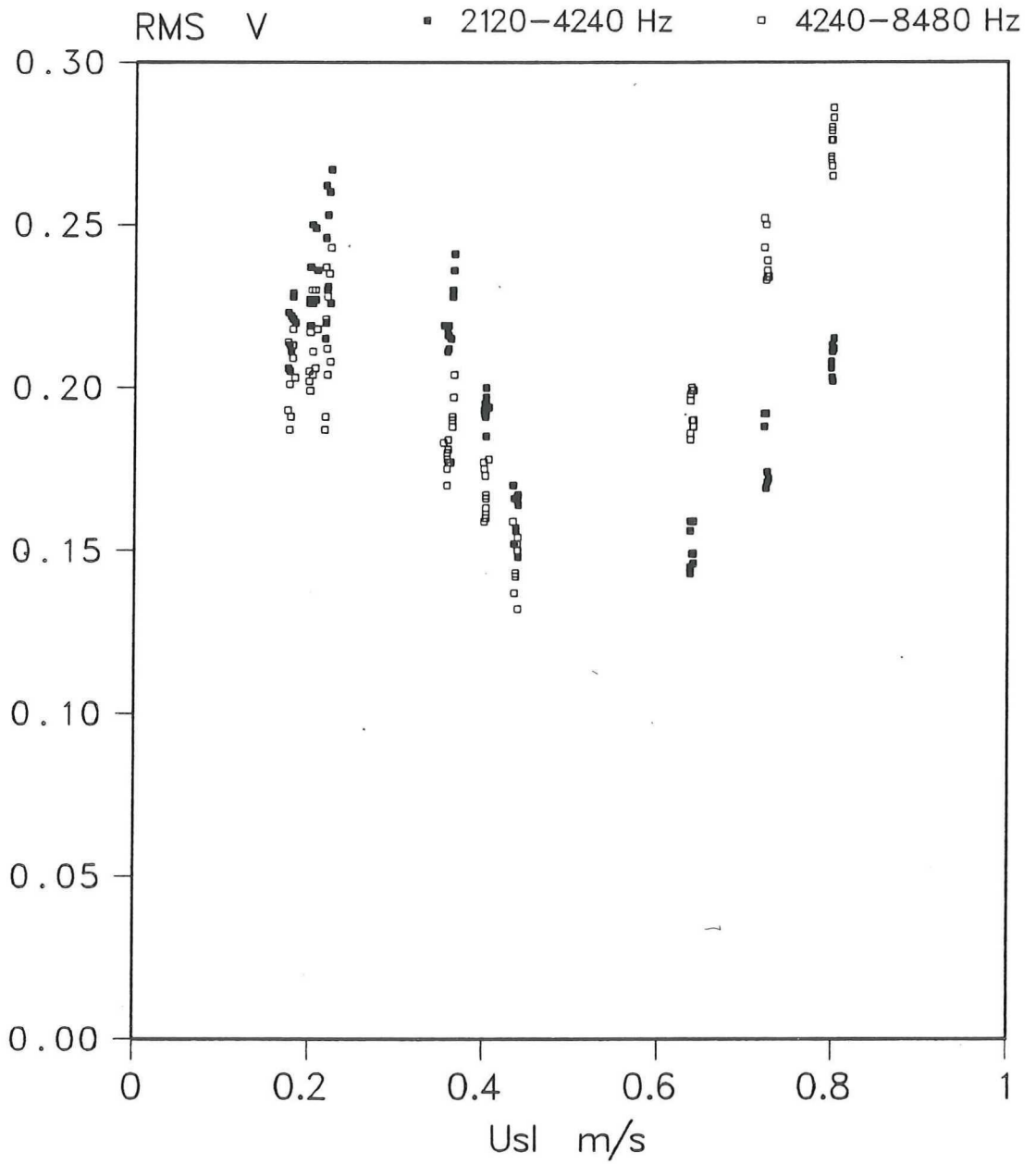


Figure 5.17. Accelerometer response to a 4 inch horizontal flow in the test-
lop Donau with the filtering as a parameter. The riser section was bypassed,
 $U_{sg} = 5U_{sl}$, and the pressure was kept at 4 Bar.

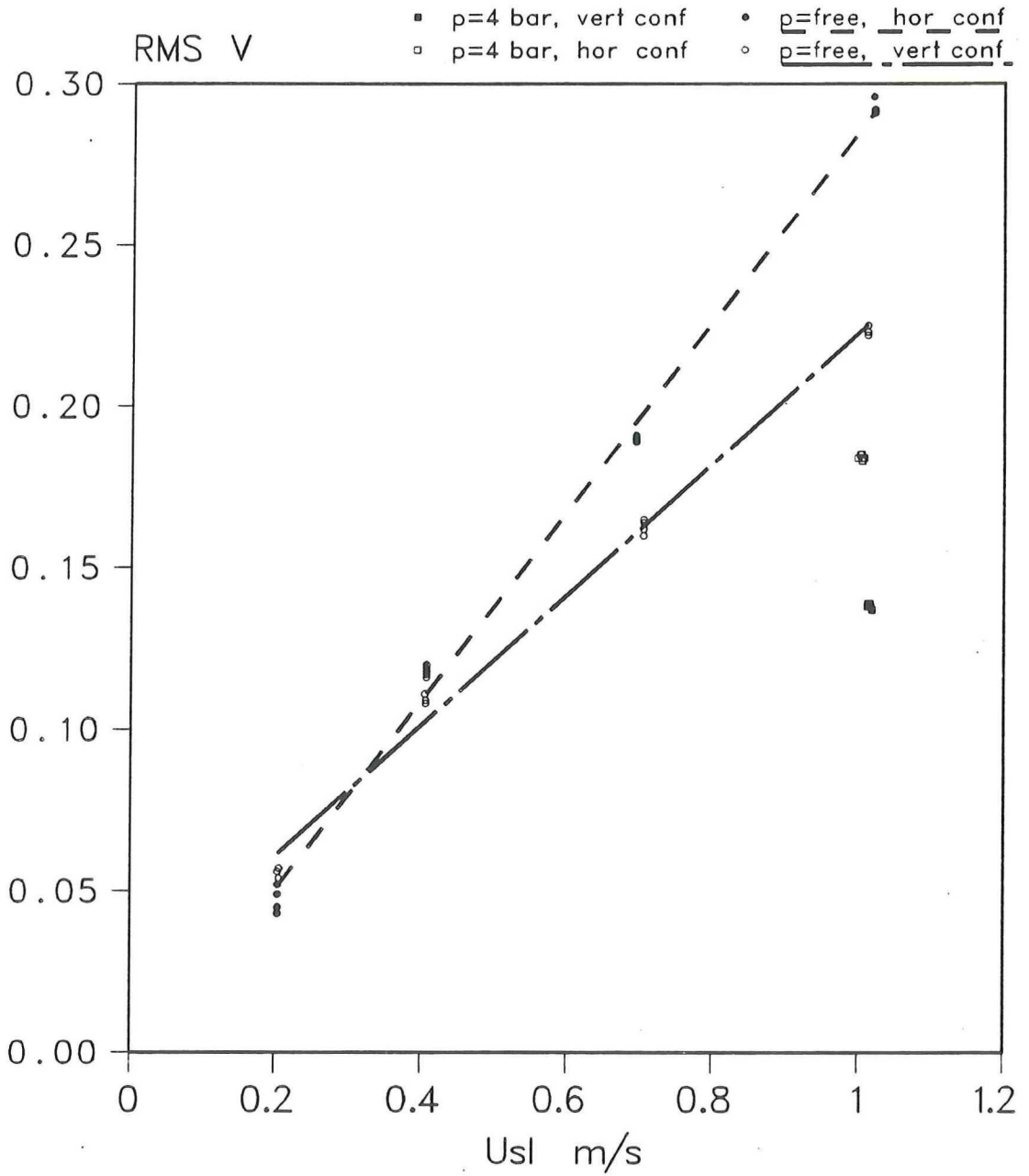


Figure 5.18. Accelerometer response to a 4 inch horizontal flow in the test-loop Donau with the test-loop configuration as a parameter (riser bypassed=hor conf.). The filtering was 4200-8500 Hz and $U_{sg}=5$ m/s.

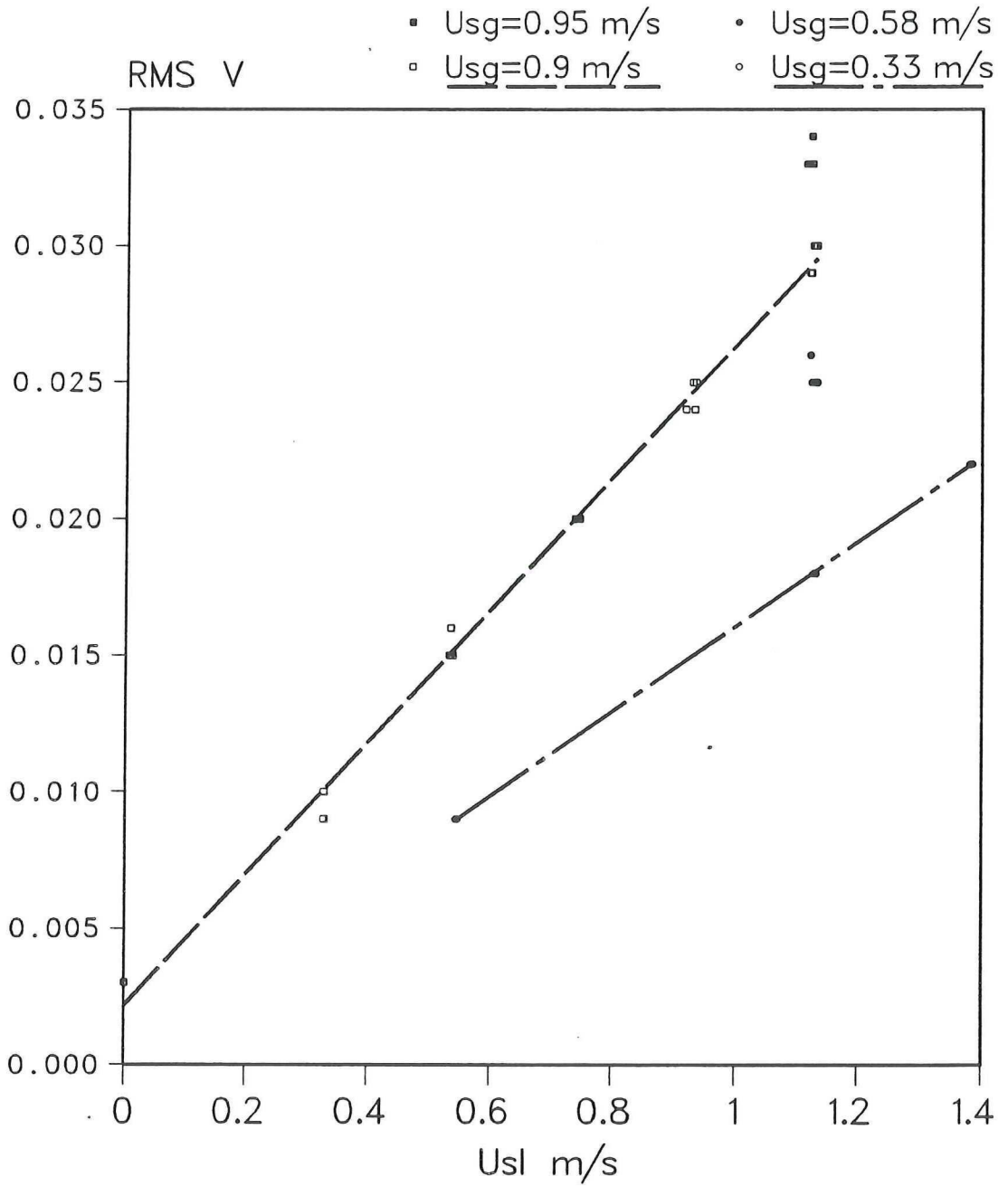
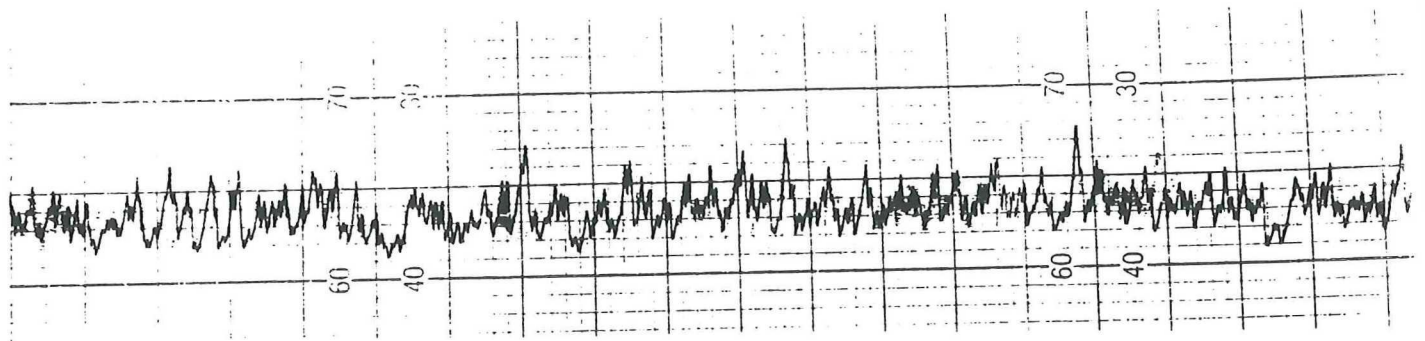
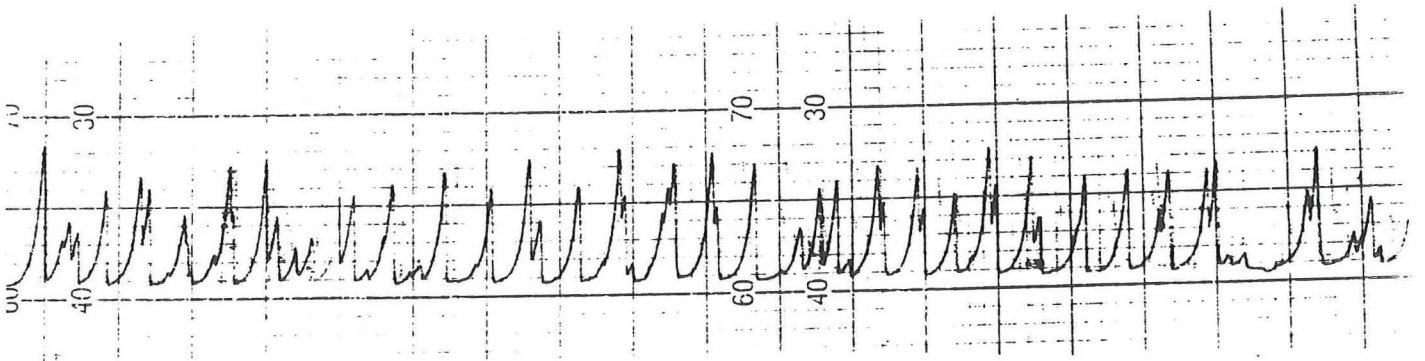


Figure 5.20. Accelerometer response to a 4 inch horizontal flow in the test-loop Donau with the superficial air velocity as a parameter. The liquid was a Tellus Oil-water emulsion. The filtering was 2k-10k Hz and the pressure was uncontrolled (free outflow).



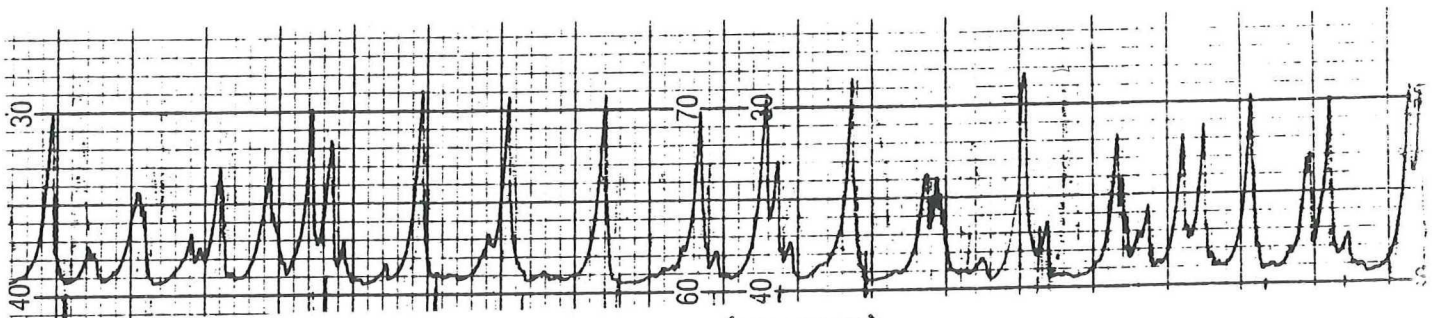
$$U_{sl} = 0.72 \text{ m/s} \quad U_{sg} = 3.9 \text{ m/s}$$

60 s



$$U_{sl} = 0.36 \text{ m/s} \quad U_{sg} = 1.8 \text{ m/s}$$

60 s



$$U_{sl} = 0.18 \text{ m/s} \quad U_{sg} = 0.9 \text{ m/s}$$

60 s

Figure 5.21. The accelerometer RMS-time signal of a 4 inch horizontal flow in the test-loop Donau for three flowrates. The pressure was kept at 4 Bar.

5.4. STATISTICAL PROCESSING

5.4.1. SLUG FREQUENCY

Averaging the RMS of the flow-noise is the simplest statistical signal processing. Some time has been spent to look into slug speed and slug frequency. For that purpose the μ -mac program was supplemented with a slug counter section. It checks every sampled RMS value of a chosen filter section whether it is above a certain level. This level is a fixed percentage above the average RMS value at that particular moment. When the RMS-value exceeds that level the number of slugs is increased by one and the detection is disabled. When the sampled RMS value is below a second level, (a fixed percentage below the average value) the slug detector is activated again. Combined with a built-in timer the μ -mac program can calculate both slug length and frequency. Unfortunately the sample interval time of the program is of such a length that it is only capable of detecting slugs with a very low frequency. It would be much better to detect the slugs with an analogous level switch fed by a fast RMS-signal instead of the signal from the RMS detector with a time constant of three seconds.

As the RMS-signal was also recorded on paper, the slug frequencies can also be determined by hand. Counting the slugs a system similar to that of the μ -mac program has been used. Consequently two slugs much closer together than the average slug separation are counted as one slug. The RMS time constant (3s) is long enough to make counting slugs easy for slug frequencies less than 0.1 Hz. For higher slug frequencies a RMS converter with a much shorter time constant is necessary.

Slugs have been counted for the flow conditions that produced the results of figure 5.17. The superficial gas velocity was kept five times the superficial water velocity. For three flow speeds the RMS time signal can be found in figure 5.21. The slug frequencies of this measurement series have been plotted as a function of the superficial water velocity in figure 5.22. Contrary to the flow-noise (see figure 5.17.) the slug frequency is linearly dependent of the superficial water velocity. This relation however is not in agreement with the results of Gregory and Scott (31).

They correlate the slug frequency f_{slug} with the superficial liquid and gas velocities and the internal diameter of the flow-line:

$$f_{slug} = 0.0226 \left(\frac{U_{sl}}{gD_i} \left(\frac{19.75}{U_{sl} + U_{sg}} + U_{sl} + U_{sg} \right) \right)^{1.2} \quad 5.1.$$

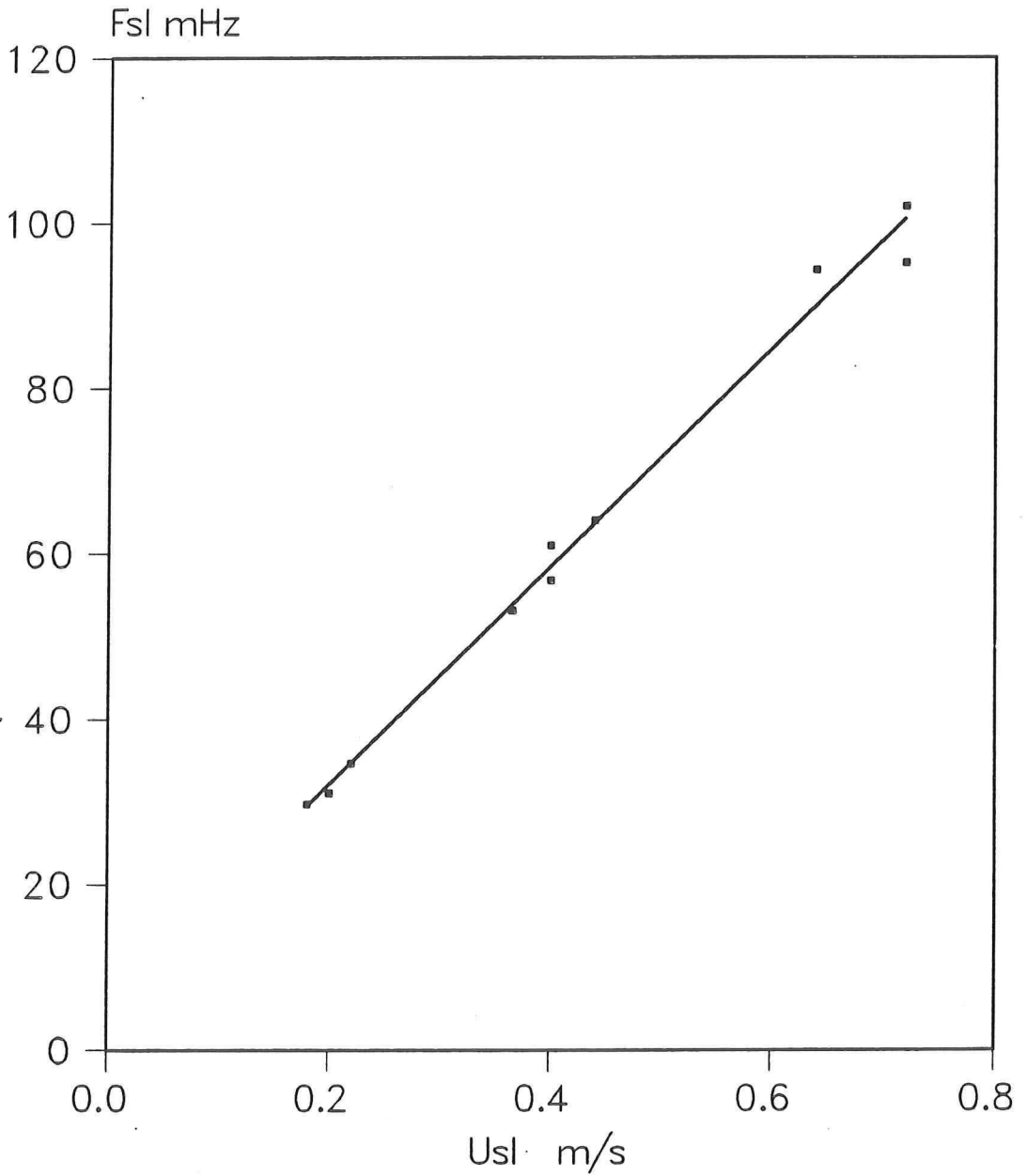


Figure 5.22. Slug frequency as a function of superficial water velocity for a 4 inch horizontal flow in the test-loop Donau. $U_{sg} = 5U_{sl}$ and the pressure was kept at 4 Bar.

For the above mentioned flow situation this is

$$f_{slug} = 0.021 (3.3 + 6 U_{sl}^2)^{1.2} \quad 5.2.$$

Apart from being a near quadratic relationship the calculated frequencies are ca twice the measured frequencies. This discrepancy is caused by the fact that Gregory and Scott measured slug frequencies for $D_i=1.9$ cm en 3.5cm. Besides that they only used one dimensionless parameter in the correlation.

It would be better to compare the results with the theoretical model of Taitel and Dukler (116) which uses five flow parameters. This model appears to agree quite well with the results of various authors.

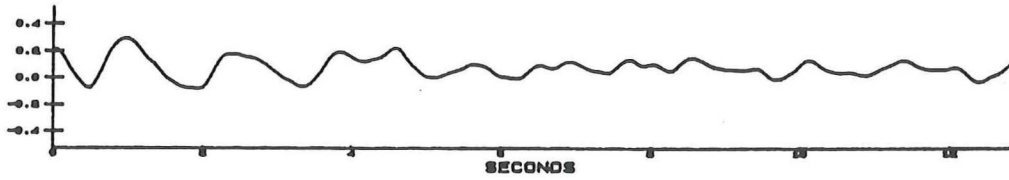
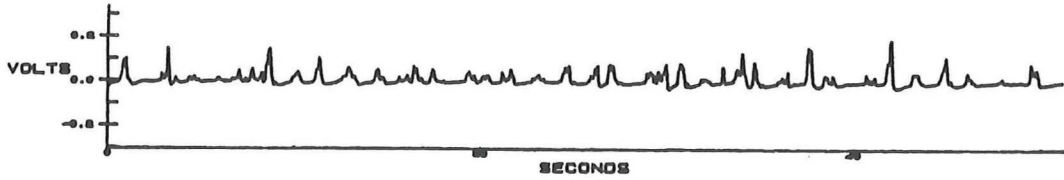
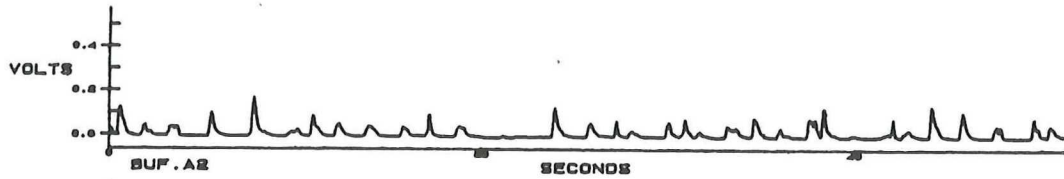
Another aspect is that using a large diameter ($D=10.82$ cm) flow line it is likely that the slug structures are determined by the geometry of the Donau. The two inch section, the vertical section or the three inch line has probably more influence on the slug formation than the Kelvin-Helmholtz instability. This phenomenon, called terrain slugging is most recently studied by Linga (117). As geometry-determined slug frequencies are usually lower and more regular than those determined by the Kelvin-Helmholtz instability, the geometry may be held responsible for the relatively low slug frequencies.

5.4.2. SLUG VELOCITY

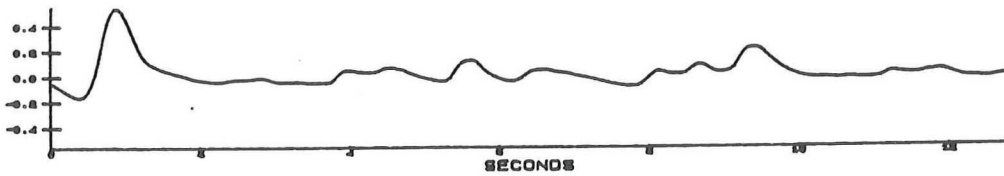
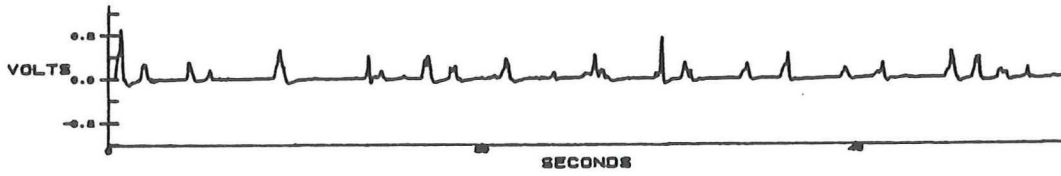
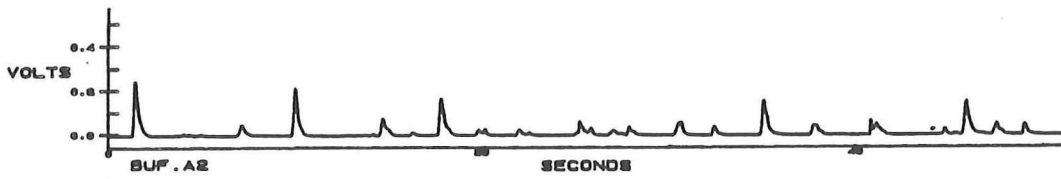
Using two accelerometers spaced out six meters the slug velocity has been determined by correlating the signals with the D6000. This has been done during the measurement of figure 5.17. Figure 5.23. shows both RMS-time signals obtained with a RMS converter with a 30 ms time constant for four flow speeds. The cross-correlations of the first with the second signal have been plotted as well. From the first peak in the cross-correlation the transition time of the slug from the first to the second accelerometer and the slug velocity is determined. The results have been plotted in figure 5.24.

The correlation between the slug velocity V_{slug} and the superficial water velocity is

$$V_{slug} = 10 U_{sl} \quad 5.3.$$

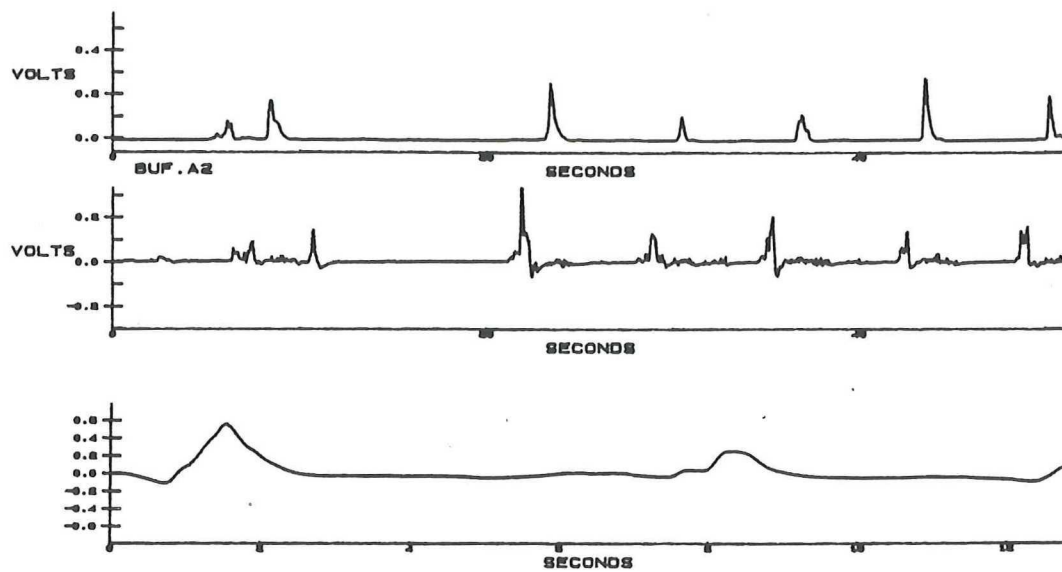


$U_{sl} = 0.8 \text{ m/s}$ $U_{sg} = 4.3 \text{ m/s}$

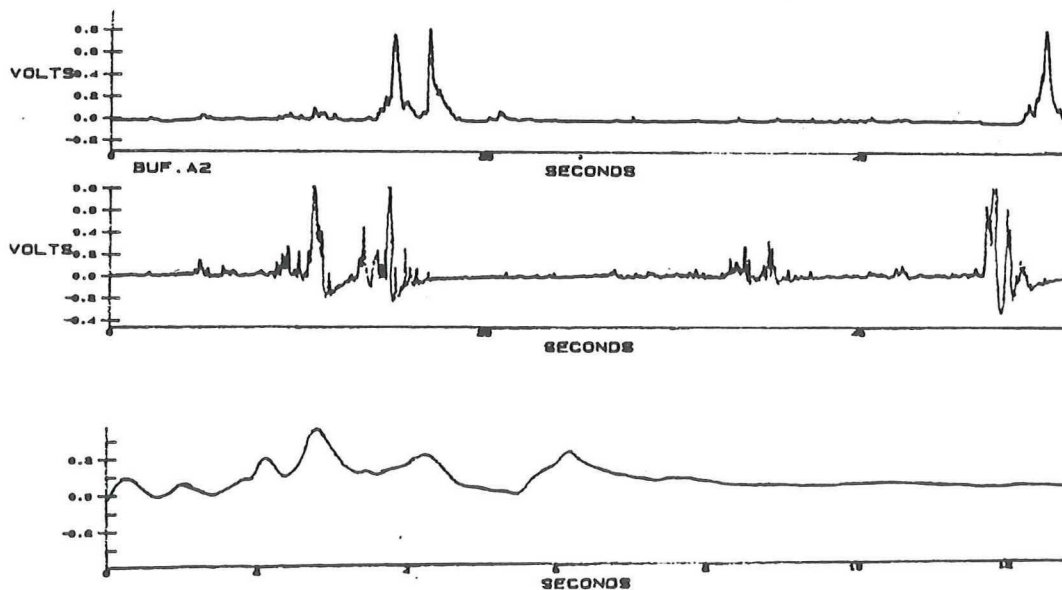


$U_{sl} = 0.64 \text{ m/s}$ $U_{sg} = 3.5 \text{ m/s}$

Figure 5.23a. Fast RMS-time ($\tau=30 \text{ ms}$) signal of two accelerometer spaced out 6 meters for a 4 inch horizontal slug flow in the test-loop Donau for two flowrates. The third graph in each case is the cross-correlation of the two signals. The pressure was kept at 4 Bar.



$U_{sl} = 0.4 \text{ m/s}$ $U_{sg} = 2.0 \text{ m/s}$



$U_{sl} = 0.18 \text{ m/s}$ $U_{sg} = 0.9 \text{ m/s}$

Figure 5.23b. Fast RMS-time ($\tau=30 \text{ ms}$) signal of two accelerometer spaced out 6 meters for a 4 inch horizontal slug flow in the test-loop Donau for two flowrates. The third graph in each case is the cross-correlation of the two signals. The pressure was kept at 4 Bar.

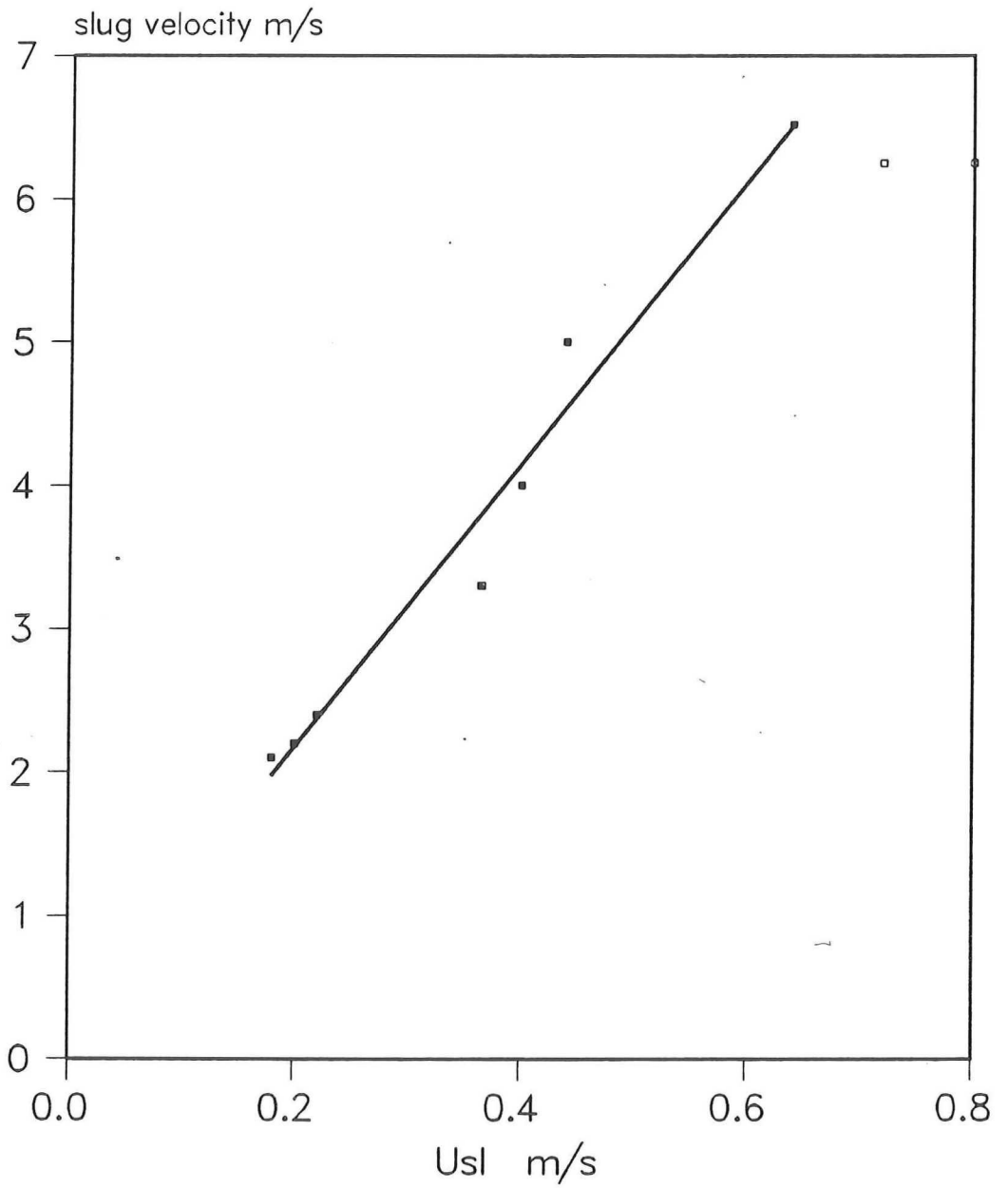


Figure 5.24. Slug velocity as a function of the superficial water velocity for a 4 inch horizontal slug flow in the test-loop Donau. $U_{sg} = 5U_{sl}$, and the pressure was kept at 4 Bar.

In literature the slug velocity is usually correlated with the no-slip velocity U_{ns} defined as

$$U_{ns} = U_{sl} + U_{sg} \tag{5.4}$$

In this case ($U_{sg} = 5U_{sl}$) formula 5.3. becomes

$$V_{slug} = 1.7 U_{ns} \tag{5.5}$$

The proportionality constant in 5.5. is not too different from the one found by Gregory and Scott (31), 1.35 or Hubbard and Dukler (26), 1.25.

For the two highest velocities the measured slug velocities do not agree with the correlation. This is caused by the fact that the consistency of the slugs structure over the distance between the two accelerometers declines with increasing slug velocity. This can be confirmed by looking at the time signals in figure 5.23.

So determining the optimum distance for measuring the slug velocity is a compromise between the consistency of the slug structure and the locality of the accelerometer. In literature a lot work can be found on slug speed and frequency measurement. They are all performed with an in-line transducer or a radiation attenuation system. In other words with a transducers determining a particular flow variable over a definite and very limited volume, area, or line segment in the flow. The tests performed with the accelerometer prove that the locality of the measurements can be sufficient to determine slug speed and frequencies.

5.4.3. OTHER SIGNAL PROCESSING

The signals obtained by the above mentioned transducers have been used to determine the flow regime by Jain ea (15), Boot ea (118), Annunziato ea (119), Jones (87), and Vince (11). As the accelerometer RMS-time signals resemble those signals there is good reason to believe that the accelerometer signal can be used for that purpose as well. Stimulated by the results from the Wolga and Donau measurements it seems worthwhile to extend the signal processing in such a way that besides the flow pattern a measure for the superficial liquid and gas velocities can be determined as well.

Considering a fast RMS time signal $f(t)$ of a specific band-width, the following statistical variables S_i to be determined as a function of the superficial velocities and other flow parameters are proposed:

$$S_1 = \frac{1}{T} \int_{-T}^0 f(t) dt \quad 5.6.$$

$$S_2 = \text{RMS} (f(t) - S_1) \quad 5.7.$$

$$S_3 = \text{RMS} \left(\frac{df(t)}{dt} \right) \quad 5.8.$$

$$S_4 = f_{\text{slug}} \quad 5.9.$$

$$S_5 = v_{\text{slug}} \quad 5.10.$$

S_6 = slug fraction, the percentage of time with a RMS signal above a certain level 5.11.

The last three variables should give enough information about the flow to constitute a basis for production surveillance in the case of low slug frequencies as encountered with gas-lift wells. The slug fraction S_6 together with the slug speed or the slug speed-related frequency gives enough information to determine the superficial velocities. For very long slugs gas bubbles are mainly dispersed in the head and the tail of the slug. In that case the slug fraction S_6 will have to be determined by counting the slugs.

For higher slug frequencies the accelerometer signal is not local enough to allow the accelerometers to be close enough to each other to safeguard the consistency of the slugs. In that case the first three variables could be of better use. Next to the normal average S_1 , an AC-average S_2 could be of use for instance to distinguish between bubbly flow (in extrema: $S_2=0$) and slug flow (in extrema: $S_1=S_2$). Variable S_3 also carries information about the frequency of the varying RMS value of the flow-noise.

As in many cases lacking sufficient theoretical predicting knowledge, the flow-noise signals call for an expert-system automatically selecting the optimum combination of variables for monitoring the production. Annunziato's (119) determination of the efficiency of the various statistical variables with respect to their ability to distinguish the various flow patterns is a good guide for designing such an expert system.

6. THEORETICAL BACKGROUND

As a clamp-on Production Surveillance Monitor could only work because of bubbles in the gas-liquid flow it is necessary to know more about the acoustic effects of bubbles in turbulent flow. As mainly water-air system were tested, this theory can determine whether an oil-gas system would yield the same results.

6.1. A BUBBLE AS SOUND SCATTERER, SINGLE BUBBLE

In "Sound & Sources of Sound" by A.P. Dowling and J.E. ffowcs Williams (35) the theory of a bubble as a sound scatterer is set out. (§ 2.2., 6.5., and 8.4.). In this paragraph the essence of those paragraphs is presented:

The case of one bubble in an infinite volume of liquid is considered. It is assumed that the gas in the bubble behaves as a perfect gas and is in a adiabatic state, meaning:

$$p_g a^{3\gamma} = p_{g0} a_0^{3\gamma} \tag{6.1.}$$

In which p_g is the pressure in the bubble, a the diameter of the bubble, γ the ratio of the constant pressure and constant volume specific heats of the gas in the bubble, and the suffix zero means the average value.

From this assumption the dependence between an incident harmonic pressure field and the resultant sound field scattered by the bubble is derived. Modelling the sound of a real turbulence as one induced by a quadrupole distribution and using this field as the incident field, the resultant scattered field is calculated. Assumed is that the distance between the quadrupole modelling the turbulence and the bubble is much less than the wavelength of the sound created by the quadrupole. In that case the amplification of the turbulent field by the bubble can be found: The intensity of the bubble-scattered field is bigger than the direct intensity of the quadrupole by a factor of order A_b :

$$A_b = \left(\frac{c}{\omega a}\right)^4 \left|1 - \frac{\omega_0^2}{\omega^2} \left(1 + \frac{i\omega a}{c}\right)\right|^{-2} \tag{6.2.}$$

in which c is the velocity of sound in the liquid, ω the angular frequency of the incident turbulent pressure field, and ω_0 the resonance angular frequency of the bubble:

$$\omega_0 = \left(\frac{3\gamma p_0}{\rho_0 a_0^2} + (3\gamma - 1) \frac{2\sigma}{\rho_0 a_0^3}\right)^{1/2} \tag{6.3.}$$

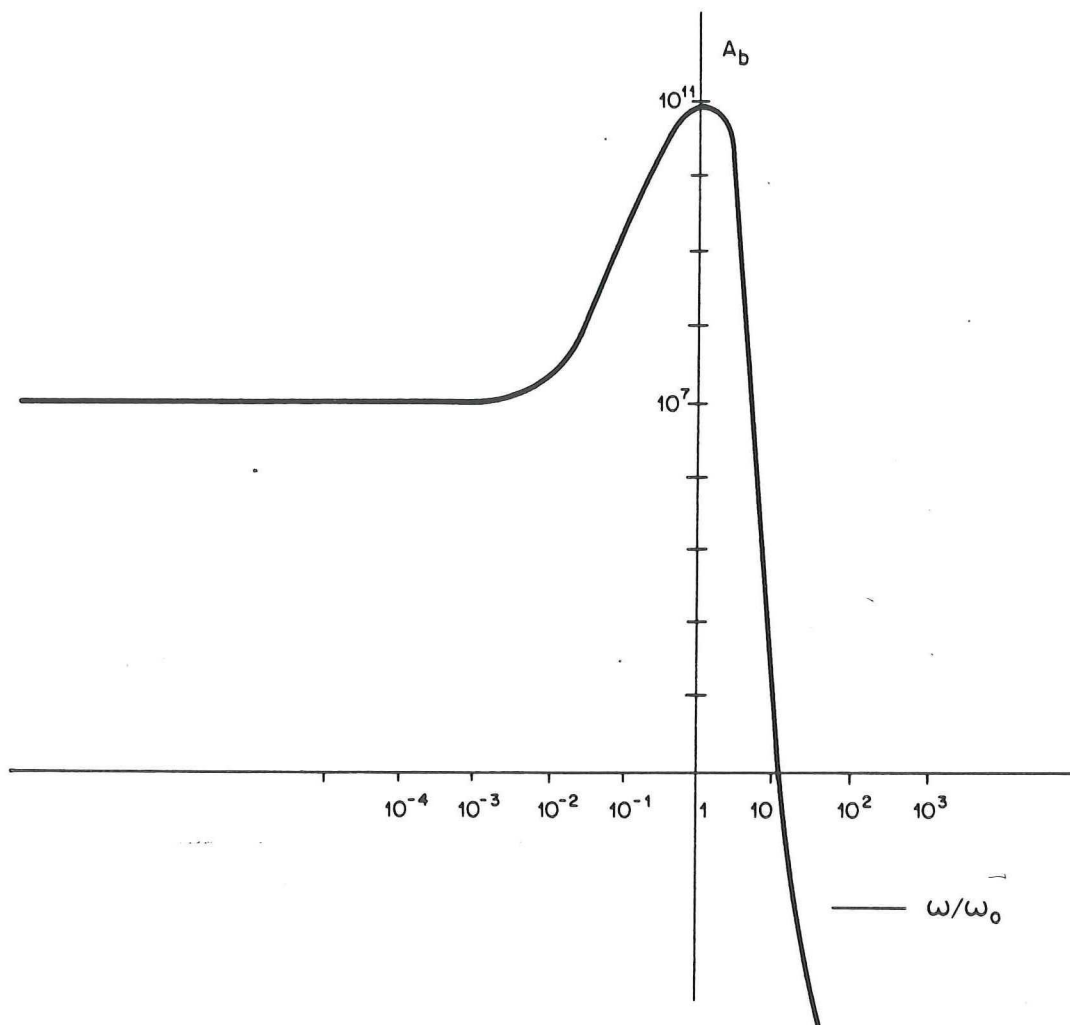


Figure 6.1. The factor by which the sound generated by a turbulent eddy is amplified by an air bubble as a function of the ratio of the incident frequency and the resonant frequency of the bubble for 1 Bar.

in which p_0 is the mean pressure in the liquid, σ the interfacial tension, and ρ_0 the average density of the liquid.

The resonant frequency is only marginally influenced by the interfacial tension. It can be neglected when

$$\sigma \ll \frac{3\gamma}{2(3\gamma-1)} p_0 a_0 \quad 6.4.$$

Even in the worst case ($\sigma=0.07$ N/m, $p_0=10^5$ N/m²) an aberration in the resonance frequency of 5% or more is only introduced for bubbles smaller than 10 μ m diameter. So equation 6.3. can be simplified to

$$\omega_0 = \left(\frac{3\gamma p_0}{\rho_0} \right)^{\frac{1}{2}} \frac{1}{a_0} \quad 6.5.$$

This is similar to a mass-spring system where the density of the liquid represents the mass and the compressibility of the gas represents the spring.

Dowling states that "Low frequency bubble vibration can be subject to sufficient heat transfer from the gas to the liquid that the gas motion is effectively isothermal in which case the foregoing analysis can be made to apply formally setting γ equal to unity in the various formulae." He does not specify "low frequency", but as the motion must be between isothermal ($\gamma \rightarrow 1$) and adiabatic ($\gamma_{\text{air}}=1.4$) the maximum error introduced by assuming $\gamma=1.4$ is 25% for ω_0^2 and 13% for ω_0 , which in this project is not of much influence.

Now for water and air we arrive at

$$\omega_0 = 0.06 \frac{\sqrt{p_0}}{a_0} \quad \text{or} \quad f_0 = 0.01 \frac{\sqrt{p_0}}{a_0} \quad 6.6.$$

So for an average pressure of 10^5 N/m² the resonance frequency f_0 lies at 30 kHz for $a_0=0.1$ mm and at 3 kHz for $a_0=1$ mm.

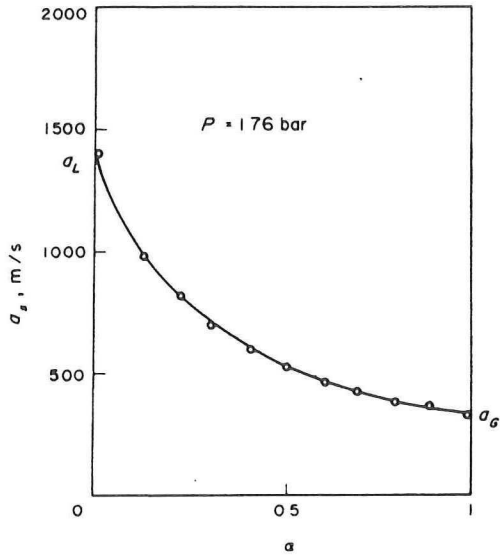
The amplification factor A_b varies enormously with the ratio of the incident frequency and the bubble resonant frequency. Figure 6.1. shows this dependency for $p_0=10^5$ N/m², and $c=1500$ m/s (i.e. from formula 6.6. : $\omega_0 a_0/c = 0.014$). Three extreme cases can be considered:

$$\omega \gg \omega_0 \quad \rightarrow \quad A_b = 0 \quad 6.7.$$

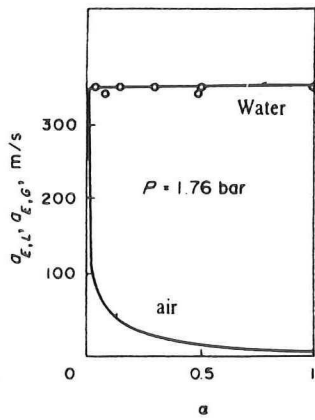
$$\omega = \omega_0 \quad \rightarrow \quad A_b = \left(\frac{c}{\omega_0 a_0} \right)^6 = 10^{11} \quad 6.8.$$

$$\omega \ll \omega_0 \quad \rightarrow \quad A_b = \left(\frac{c}{\omega_0 a_0} \right)^4 = 10^7 \quad 6.9.$$

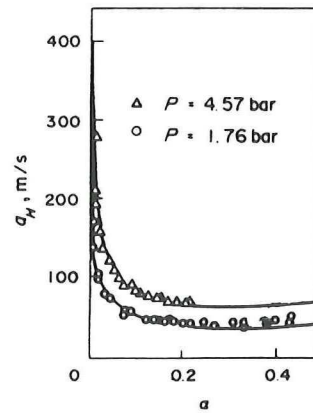
So even for frequencies below the resonance frequency of the bubble the amplification factor is considerable. This explains the importance of bubbles as sound scatterers in a turbulent pressure field



SLUG FLOW



STRATIFIED FLOW



HOMOGENEOUS FLOW

Figure 6.2. The dependence of the velocity of sound as a function of the void fraction for a slug, stratified, and homogeneous flow as determined by Nguyen (22).

6.2. A BUBBLE AS SOUND SCATTERER, DISPERSED BUBBLES

So far only the case of one bubble in an infinite volume of liquid has been looked into. In a gas-liquid flow this is very rarely the case. If we consider a single bubble in a homogeneous mixture of air bubbles dispersed in water, the density and the speed of sound of the surrounding fluid is less than the density and speed of sound of pure water. For the angular resonance frequency (formula 6.5.) only the density is of any importance. According to Gregory et al (115) the gas fraction in a slug is less than 50 % when the total of the superficial velocities is less than 10 m/s. For bubbles, 50% by volume dispersed in water the density will only halve and the resonance frequency will be 40% higher. So the order of magnitude of the resonance frequency will be similar to that in case of a single bubble in a pure liquid.

The amplification factor A_b however will be greatly influenced by the presence of more bubbles, as the speed of sound decreases sharply with a small increase of the volumetric air fraction. Figure 6.2. shows the dependence of the speed of sound as a function of the gas fraction for the case of stratified flow, slug flow, and dispersed bubble flow, as determined by Nguyen et al (22). In the case of dispersed bubble flow the speed of sound may be as low as 20 m/s for atmospheric pressure. Supposing the bubble amplification factor is still determined by formula 6.2. the amplification will be unity. This might well be the reason that for a certain void fraction more air does not create more high frequency sound (cf paragraph 5.1.6.).

Another effect of the gas entrainment in the liquid is the attenuation of the sound. As the propagation of sound decreases with a higher gas fraction so does the transmitted sound energy. Davis (110) has experimentally confirmed that the attenuation of incident pressure fluctuations along a two-phase pipe flow increases with increasing void fraction and increasing frequency. Because of this the signal from the accelerometer is only related to a certain region of the flow. The dimension of this region depends on the attenuation of the sound and consequently on the gas fraction and flow-pattern. As a result sound caused by valves and other disturbances will not interfere with the flow-noise if not too close to the accelerometer. Unfortunately sound propagating through the pipe-wall will not be attenuated, so kicking the pipe will decrease the signal to noise ratio.

The decrease in speed of sound is also important for the mode of sound propagation through the gas-liquid mixture in the pipe. The wavelength of the sound is defined as the ratio of the speed of sound in the mixture and the frequency of the sound-source. Dowling ea (35) shows in chapter 3.2. that sound with a wavelength larger than twice the diameter propagates only in the plane-wave mode as the higher modes are evanescent. Therefore those waves excite two opposed accelerometers identically. Smaller wavelengths result in higher mode (three dimensional) waves having an uncorrelated effect on both transducers.

6.3. TURBULENT EDDIES

Until now the sound scattering effect of bubbles has been talked about. It is also necessary to have turbulent eddies which pressure fields can be scattered. Well known is Kolmogoroff's theory of local isotropic turbulence (for a single-phase high Reynolds number flow) as described for instance by Levich (113).:

The size of the largest eddy is in the order of the diameter of the pipe. This eddy creates several smaller eddies which break up in turn. This goes on until such an eddy scale is reached that the viscous and inertial forces are in equilibrium, i.e. the corresponding Reynolds number is approximately equal to unity. For smaller eddies viscous effects will overcome turbulent effects and the eddies will dissipate their energy.

Taking the superficial velocity as the characteristic velocity the frequency of the largest eddy is U_{sl}/D_i . This compares quite well with the Wolga pressure signal shown in figure 5.4.: $U_{sl}=1.45$ m/s, $D_i=7$ cm, so the lowest frequency should be ca 20 Hz, which is about the lowest frequency in the pressure signal.

According to the Kolmogoroff theory (see Levich (113)) the length scale of the eddies with their viscous and inertia forces in balance, λ_k is determined by

$$\lambda_k = (\eta/\rho\epsilon)^{1/4} \tag{6.10.}$$

in which η is the dynamic viscosity of the liquid, and ϵ the energy dissipated by the turbulent flow per unit mass and per unit time. This dissipated power can be calculated from

$$\epsilon = \frac{\Delta p \cdot Q}{A \Delta l \cdot \rho} \tag{6.11.}$$

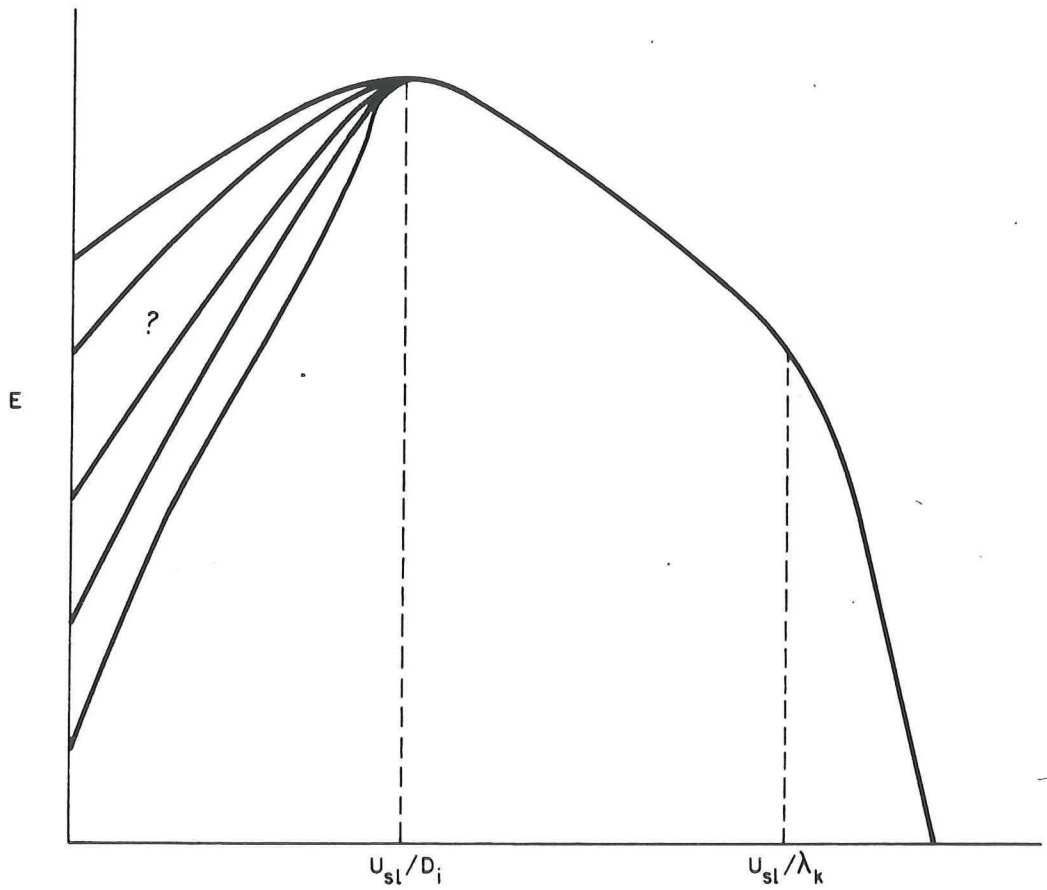


Figure 6.3. Sketch of the dependency of the eddie energy as a function of the eddie caused pressure fluctuation frequency.

in which Δp is the pressure drop over a length Δl , Q the volume rate, and A the area of the cross section of the pipe. This is equal to

$$\epsilon = \frac{\Delta p}{\Delta l} \frac{U_{sl}}{\rho} \tag{6.12}$$

Using the Blasius expression for the turbulent friction factor the pressure drop is

$$\frac{\Delta p}{\Delta l} = 0.316 \text{Re}^{-1/4} \frac{1}{2} \rho U_{sl}^2 D_i^{-1} \tag{6.13}$$

in which Re is the Reynolds number. Now ϵ becomes

$$\epsilon = 0.158 \text{Re}^{-1/4} \frac{U_{sl}^3}{D_i} \tag{6.14}$$

For a water flow of 1 m/s in a 10 cm internal diameter pipe the specific power consumption will be $\epsilon=0.1$ W/kg so the Kolmogoroff length scale will be (formula 6.10) $\lambda_k=56\mu\text{m}$. Again taking U_{sl} as the characteristic velocity the resultant frequency is 18 kHz. As the pressure transducer has an effective diameter of ca 1cm and the pressure amplitude caused by such small eddies will be very low such small eddies will not be detected by the transducer. (cf Corcos, (36): resolution of pressure in turbulence).

Figure 6.3. presents a rough sketch of the dependency of the eddy energy on the eddy-caused-frequency. The energy between U_{sl}/D_i and U_{sl}/λ_k is declining with frequency as the energy is distributed among the smaller and more numerous eddies. At higher frequency the eddies will start dissipating and their energy will decline even more. About the frequency less than U_{sl}/D_i not much can be said as the turbulence responsible for those frequencies will be determined by the geometry of the total flow-line.

The main relevant conclusion from this discussion about the energy distribution is that the turbulent frequency band is broad enough to to generate pressure fields in the appropriate frequency to be modulated by the bubbles. In gas-liquid flow the same general conclusion will apply as the scale of turbulence in the liquid will have the same order of magnitude.

6.4. BUBBLE FORMATION

Finally the formation of bubbles in the turbulent gas-liquid flow has to be looked into. Levich (113, chapter 89) derives a criterion for bubble brake-up in turbulent liquid flow by balancing the capillary pressure of a bubble with the dynamic pressure difference over the bubble. This pressure difference is caused by the velocity difference of the turbulent eddies

surrounding the bubble. Using the Kolmogoroff homogeneous turbulence model he finds a critical bubble diameter a_{cr} above which the bubble will break up:

$$a_{cr} = 2 L^{2/3} \left(\frac{\sigma}{k_f \rho_l} \right)^{3/5} U^{-6/5} \left(\frac{P_l}{\rho_g} \right)^{1/5} \quad 6.15.$$

in which L is the scale of the turbulence, in this case the internal diameter D_i . k_f is a constant equal to 0.5, and U is the fluid velocity. For homogeneous flow the no-slip velocity $U_{sn} = U_{sl} + U_{sg}$ is to be used as the fluid velocity. For determining the bubble scale in slugs the fluid speed should be replaced by slug speed, which is (see chapter 5.4.2.) proportional to the no slip velocity.

The mechanism opposing the effects of bubble fracture is coalescence. This is a very complicated mechanism determined by the liquid viscosity, the interfacial tension and the shear forces. Also the structure of the flow is of importance, for instance in an undispersed bubbly flow in the Wolga it has been observed that coalescence rarely occurs. This is probably caused by the fast rotation of the bubbles between the pipe wall and the fast flowing liquid. This rotation prevents the liquid layer separating the bubbles to deplete and coalescence will not take place. Certain additives like salt and surfactants influence coalescence often without even influencing the static interfacial tension.

As after coalescence the bubbles will probably immediately break up again by the turbulent eddies, the largest number of bubbles is expected to have a diameter in the order of the critical diameter as formulated in 6.15. Comparing the criterion with the pictures of the bubbles in the Wolga, (figure 5.6.), the predicted bubble diameter agrees quite nicely with the observed bubble diameter. For $L=D_i=0.07$ m, $\sigma=0.05$ N/m, $k_f=0.5$, $\rho_l=10^3$ kg/m³, $\rho_g=2$ kg/m³ ($P=180$ kN/m²), and $U=1.7$ m/s the critical diameter works out to be 2.5 mm. In the second picture of figure 5.6. corresponding with the flow conditions as mentioned, the average diameter is ca 3mm. In the first picture of the same figure the bubbles are three times smaller. This is caused by the fact that since being introduced into the system no coalescence has taken place because of the small number of bubbles. So in that case the bubble is smaller than the critical diameter already and is consequently not determined by the turbulence but by the initial diameter.

A second criterion is the balance between turbulent forces and buoyancy forces determining whether the bubbles will be dispersed or floating on top of the liquid. This has been modelled by Taitel and Dukler (30). At first approximation the difference in sound scattering between dispersed and undispersed bubbles is thought to be of little significance, so this criterion has not been looked into further.

So if in future flow noise of systems other than water-air will be investigated the main criterion to look into will probably be 6.15. For oil-gas mixtures the main difference will be caused by the much lower interfacial tension (down to 10^{-3} N/m) resulting in much smaller bubbles.

6.5. THEORY: CONCLUDING REMARKS

At the start of the project it was planned to devise a scheme to show the relationship between the flow parameters on the one side and the bubble formation, turbulence, and bubble resonance and consequently the flow noise on the other side. From the theory discussed it is clear that the parameters influencing the flow-noise generation are mutually influential in a complex way. Unfortunately it is impossible to distill a simple flow-noise model from this multitude of influences. So the theory in this chapter does not pretend to give a complete prediction of the flow-noise as a function of the various flow-parameters but tries to clarify the mechanism responsible for the possibility of detecting flow-related noise outside the pipe.

From this theory it can be concluded that an oil-gas system will not behave fundamentally different with respect to the flow-noise generation than the tested air-water systems.

7. CONCLUSIONS AND RECOMMENDATIONS

It has been found that gas-liquid flow-noise detected with a clamp on accelerometer contains information about the flow. Under certain circumstances the average of the RMS value of the high pass (ca 2kHz) filtered flow-noise is such a function of the superficial gas and liquid velocities that it can indicate the superficial liquid velocity within 10%. This has been found for a horizontal flow of water and air, for a horizontal flow of water-oil emulsion ($\eta=200$ kg/ms) with air, and for a vertical down flow of water and air. Unfortunately the flow-noise is also dependent on the geometry of the test-loop and the line-pressure regulation.

The detected flow-noise has been found to be only related to a limited volume of gas-liquid mixture. For certain conditions this signal locality is sufficient to measure slug frequencies and slug speeds, which proves to be a good indication of the superficial velocities if the ratio of the superficial gas and liquid velocities is known. In general the flow-noise signal is sufficiently similar to the various in-line transducer signals, (such as void fraction meters and differential pressure transducers), to be used as a flow pattern indicator.

As the flow-noise itself has a near white-noise frequency distribution, the real flow information is found in the RMS value of the flow noise. This agrees well with the "modulation idea" that the in-line pressure fluctuation are modulated by bubbles, and that RMS value (a kind of demodulated signal) carries the same information as the pressure fluctuations.

At present various researchers e.g. Toral (Imperial College, Petroleum Engineering Multi-phase Flow Laboratories) are working on an improved signal processing of the in-line measured signals to increase the resolution of the flow-pattern recognition. In other words the purpose in those studies is to find an indication of the superficial gas and liquid velocities.

- Putting together:
1. the resemblance of in-line transducer and accelerometer signals, because of sufficiently local measurement of the accelerometer,
 2. the efforts of various researchers to derive an indication of the superficial gas and liquid velocities from those in-line transducer signals,
 3. the fact that from the theory no reason has been found that clamp-on flow-noise measurement of an oil-gas flow would be fundamentally different from an air-water flow,

it is concluded that further work on the statistical processing of clamp-on acquired gas-liquid flow-noise is worth the effort.

So it is recommended to devise a computer program determining certain statistical parameters (as specified in Chapter 5.4) as a function of the various flow parameters. For various flow situations a digitized recording (for instance with the available PDP-Minc-23 computer) should be made of a fast ($\tau=30$ ms) RMS value of the flow-noise, to be analysed by the computer program. The efficiency of the statistical variables in their ability to determine the flow pattern and, more specifically the superficial velocities should then be assessed.

Initially the flow-noise of the Donau should be recorded and analysed. When it has been proved that the analysing program is working properly a recording of a producing pipe-line should be made. It can than be checked whether the oil-gas system produces sufficient flow-noise. In addition it gives the opportunity to process flow-noise from low frequency but very long slugs.

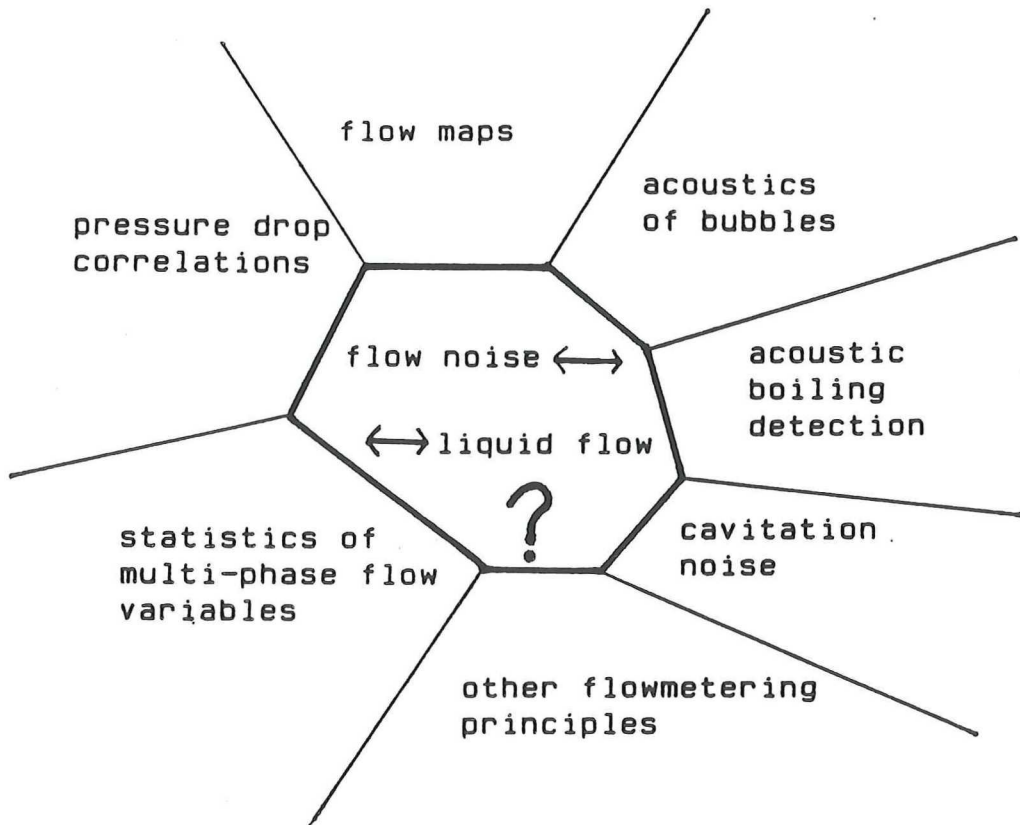


Figure 8.1. Schematic representation of the literature related to the subject of this study.

8. LITERATURE

In literature nothing has been found on the quantitative analysis of clamp-on acquired gas-liquid flow-noise. Much however has been published on related subjects. For instance a lot of work has been done on acoustic boiling detection especially for cooling systems of nuclear reactors (e.g. De (71)). Another example is the work of Sami (34) on the relation between pressure fluctuation and flow velocity in single-phase flow. In figure 8.1. other closely related fields of interest are schematically presented.

With the systems Compendex and Inspec a search for literature on, or closely related to the field of interest of the present study has been carried out. A selection of the articles found by the computer combined with literature found by other means was collected and categorised. To facilitate further work, not only the references used in this report but all the collected literature is listed below.

Firstly the references are listed by the numbers corresponding to the references in this report. For cross reference and further work the list is printed again in alphabetical order with abbreviated titles. And thirdly, they are presented by topic. The topic abbreviations are:

AC acoustics
BU theory on acoustics of gas bubbles
DE flowmetering device
GE general
MA flow pattern map
OT other literature
PS production surveillance monitor
ST statistics
TH theory

- 001 OOSTEROM, M.H.VAN; R.G.SMEENK
ISEFL RIJSWIJK
NEDERLANDS TIJDSCHRIFT VOOR NATUURKUNDE, A52(2)1986
- 002 JAMIESON, A.W.; R.G. SMEENK; P.B. VRIEZEN
MULTI-PHASE FLOW MEASUREMENTS AT PRODUCTION PLATFORMS
PETROLEUM REVIEW, PUBLICATION 737, NOV 1985
- 003 SKUDRZYK, E.J.; G.P. HADDLE
NOISE PRODUCTION IN A TURBULENT BOUNDARY LAYER BY SMOOTH AND
ROUGH SURFACES
J. OF ACOUST. SOC. OF AMERICA, VOL 32, NO 1, JAN 1960
- 004A HENDRINKS, J.J.R.; G. SMILDE
DETECTIE VAN RESTEREND WANDDIKTE MET EEN CAPACITIEVE
VERPLAATSING OPNEMER
EINDONDERZOEK TN-THDELFT
- 004B HERWEIJER, E.J.J.
ONDERZOEK NAAR DE BRUIKBAARHEID VAN CAPACITIEVE DETECTIE BIJ DE
BEPALING VAN WANDSLIJTAGE IN PIJPEN
EIND ONDERZOEK TN-THDELFT
- 005 SMITH, J.M.; I. BOUWMANS
MEERFASE STROMING EN WARMTE OVERDRACHT BIJ GASONTSNAPPINGEN
ONDER WATER
FUEL IN VOORB FT-TN-THDELFT, APRIL 86
- 007 PATTERSON, M.M.
A FLOWLINE MONITOR FOR PRODUCTION SURVEILLANCE
SOCIETY OF PETROLEUM ENGINEERS OF AIME, SPE 5769, 1976
- 008 ALFORD, E.J.; M.M. PATTERSON; F.A. WOMACK
DEVELOPMENT AND FIELD EVALUATION OF THE PSM
J OF PETROLEUM TECHNOLOGY, FEBR 1978
- 009 MATSUI, G.
IDENTIFICATION OF FLOW REGIMES IN VERTICAL GAS-LIQUID TWO-PHASE
FLOW USING DIFFERENTIAL PRESSURE FLUCTUATIONS
INT. J. MULTIPHASE FLOW, VOL 10, NO 6, PP711-720, 1984
- 010 TUTU, N.K.
PRESSURE DROP FLUCTUATIONS AND BUBBLE-SLUG TRANSITION IN A
VERTICAL TWO PHASE AIR-WATER FLOW
INT. J. MULTIPHASE FLOW VOL 10, NO 2, PP 211-216, 1984
- 011 VINCE, M.A.; R.T. LAHEY JR
ON THE DEVELOPMENT OF AN OBJECTIVE FLOW REGIME INDICATOR
INT J. MULTIPHASE FLOW VOL 8 NO 2 PP 93-124, 1982
- 012 TORAL, H
A STUDY OF THE HOT-WIRE ANEMOMETER FOR MEASURING VOID FRACTION IN
TWO PHASE FLOW
J PHYS. E:SCI. INSTRUM VOL 14 1981
- 013 MAKHOUL, J
LINEAR PREDICTION: A TUTORIAL PREVIEW
PROCEEDINGS OF THE IEEE VOL 63 NO 4, APRIL 1975
- 015 JAIN, P.K.; R.P. ROY
STOCHASTIC CHARACTERISATION OF VAPOR FRACTION AND WALL PRESSURE
FLUCTUATIONS IN BOILING FLOWS
INT.J. MULTIPHASE FLOW VOL 9 NO 3 PP 463-489 1983
- 016 BRUEL & KJAER
VIBRATION TRANSDUCERS AND ACCESSORY EQUIPMENT
SPECIFICATIES
- 021 OHLMER, E.; T.FORTESCUE; W.RIEBOLD; B. BORS; J. IMMINK; U. WESSER
TWO PHASE FLOW IDENTIFICATION BY CALIBRATION WITH STOCHASTIC
PARAMETERS
IUTAM SYMPOSIUM, MEASURING TECHNIQUES IN GAS/LIQUID TWO PHASE
FLOWS, NANCY. FRANCE 1983; SPRINGER VERLAG
- 022 NGUYEN, D.L.; E.R.F. WINTER; M. GREINER
SONIC VELOCITY IN TWO-PHASE SYSTEMS
INT. J. MULTIPHASE FLOW VOL 7 PP 311-320, 1981
- 023 MANDHANE, J.M.; G.A. GREGORY; K. AZIZ
A FLOW PATTERN MAP FOR GAS-LIQUID FLOW IN HORIZONTAL PIPES
INT J. MULTIPHASE FLOW VOL 1 PP 537-553, 1974
- 024 CHESTERS, A.K.
STROMING EN WARMTE OVERDRACHT III
DICTAAT TH-DELFT, BW75
- 025 BRILL, J.P.
TWO PHASE FLOW IN PIPES
FLUID FLOW PROJECTS TULSA/BHRA MAART 1985

026 HUBBARD, M.G.; A.E. DUKLER
THE CHARACTERIZATION OF FLOW REGIMES FOR HORIZONTAL TWO-PHASE
FLOW; 1. STATISTICAL ANALYSIS OF WALL PRESSURE FLUCTUATION
PROCEEDINGS OF THE 1966 HEAT TRANSFER & FLUID MECHANICS INSTITUTE
UN. OF ST. CLARA, CALIFORNIA, JUNE 1966; ED. SAAD & MILLER

027 ANNUNZIATO, M.; G. GIRALDI
STATISTICAL METHODS TO IDENTIFY TWO-PHASE REGIMES; EXPERIMENTAL
RESULTS FOR VERTICAL LARGE DIAMETER TUBES
2ND INTERNATIONAL CONFERENCE ON MULTI PHASE FLOW, LONDON JUNE 1985

028 HINZE, J. O.
TURBULENCE
MCGRAW HILL BOOK COMPANY, 2ND EDITION, 1975

030 TAITEL, Y.; A.E. DUKLER
A MODEL FOR PREDICTING FLOW REGIME TRANSITIONS IN HORIZONTAL AND
NEAR HORIZONTAL GAS-LIQUID FLOW
AIChE JOURNAL, VOL 22 NO 1 PP 47 JAN 1976

031 GREGORY, G. A.; D.S. SCOTT
CORRELATION OF LIQUID SLUG VELOCITY AND FREQUENCY IN HORIZONTAL
COCURRENT GAS-LIQUID SLUG FLOW
AIChE JOURNAL VOL 15, NO 6, PP 933, NOV 1969

032 GOVIER, G. W.; M. M. OMER
THE HORIZONTAL PIPELINE FLOW OF AIR-WATER MIXTURES
CAN. J. OF CHEM. ENG., JUNE 1962

033 ABESSEKERA, S.A.; M.S. BECK
LIQUID FLOW MEASUREMENT BY CROSS CORRELATION OF TEMPERATURE
FLUCTUATIONS
TRANS OF THE INST OF MEASUREMENT AND CONTROL, VOL 5, NO 11
P 435, NOV 1972

034 SAMI, S.M.; A.A. LAKIS
SPECTRAL ANALYSIS OF WALL-PRESSURE FLUCTUATIONS IN TURBULENT
TWO-PHASE FLOW
J ACOUST. SOC. AM. 80 (5), NOV 1986

035 DOWLING, A.P.; J.E. FLOWERS WILLIAMS
SOUND AND SOURCES OF SOUND
ELLIS HORWOOD LTD, JOHN WILEY & SONS

036 CORCOS, G.M.
RESOLUTION OF PRESSURE IN TURBULENCE
JOURNAL OF THE ACOUSTICAL SOC OF AM VOL 35 NO 1 FEB 1963

037 ARNAUDEAU, M.; P. ROUSSET
PROCESS AND DEVICE FOR MEASURING THE FEED OF LIQUID AND GASEOUS
PHASES OF A TWO PHASE FLUID DURING FLOW
UK PATENT APPLICATION 8432800, 31-12 1984

038 CRAWFORD, T.J.; C.B. WEINBERGER; J. WEISMAN
TWO-PHASE FLOW PATTERNS AND VOID FRACTIONS IN DOWNWARD FLOW;
PART I: STEADY STATE FLOW PATTERNS
INT. J. MULTIPHASE FLOW VOL 11 NO 6 PP 761-782 1985

039 ABRIOLO, L.M.; W.G. GRAY
ON THE EXPLICIT INCORPORATION OF SURFACE EFFECTS INTO THE
MULTIPHASE MIXTURE BALANCE LAWS
INT. J. MULTIPHASE FLOW VOL 11 NO 6 PP 837-852 1985

040 BEYERLEIN, S.W.; R.K. COSSMANN; H.J. RICHTER
PREDICTION OF BUBBLE CONCENTRATION PROFILES IN VERTICAL TURBULENT
TWO-PHASE FLOW
INT. J. MULTIPHASE FLOW VOL 11 NO 5 PP 629-641 1985

041 HASHIZUME, K.; H. OGIWARA; H. TANIGUCHI
FLOW PATTERN, VOID FRACTION, PRESSURE DROP OF REFRIGERANT 2 PHASE
FLOW IN A HORIZONTAL PIPE-II; ANALYSIS OF FRICTIONAL PRESSURE DROP
INT. J. MULTIPHASE FLOW VOL 11 NO 5 PP 643-658 1985

042 GUNN, D.J.; H.H. AL-DOORI
THE MEASUREMENT OF BUBBLE FLOWS IN FLUIDISED BEDS BY ELECTRICAL
PROBE
INT. J. MULTIPHASE FLOW VOL 11 NO 4 PP 535-551 1985

043 BISWAS, JAYDEEP; P.F. GREENFIELD
TWO PHASE FLOW THROUGH VERTICAL CAPILLARIES-EXISTENCE OF A
STRATIFIED FLOW PATTERN
INT. J. MULTIPHASE FLOW VOL 11 NO 4 PP 553-563 1985

044 MUKHERJEE, H; J.P. BRILL
EMPIRICAL EQUATIONS TO PREDICT FLOW PATTERNS IN TWO PHASE
INCLINED FLOW
INT. J. MULTIPHASE FLOW VOL 11 NO 3 PP 299-315 1985

045 WELLE, R. VAN DER
VOID FRACTION, BUBBLE VELOCITY AND BUBBLE SIZE IN TWO PHASE FLOW
INT. J. MULTIPHASE FLOW VOL 11 NO 3 PP 317-345 1985

046 THORLEY, A.R.D.; D.C. WIGGERT
THE EFFECT OF VIRTUAL MASS ON THE BASIC EQUATIONS FOR UNSTEADY
ONE DIMENSIONAL HETEROGENEOUS FLOWS
INT. J. MULTIPHASE FLOW VOL 11 NO 2 PP 149-160 1985

047 MCOUILLAN, K.W.; P.B. WHALLEY
FLOW PATTERS IN VERTICAL TWO-PHASE FLOW
INT. J. MULTIPHASE FLOW VOL 11 NO 2 P 161-175 1985

048 BARNEA, D; N. BRAUNER
HOLDUP OF THE LIQUID SLUG IN TWO PHASE INTERMITTANT FLOW
INT J MULTIPHASE FLOW VOL 11 NO 1 P 43-49 1985

049 DAVIS, M.R.; B. FUNGTAMASAN
LARGE SCALE STRUCTURES IN GAS-LIQUID MIXTURE FLOWS
INT J MULTIPHASE FLOW VOL 10 NO 6 P 663-676 1984

050 DALLMAN J.C.; J.E. LAURINAT; T.J. HANRATTY
ENTRAINMENT FOR HORIZONTAL ANNULAR GAS-LIQUID FLOW
INT J MULTIPHASE FLOW VOL 10 NO 6 P 677-690 1984

051 CLARK, N.N.; R.L.C. FLEMMER
A METHOD FOR DETERMINING FRICTIONAL PRESSURE LOSSES IN TWO-PHASE
FLOW
INT J MULTIPHASE FLOW VOL 10 NO 6 P 737-738 1984

052 HARDY, J.E.; J.O. HYLTON
ELECTRICAL IMPEDANCE STRING PROBESFOR TWO-PHASE VOID AND VELOCITY
MEASUREMENTS
INT J MULTIPHASE FLOW VOL 10 NOS P 541-556 1984

053 SINAI, Y.L.
ACOUSTIC SPEEDS FOR TRATIFIED TWO-PHASE FLUIDS IN
RECTANGULAR DUCTS
INT J MULIPHASE FLOW VOL 10 NO 4 P 415-423 1984

054 PROSPERETTI, A.; A.V. JONES
PRESSURE FORCES IN DISPERSE TWO-PHASE FLOW
INT J MULTIPHASE FLOW VOL 10 NO 4 P 425-440 1984

055 KVERNOLD, O.;V. VINDOY; T. SONTVEDT;A. SAASEN; S. SELMER-OLSEN
VELOCITY DISTRIBUTION IN HORIZONTAL SLUG FLOW
INT J MULTIFHASE FLOW VOL 10 NO 4 441-457 1984

056 AZZOPARDI, B.J.;
THE EFFECT OF A SIDE ARM DIAMETER ON THE TWO PHASE FLOW SPLIT
AT A "T" JUNCTION
INT J MULTIPHASE FLOW VOL 10 NO 4 P 509-512

057 KAMATH, P.S.; R.T. LAHEY JR.; D.R. HARRIS
MEASUREMENT OF VIRTUAL MASS AND DRAG COEFFICIENT OF A DISK
OSCILLATING SINUSOIDALLY IN A TWO-PHASE MIXTURE
INT J MULTIPHASE FLOW VOL 10 NO3 P 249-272 1984

058 SPEDDING, P.L.; J.J.J. CHAN
HOLDUP IN TWO PHASE FLOW
INT J MULTIPHASE FLOW VOL 10 NO 3 P 307-339 1984

059 MATSUMOTO, S.; M. SUZUKI
STATISTICAL ANALYSIS OF FLUCTUATIONS OF FROTH PRESSURE ON
PERFORATED PLATES WITHOUT DOWNCOMERS
INT J MULTIPHASE FLOW VOL 10 NO 2 P 217-227 1984

060 ELAMVALUTHI, G.;N.S. SRINIVAS
TWO-PHASE HEAT TRANSFER IN TWO COMPONENT VERTICAL FLOW
INT J MULTIPHASE FLOW VOL 10 NO 2 P 237-242 1984

061 WIJNGAARDEN, L. VAN
GAS/LIQUID FLOW RESEARCH IN THE NETHERLANDS
INT J MULTIPHASE FLOW VOL 10 NO 1 P 107-111 1984

062 BLAKE W.K.
MECHANICS OF FLOW-INDUCED SOUND AND VIBRATION
ACADEMIC PRESS, INC 1986

063 CRIGHTON, D.G.; J.E. FFWCS WILLIAMS
SOUND GENERATION BY TURBULENT TWO-PHASE FLOW
J FLUID MECHANICS VOL 36 P 585-603 1969

065 ROUHANI, S.Z.; M.S. SOHAL
TWO-PHASE FLOW PATTERNS; A REVIEW OF RESEARCH RESULTS
PROGRESS IN NUCLEAR ENERGY VOL 11 NO 3 P 219-259 1983

066 AKAGAWA, K.;H. HAMAGUCHI, T SAKAGUCHI, T. IKARI
STUDIES OF THE FLUCTUATION OF PRESSURE DROP IN TWO-PHASE
SLUG FLOW
BULL JSME VOL 14 P447 1971

067 ANDO, Y.;N. HAITO; A. TANABE; N. KITAMURA
VOID DETECTION IN BWR BY NOISE ANALYSIS
J NUCLEAR SCIENCE AND TECHNOLOGY VOL 12 NO 9 P 597-599 1975

068 BESSHO, Y.; H. NISHIHARA
BOILING ACOUSTIC EMISSION AND BUBBLE DYNAMICS IN NUCLEATE BOILING
J NUCLEAR SCIENCE AND TECHNOLOGY VOL 13 P 520 1976

069 BANERJEE, S.; R.T. LAHEY JR
ADVANCES IN TWO-PHASE FLOW INSTRUMENTATION
ADVANCES IN NUCLEAR SCIENCE AND TECHNOLOGY VOL 13 P 227

070 BAKER, D.
SIMULTANEOUS FLOW OF OIL AND GAS
OIL AND GAS JOURNAL VOL 53 P 185 1954

071 DE, M.K.
STATISTICAL CHARACTERISTICS OF INCIPIENT TWO-PHASE NOISE FOR
REACTOR DIAGNOSIS
NUCLEAR TECHNOLOGY VOL 62 P 94 1983

072 FOUDA, A.E.; G.A. GREGORY; E. RHODES; D.S. SCOTT
PROBLEMS OF TWO PHASE FLOW IN NETWORKS AND METERING OF QUALITY,
MASS FLOW AND VOID FRACTION
CANADIAN INSTITUTE OF MINING AND METALURGY SPECIAL VOLUME 17
P 663 1977

073 BARTHELS, H.
MESSVERFAHREN FUER ZWEIFHASENSTROMUNGEN
CHEMIE-ING-TECHN VOL 40 NO 11 P 530 1968

074 ERMAKOV, P.P.; V.M. ZADORSKII
EXP. INVEST. OF THE ACOUSTICAL AND MASS-TRANSFER CHARACT. OF GAS-
LIQUID SYSTEMS WITH SELF-EXCITED OSCILLATIONS OF THE GAS FLOW
J ENG. PHYS VOL 47 NO 3 P 1080 1984

075 HSIEH, D.Y.
FORCED OSCILLATIONS OF NONSPHERICAL BUBBLES
JOURNAL DE PHYSIQUE COLL CB P CB-278 1979

076 CRUM, L.A.
SURFACE OSCILLATIONS AND JET DEVELOPMENT IN PULSATING BUBBLES
JOURNAL DE PHYSIQUE COLL CB P CB-284 1979

077 KEDRINSKII, V.K.; S.I. FLAKSIN
STRUCTURE OF PERIODICAL DISTURBANCES IN REAL LIQUID
JOURNAL DE PHYSIQUE COLL CB P CB-292 1979

078 CRAMER, E.; W. LAUTERBORN
ON RESPONSE CURVES OF BUBBLES THE OSCILLATIONS OF WHICH ARE
DAMPED BY SOUND RADIATION
JOURNAL DE PHYSIQUE COLL CB P CB-296 1979

079 MALYKH, N.V.; I.A. OGORODNIKOV
STRUCTURE OF PRESSURE PULSES IN LIQUID WITH GAS BUBBLES
JOURNAL DE PHYSIQUE COLL CB P CB-300 1979

080 NABERGOJ, R.; A. FRANCESCUTTO
ON THRESHOLD FOR SURFACE WAVES ON RESONANT BUBBLES
JOURNAL DE PHYSIQUE COLL CB P CB-306 1979

081 NAYFEH, A.H.; D.T. MOOK
NONLINEAR RESPONSE OF A SPHERICAL BUBBLE TO A MULTY-FREQUENCY
EXCITATION
JOURNAL DE PHYSIQUE COLL CB P CB-310 1979

082 GASENIKO, V.G.; V.E. NAKORYAKOV; I.R. SHREIBER
NONLINEAR DISTURBANCES IN A LIQUID CONTAINING GAS BUBBLES
SOV PHYS ACOUST VOL 25 NO 5 P 385 1979

083 GAUNAURD, G.C.; H. UEBERALL
RESONANCE THEORY OF BUBBLY LIQUIDS
J ACOUST SOC AM VOL 69 NO 2 P 362 1981

084 CHALOV, A.V.
SOUND EMISSION BY A BUBBLE MOVING IN A LIQUID FLOW NEAR AN
ELLIPTICAL CILINDER
SOV PHYS ACOUST VOL 20 NO 4 P 370 1975

085 BAKER R.C.
THEORIE UND PRAXIS DER ELEKTROMAGNETISCHEN DURCHFLUSSMESSUNG
TECHN MESSEN VOL 52 P 4 1985

086 FRANCESCUTTO, A.; R. NABERGOJ
ANALYTICAL PREDICTIONS FOR THE MAXIMUM AMPLITUDES OF
OSCILLATING BUBBLES
ACOUSTICS LETTERS VOL 7 NO 3 P 43 1983

087 JONES JR, O.C.; J.M. DELHAYE
TRANSIENT AND STATISTICAL MEASUREMENT TECHNIQUES FOR TWO-PHASE
FLOWS: A CRITICAL REVIEW
INT. J. MULTIPHASE FLOW VOL 3 NO 2 P 89-116 1976

- 088 HEWITT, G.F.
ROLE OF EXPERIMENTS IN TWO-PHASE SYSTEMS WITH PARTICULAR
REFERENCE TO MEASURE TECHNIQUES
J BRIT NUCL ENERGY SOC VOL 12 P 213 1973
- 089 SCHROCK, V.E.
RADIATION ATTENUATION TECHNIQUES IN TWO-PHASE FLOW MEASUREMENTS
ASME 11TH NAT ASME/AICHE HEAT TRANSFER CONF MINNEAPOLIS P24 1969
- 090 NISHIHARA, H.; H. KONISHI
A NEW CORRELATION METHOD FOR TRANSIT-TIME ESTIMATION
PROGR IN NUCLEAR ENERGY VOL 1 P 219 1977
- 091 GELFAND, B.E.; B.V. STEPANOV; E.I. TIMOFEEV; S.A. TSYGANOV
AMPLIFICATION OF SHOCK WAVES IN A NONEQUILIBRIUM SYSTEM
CONSISTING OF A LIQUID AND SOLVENT GAS BUBBLES
SOV PHYS DOFL VOL 23 P 176 1978
- 092 BUTENKO, A.N.; A.E. POTAPENKO; E.S. CHYSTIAKOV
ACOUSTIC METHOD OF MEASURING CONCENTRATION OF THE GASEOUS PHASE
IN A TWO-PHASE MEDIUM
IND LAB VOL 43 P 547 1977
- 093 JONES JR., D.C.
TWO-PHASE FLOW MEASUREMENT TECHNIQUES IN GAS-LIQUID SYSTEMS
FLUID MECHANICS MEASUREMENTS ED R.J. GOLDSTEIN HEMISPHERE PUBL
CORP CHAPT 10 1983
- 094 PURSHLEY, W.C.; J.S. HUMPHREYS
TWO-PHASE FLOW MEASUREMENT AT NEL
FLUID MECHANICS SILVER JUBILEE CONFERENCE NEL GLASGOW
PAPER 6.4 1979
- 095 FELL, R.
A NEW ULTRASONIC CORRELATION FLOWMETER
FLUID MECHANICS SILVER JUBILEE CONFERENCE NEL GLASGOW
PAPER 9.1 1979
- 096 HARRISON, P.
FLOW MEASUREMENT- A STATE OF THE ART REVIEW
CHEMICAL ENGINEERING VOL 67 P 97 1980
- 097 HOOGENDOORN, C.J.
GAS-LIQUID FLOW IN HORIZONTAL PIPES
CHEMICAL ENGINEERING SCIENCE VOL 9 P 205 1959
- 098 DUKLER, A.E.
GAS-LIQUID FLOW IN PIPELINES
RESEARCH RESULTS PROJECT NX-28 UNIV OF HOUSTON 1969
- 099 MAKHIN, V.A.; V.I. MELNIKOVA; V.A. SHATROV
ESTIMATE OF THE ERROR IN MEASURING THE VOID FRACTION BY THE
ACOUSTIC SOUNDING METHOD
FLUID MECHANICS-SOVIET RESEARCH VOL 11 NO 3 P31 1982
- 100 PETERS, R.; F. BLISCHKE; H. MEYR
PARAMETERSCHAETZVERFAHREN ZUR BESTIMMUNG DER DURCHFLUSSGESCHWIN-
DIGKEIT AUF DER BASIS DES KORRELATIONSPRINZIPI
TECHNISCHES MESSEN VOL 53 P 17 1986
- 101 LAHEY JR, R.T.
REVIEW OF SELECTED NONINTRUSIVE NUCLEAR AND OPTICAL TECHNIQUES
FOR DETERMINATION OF VOID FRACTION, FLOW REGIME, TWO-PHASE FLOW RATE
TRANS AM NUCL SOC VOL 39 P 1006 1981
- 102 LAHEY JR, R.T.
THERMAL-HYDROLOGIC INSTRUMENTATION FOR LWR EXPERIMENTS- A REVIEW
TRANS AM NUCL SOC VOL 38 P 12 1981
- 103 HSU, Y.Y.; A.L.M. HON
SUMMARY OF USNRC-SPONSORED TWO-PHASE-FLOW INSTRUMENTATION FOR
SAFETY EXPERIMENTS
TRANS AM NUCL SOC VOL 34 P 74 1980
- 104 KIPPAN, H.; F. MESCH
FLOW MEASUREMENT SYSTEMS USING TRANSIT-TIME CORRELATION
FLOW MEASUREMENT OF FLUIDS ED H.H. DIJSTELBERGEN, E.A. SPENCER,
NORTH-HOLLAND PUBLISHING COMPANY P 409 1978
- 105 JONES JR, D.C.; N. ZUBER
THE INTERRELATION BETWEEN VOID FRACTION FLUCTUATIONS AND FLOW
PATTERNS IN TWO-PHASE FLOW
INT. J. MULTIPHASE FLOW VOL 2 P 273 1975
- 106 DUNS JR., H.; N.C.J. ROS
VERTICAL FLOW OF GAS AND LIQUID MIXTURES IN WELLS
SIXTH WORLD PETROLEUM CONGRESS, DRILLING AND PRODUCTION,
FRANKFURT/MAIN, JUNE 19-26, 1963
- 107 DELHAYE, J.M.; J.L. ACHARD
ON THE USE OF AVERAGING OPERATORS IN TWO-PHASE FLOW MODELING
SYMPOSIUM ON THE THERMAL AND HYDROLOGIC ASPECTS OF NUCLEAR REACTOR
SAFETY, VOL 1, LIGHT WATER REACTORS, AM SOC MECH ENG 1977

- 108 KEMENY, L.G.
NEUTRONIC AND ACOUSTIC TECHNIQUES FOR VOIDAGE MEASUREMENT IN
TWO-PHASE FLOW
5TH AUSTRALASIAN CON. ON HYDROLOGICS AND FLUID MECHANICS, UNIVERSITY
OF CANTERBURY, CHRISTCHURCH, NEW ZEALAND, 9-13 DECEMBER 1974
- 109 ELMENDORP, J.J.
A STUDY ON POLYMER BLENDING MICRORHEOLOGY
PHD THESIS, TECHNICAL UNIVERSITY DELFT, 1-4-1986
- 110 DAVIS, M.R.
PRESSURE FLUCTUATIONS IN A VAPOUR-LIQUID MIXTURE FLOW
INT. J. HEAT MASS TRANSFER, VOL 16, PP 2043-2054, PERGAMON 1973
- 111 HENRY, R.E.; M.A. GROLMES; H.K. FAUSKE
PRESSURE PULSE PROPAGATION IN TWO-PHASE ONE AND TWO COMPONENT
MIXTURES
REPORT ANL-7792, REACTOR TECHNOLOGY, ARGONNE NATIONAL LABORATORY,
ARGONNE, ILLINOIS, MARCH 1971
- 112 WAMBSGANSS, M.W.; P.L. ZALESKI
MEASUREMENT, INTERPRETATION AND CHARACTERIZATION OF NEARFIELD
FLOW-NOISE
ARGONNE NATIONAL LABORATORY REPORT ANL-7685, 1970
- 113 LEVICH, G.
PHYSICO-CHEMICAL HYDRODYNAMICS
PRENTICE HALL, ENGLEWOOD CLIFFS, 1962
- 114 HSU, Y.Y.; R.J. SIMONEAU, F.F. SIMON, R.W. GRAHAM
PHOTOGRAPHIC AND OTHER OPTICAL TECHNIQUES FOR STUDYING TWO-PHASE
FLOW
11TH NATIONAL ASME/AICHE HEAT TRANSFER CONFERENCE, AUGUST 3-6,
1969, MINNEAPOLIS, MINNESOTA
- 115 GREGORY, G.A.; M.K. NICHOLSON, K. AZIZ
CORRELATION OF THE LIQUID VOLUME FRACTION IN THE SLUG FOR
HORIZONTAL GAS-LIQUID SLUG FLOW
INT J MULTIPHASE FLOW VOL 4, PP 33-39, 1978
- 116 TAITEL, Y; A.E. DUKLER
A MODEL FOR SLUG FREQUENCY DURING GAS-LIQUID FLOW IN HORIZONTAL
AND NEAR HORIZONTAL PIPES
INT J MULTIPHASE FLOW, VOL 3, PP 585-596, 1977
- 117 LINGA, H.
TERRAIN SLUGGING PHENOMENA. SOME EXPERIMENTAL RESULTS OBTAINED AT
THE SINTAF TWO-PHASE FLOW LABORATORY
3RD INTERNATIONAL CONFERENCE ON MULTI-PHASE FLOW, THE HAGUE, THE
NETHERLANDS, 18-20 MAY, 1987
- 118 BOOT, P.G.M.T.; C.W.M. VAN DER GELD; H.A.M. HENDRIKSEN
FLOW-PATTERN MEASUREMENTS IN A VERTICAL EVAPORATOR TUBE
3RD INTERNATIONAL CONFERENCE ON MULTI-PHASE FLOW, THE HAGUE
THE NETHERLANDS, 18-20 MAY, 1987
- 119 ANNUNZIATO, M.; G. GIRALDI
HORIZONTAL TWO-PHASE FLOW: A STATISTICAL METHOD FOR FLOW PATTERN
RECOGNITION
3RD INTERNATIONAL CONFERENCE ON MULTI-PHASE FLOW, THE HAGUE
THE NETHERLANDS, 18-20 MAY, 1987
- 120 JEPSON, W.P.
THE FLOW CHARACTERISTICS IN HORIZONTAL SLUG FLOW
3RD INTERNATIONAL CONFERENCE ON MULTI-PHASE FLOW, THE HAGUE,
THE NETHERLANDS, 18-20 MAY, 1987
- 121 MILLER, N.; R.E. MITCHIE
THE DEVELOPMENT OF A UNIVERSAL PROBE FOR MEASUREMENT OF LOCAL
VOIDAGE IN LIQUID/GAS TWO-PHASE FLOW SYSTEMS
11TH NAT ASME/AICHE HEAT TRANSFER CONFERENCE, MINNEAPOLIS,
3-6 AUG, 1969
- 122 NAGULESWARAN, S.; C.J.H. WILLIAMS
LATERAL VIBRATION OF A PIPE CONVEYING A FLUID
JOURNAL OF MECHANICAL ENGINEERING SCIENCE, 1968
- 123 JAMIESON, A.W.; R.G. SMEENK; P.B. VRIEZEN
MULTI-PHASE FLOW MEASUREMENT AT PRODUCTION PLATFORMS
PETROLEUM REVIEW, NOVEMBER 1985
- 124 WOOD, J.D.; A.N. DICKSON
METERING OF OIL/AIR MIXTURES WITH SHARP-EDGED ORIFICES
HERIOT-WATT UNIVERSITY, DPT OF MECHANICAL ENGINEERING REPORT,
JUNE 1973
- 125 HARRIS, D.M.; G.L. SHIRES
TWO-PHASE PRESSURE DROP IN A VENTURI
NEL REPORT NO 549 NATIONAL ENGINEERING LABORATORY, EAST KILBRIDGE
GLASGOW, 1972
- 126 ENERGIEONDERZOEK CENTRUM NEDERLAND
PROCESBEHEERSING MET BEHULP VAN ON-LINE RUIS ANALYSE
ECN-BROCHURE, WITH NEDERLANDS TIJDSCHRIFT VOOR NATUURKUNDE
AUG 1987

SUBJECT	NR	AUTHOR	TITEL	PAPER
DE	033	ABESEKERA	CROS COR TEMP FLUCT	MEAS & CONTR 1972
TH	039	ABRIOLA	SURFACE EFFECTS	I J MULT F 1985
ST	046	AKAGAWA	PRESS FLUCT SLUG	JSME 1971
FSM	008	ALFORD	DEV,EVAL FSM	J PETR TECHN 78
AC	067	ANDO	VOID DET NOISE ANAL	J NUCL SC&TECHN 1975
ST MA	119	ANNUNZIATO	STAT RECOGN FLOW PAT	MULT P F CONF 1987
MA ST	027	ANNUNZIATO	STAT VERT TP FLOW	CONF MULT FLOW 1985
DE	037	ARNAUDEAU	L/G FEED MEAS	UK FAT 1984
OT	056	AZZOPARDI	TP FLOW SPLIT	I J MULT F 1984
DE	085	BAKER	ELECTROMAGNFLOWMETER	TECHN MESSEN 1985
MA	070	BAKER	SIMULT FLOW OIL-GAS	OIL-GAS J 1954
DE	069	BANERJEE	ADVANCES TPF INSTRUM	ADV NUCL SC&TECHN 13
MA	048	BARNEA	SLUGHOLDUP INTERM FL	I J MULT F 1985
DE	073	BARTHELS	REVIEW TPF MEAS	CHEMIE-ING-TECHN1968
AC	068	BESSHO	BOILING BUBBLE ACOUS	J NUCL SC&TECHN 1976
BU	040	BEYERLEIN	BUBBLE CONC PROFILE	I J MULT F 1985
MA	043	BISWAS	CAPILLARY FLOW MAP	I J MULT F 1985
TH	062	BLAKE	FLOW SOUND&VIBR	ACADEMIC PRESS 1986
DE MA ST	118	BOOT	VERT FLOW PATTERN	MULT P F CONF 1987
MA	025	BRILL	TWO P FLOW IN PIPES	TULSA/BHRA PROJECTS
OT	016	B&K	VIBR TRANSD	SPECS
DE	092	BUTENKO	ACOUST GAS CONC MEAS	IND LAB 1977
AC	084	CHALOV	BUBBLESOUND NEAR CIL	SOV PHYS AC 1975
TH	024	CHESTERS	SWD III	DICT TH DELFT
DE	051	CLARK	FRICT PRESS LOSS TPF	I J MULT F 1984
TH	036	CORCOS	RESOLUTION TURB PRES	ACOUST SOC AM 1983
AC	078	CRAMER	OSCILL BUBBLES RADIA	J DE PHYS CB 1979
MA	038	CRAWFORD	FLOW PAT-VOID FRACT	I J MULT F 1985
AC TH	063	CRIGHTON	TWO PHASE SOUND GEN	J FLUID MECH 1969
AC	076	CRUM	OSCILL BUBBLES	J DE PHYS CB 1979
ST MA	050	DALLMAN	ENTRAINM HOR ANNULAR	I J MULT F 1984
AC	110	DAVIS	PRES FL VAP-LIQ FLOW	I.J. HEAT MASS 1973
ST	049	DAVIS	LARGE STRUCT G-L FL	I J MULT F 1984
AC ST	071	DE	STAST INCIP TP NOISE	NUCL TECHN 1983
ST	107	DELHAYE	AVER OP TPF MONITOR	SYM AS MECH ENG 1977
TH	035	DOWLING	SOURCES OF SOUND	JOHN WILEY
MA	098	DUKLER	GAS LIQ FLOW IN PIPE	HOUSTON NX28 1969
OT	106	DUNS	VERT TPF IN WELLS	6TH PETR CONGR 1963
OT	060	ELAMVALUTHI	HEAT TRANSF VERT TPF	I J MULT F 1984
TH	109	ELMENDORP	POLYMER BLENDING	PHD THESIS TUD 1986
ST	126	ECN	NOISE ANALYSIS	ECN-BROCHURE 1987
AC	074	ERMAKOV	GAS OSCILL-AC/MASSTR	J ENG PHYS 1984
DE	095	FELL	ULTRAS CORR FL METER	FL MECH CONF NEL1979
OT	072	FOUDA	TP NETWORK FLOW MEAS	CIM 1977
AC TH	086	FRANCESCUTTO	OSCILL BUBBLES ANALY	AC LETTERS 1983
AC TH	082	GASENKO	NONLIN DIST LIQ-BUBB	SOV PHYS ACOUST 1979
AC TH	083	GAUNAURD	RES BUBBLY LIQUIDS	J AC SOC AM 1981
AC	091	GELFAND	SHOCK WAVES- GAS/LIQ	SOV PHYS DOKL 1978
MA	032	GOVIER	HOR AIR-WATER FLOW	CAN J CHEM ENG 1962
OT	031	GREGORY	SLUG VEL-FREQ CORR	AICHE 1969
OT	115	GREGORY	SLUG LIQ VOL FRACT	I J MULT F 1978
DE	042	GUNN	ELECTRICAL PROBE	I J MULT F 1985
DE	052	HARDY	VOID VEL MEAS,EL IMP	I J MULT F 1984
DE	125	HARRIS	VENTURI TPF PR. DROP	NEL REPORT 549 1972
DE	096	HARRISON	REVIEW FLOW MEAS	CHEM ENG 1980
MA	041	HASHIZUME	PAT, VOID, PRES DROP	I J MULT F 1985
OT	004A	HENDRIKS	WANDD. CAPACITIEF	EO TN-THD
TH	111	HENRY	PRES PROP TPF	ARGONNE NAT LAB 1971
OT	004B	HERWEIJER	WANDSLIJTAGE	EO TN-THD
DE	088	HEWITT	REVIEW TPF MEAS	J BR NUCL EN SOC1973

SUBJECT	NR	AUTHOR	TITEL	PAPER
TH	028	HINZE	TURBULENCE	MCGRAW HILL 1975
MA	097	HOOGENDOORN	GL FLOW HOR PIPES	CHEM ENG SC 1959
AC	075	HSIEH	OSCILL NONSPHER BUBB	J DE PHYS C8 1979
DE	103	HSU	TPF INSTRUM	TRANS AM NUCL S 1980
DE	114	HSU	OPT TECHN TPF STUDY	ASME/AICHE CONF 1969
MA ST	026	HUBBARD	STAT PRESS FLOW REG	HTFM ST CLARA 1966
ST	015	JAIN	STOCH. FRACT&PRESS	I J MULT F 1983
GE	002	JAMIESON	M-P FLOW MEAS	PETR REV
GE	123	JAMIESON	M P F MEAS PLATFORMS	PETR REVIEW 1985
OT	120	JEPSON	HOR SLUG CHARACT	MULTI P F CONF 1987
DE ST	087	JONES	REVIEW TPF MEAS TECH	I J MULT F 1976
ST MA	105	JONES	VOID FRACT/F-PATTERN	I J MULT F 1975
DE	093	JONES	TPF MEAS TECHN	FL MECH MEAS 1983
OT	057	KAMATH	VIRT MASS DRAG COEF	I J MULT F 1984
AC	077	KEDRINSKII	CAVITATION IN TPF	J DE PHYS C8 1979
DE ST	108	KEMENY	NEUTR/ACOUST VOID M	CONF HYDR/F.MEC 1974
DE	104	KIPPHAN	CORR FLOW MEAS	NORTH H PUBL 1978
MA ST	055	KVERNOLD	VEL DITR HOR SLUG	I J MULT F 1984
DE	101	LAHEY	REV TP FLOW MEAS	TRANS AM NUCL S 1981
DE	102	LAHEY	REVIEW THER-HYDR INS	TRANS AM NUCL S 1981
TH	113	LEVICH	PHYSICOCHEM HYDRODAN	PRENTICE HALL 1962
ST MA	117	LINGA	TERRAIN SLUGGING	MULT-P F CONF 1987
DE	099	MAKHIN	ACOUST VOID FRACT	FLUID MECH 1982
TH	013	MAKHOUL	LIN PREDICTION	PROC IEEE 1975
AC	079	MALYKH	PRESS PULSE LIQ-BUBB	J DE PHYS C8 1979
MA	023	MANDHANE	HOR FLOW PATTERN MAP	I J MULT FLOW 1974
MA ST	009	MATSUI	FLOW REG PRESS FLUCT	I.J.MULT.F.1984
OT	059	MATSUMOTO	FLUCT FROTH PRESS	I J MULT F 1984
MA	047	MCQUILLAN	VERT T P FLOWPATTERN	I J MULT F 1985
DE	121	MILER	VOID MEAS PROBE	ASME/AICHE CON 1969
MA	044	MUKHERJEE	FLOW PAT INCLINED FL	I J MILT F 1985
AC	080	NABERGOJ	SURF WAVES ON BUBBLE	J DE PHYS C8 1979
DE	122	NAGULESWARAN	FLUID CONV PIPE VIBR	J MECH ENG SC, 1968
AC	081	NAYFEH	MULT FREQ BUBB RESP	J DE PHYS C8 1979
TH	022	NGUYEN	TWO PHASE SON VEL	I J MULT FLOW 1981
TH	090	NISHIHARA	CORRELATION TECHN	FR NUCL EN 1977
MA ST	021	OHLMER	STOCH TWO P FL	IUTAM SYMP 1983
GE	001	OOSTEROM	KSEPL	NED.TIJD.NAT. 86
FSM	007	PATTERSON	PSM	SPE-AIME, 1976
DE	100	PETERS	FLOWSPEED-CORREL	TECHN MESSEN 1986
TH	054	PROSPEREETI	PRESS FORCE DISPERSE	I J MULT F 1984
DE	094	PURSHLEY	TPF MEAS AT NEL	FL MECH CONF NEL1979
MA ST	065	ROUHANI	REVIEW TP FLOW PAT	NUCL ENERGY 1983
ST	034	SAMI	SPECTR PRESS FLUCT	ACOUST SOC AM 1986
DE	089	SCHROCK	RAD ATTEN TPF MEAS	ASME/AICHE CONF 1969
AC TH	053	SINAI	AC SPEED STRAT RECT	I J MULT F 1984
AC	003	SKUDRZYK	NOISE PROD	J ACOUST SOC AM
OT	005	SMITH	GASONTSNAPPING	FT-TN-THD
ST MA	058	SPEDDING	HOLDUP TP FLOW	I J MULT F 1984
MA	030	TAITEL	FL REG TRANSITIONS	AICHE 1976
MA ST	116	TAITEL	HOR SLUG FREQ	I J MULT F 1977
TH	046	THORLEY	VIRTUEL MASS-MP FLOW	I J MULT F 1985
DE	012	TORAL	HOT WIRE-VOID FRACT	J PHYS E
ST MA	010	TUTU	PRESS FLUCT BS TRANS	I.J.MULT.F. 1984
DE MA	011	VINCE	FLOW REG INDICATOR	I J MULT F 1982
DE ST	112	WAMBGANSS	FLOW NOISE MEASUREMENT	ARGONNE NAT LAB 1970
BU	045	WELLE, VAN DER	VOID/BUBBLE VEL,SIZE	I J MULT F 1985
GE	061	WIJNGAARDEN	G-L FLOW RES NL	I J MULT F 1984
DE	124	WOOD	ORIFICE TPF MEASUR.	HERIOT-WATT UN 1973

SUBJECT	NR	AUTHOR	TITEL	PAPER
AC	067	ANDO	VOID DET NOISE ANAL	J NUCL SC&TECHN 1975
AC	068	BESSHO	BOILING BUBBLE ACOUS	J NUCL SC&TECHN 1976
AC	084	CHALOV	BUBBLESOUND NEAR CIL	SOV PHYS AC 1975
AC	078	CRAMER	OSCILL BUBBLES RADIA	J DE PHYS C8 1979
AC	076	CRUM	OSCILL BUBBLES	J DE PHYS C8 1979
AC	110	DAVIS	PRES FL VAP-LIQ FLOW	I.J. HEAT MASS 1973
AC	074	ERMAKOV	GAS OSCILL-AC/MASSTR	J ENG PHYS 1984
AC	091	GELFAND	SHOCK WAVES- GAS/LIQ	SOV PHYS DOKL 1978
AC	075	HSIEH	OSCILL NONSPHER BUBB	J DE PHYS C8 1979
AC	077	KEDRINSKII	CAVITATION IN TPF	J DE PHYS C8 1979
AC	079	MALYKH	PRESS PULSE LIQ-BUBB	J DE PHYS C8 1979
AC	080	NABERGOJ	SURF WAVES ON BUBBLE	J DE PHYS C8 1979
AC	081	NAYFEH	MULT FREQ BUBB RESP	J DE PHYS C8 1979
AC	003	SKUDRZYK	NOISE PROD	J ACOUST SOC AM
AC ST	071	DE	STAST INCIP TP NOISE	NUCL TECHN 1983
AC TH	063	CRIGHTON	TWO PHASE SOUND GEN	J FLUID MECH 1969
AC TH	086	FRANCESCUTTO	OSCILL BUBBLES ANALY	AC LETTERS 1983
AC TH	082	GASENKO	NONLIN DIST LIQ-BUBB	SOV PHYS ACOUST 1979
AC TH	083	GAUNAURD	RES BUBBLY LIQUIDS	J AC SOC AM 1981
AC TH	053	SINAI	AC SPEED STRAT RECT	I J MULT F 1984
BU	040	BEYERLEIN	BUBBLE CONC PROFILE	I J MULT F 1985
BU	045	WELLE, VAN DER	VOID/BUBBLE VEL,SIZE	I J MULT F 1985
DE	033	ABESEKERA	CROS COR TEMP FLUCT	MEAS & CONTR 1972
DE	037	ARNAUDEAU	L/G FEED MEAS	UK PAT 1984
DE	085	BAKER	ELECTROMAGNFLOWMETER	TECHN MESSEN 1985
DE	069	BANERJEE	ADVANCES TPF INSTRUM	ADV NUCL SC&TECHN 13
DE	073	BARTHELS	REVIEW TPF MEAS	CHEMIE-ING-TECHN1968
DE	092	BUTENKO	ACOUST GAS CONC MEAS	IND LAB 1977
DE	051	CLARK	FRICT PRESS LOSS TPF	I J MULT F 1984
DE	095	FELL	ULTRAS CORR FL METER	FL MECH CONF NEL1979
DE	042	GUNN	ELECTRICAL PROBE	I J MULT F 1985
DE	052	HARDY	VOID VEL MEAS,EL IMP	I J MULT F 1984
DE	125	HARRIS	VENTURI TPF PR. DROP	NEL REPORT 549 1972
DE	096	HARRISON	REVIEW FLOW MEAS	CHEM ENG 1980
DE	088	HEWITT	REVIEW TPF MEAS	J BR NUCL EN SOC1973
DE	103	HSU	TPF INSTRUM	TRANS AM NUCL S 1980
DE	114	HSU	OPT TECHN TPF STUDY	ASME/AICHE CONF 1969
DE	093	JONES	TPF MEAS TECHN	FL MECH MEAS 1983
DE	104	KIPPHAN	CORR FLOW MEAS	NORTH H PUBL 1978
DE	101	LAHEY	REV TP FLOW MEAS	TRANS AM NUCL S 1981
DE	102	LAHEY	REVIEW THER-HYDR INS	TRANS AM NUCL S 1981
DE	099	MAKHIN	ACOUST VOID FRACT	FLUID MECH 1982
DE	121	MILER	VOID MEAS PROBE	ASME/AICHE CON 1969
DE	122	NAGULESWARAN	FLUID CONV PIPE VIBR	J MECH ENG SC, 1968
DE	100	PETERS	FLOWSPEED-CORREL	TECHN MESSEN 1986
DE	094	PURSHLEY	TPF MEAS AT NEL	FL MECH CONF NEL1979
DE	089	SCHROCK	RAD ATTEN TPF MEAS	ASME/AICHE CONF 1969
DE	012	TORAL	HOT WIRE-VOID FRACT	J PHYS E
DE	124	WOOD	ORIFICE TPF MEASUR.	HERIOT-WATT UN 1973
DE MA	011	VINCE	FLOW REG INDICATOR	I J MULT F 1982
DE MA ST	118	BOOT	VERT FLOW PATTERN	MULT P F CONF 1987
DE ST	087	JONES	REVIEW TPF MEAS TECH	I J MULT F 1976
DE ST	108	KEMENY	NEUTR/ACOUST VOID M	CONF HYDR/F.MEC 1974
DE ST	112	WAMBGANSS	FLOW NOISE MEASUREM.	ARGONNE NAT LAB 1970
GE	002	JAMIESON	M-P FLOW MEAS	PETR REV
GE	123	JAMIESON	M P F MEAS PLATFORMS	PETR REVIEW 1985
GE	001	OOSTEROM	KSEPL	NED.TIJD.NAT. 86
GE	061	WIJNGAARDEN	G-L FLOW RES NL	I J MULT F 1984
MA	070	BAKER	SIMULT FLOW OIL-GAS	OIL-GAS J 1954
MA	048	BARNEA	SLUGHOLDUP INTERM FL	I J MULT F 1985

SUBJECT	NR	AUTHOR	TITEL	PAPER
MA	043	BISWAS	CAPILLARY FLOW MAP	I J MULT F 1985
MA	025	BRILL	TWO P FLOW IN PIPES	TULSA/BHRA PROJECTS
MA	038	CRAWFORD	FLOW PAT-VOID FRACT	I J MULT F 1985
MA	098	DUKLER	GAS LIQ FLOW IN PIPE	HOUSTON NX28 1969
MA	032	GOVIER	HOR AIR-WATER FLOW	CAN J CHEM ENG 1962
MA	041	HASHIZUME	PAT, VOID, PRES DROP	I J MULT F 1985
MA	097	HOOGENDOORN	GL FLOW HOR PIPES	CHEM ENG SC 1959
MA	023	MANDHANE	HOR FLOW PATTERN MAP	I J MULT FLOW 1974
MA	047	MCQUILLAN	VERT T P FLOWPATTERN	I J MULT F 1985
MA	044	MUKHERJEE	FLOW PAT INCLINED FL	I J MILT F 1985
MA	030	TAITEL	FL REG TRANSITIONS	AICHE 1976
MA ST	027	ANNUNZIATO	STAT VERT TP FLOW	CONF MULT FLOW 1985
MA ST	026	HUBBARD	STAT PRESS FLOW REG	HTFM ST CLARA 1966
MA ST	055	KVERNVDL	VEL DITR HOR SLUG	I J MULT F 1984
MA ST	009	MATSUI	FLOW REG PRESS FLUCT	I.J.MULT.F.1984
MA ST	021	OHLMER	STOCH TWO P FL	IUTAM SYMP 1983
MA ST	065	ROUHANI	REVIEW TP FLOW PAT	NUCL ENERGY 1983
MA ST	116	TAITEL	HOR SLUG FREQ	I J MULT F 1977
OT	056	AZZOPARDI	TP FLOW SPLIT	I J MULT F 1984
OT	016	B&K	VIBR TRANSD	SPECS
OT	106	DUNS	VERT TPF IN WELLS	6TH PETR CONGR 1963
OT	060	ELAMVALUTHI	HEAT TRANSF VERT TPF	I J MULT F 1984
OT	072	FOUDA	TP NETWORK FLOW MEAS	CIM 1977
OT	031	GREGORY	SLUG VEL-FREQ CORR	AICHE 1969
OT	115	GREGORY	SLUG LIQ VOL FRACT	I J MULT F 1978
OT	004A	HENDRIKS	WANDD. CAPACITIEF	EO TN-THD
OT	004B	HERWEIJER	WANDSLIJTAGE	EO TN-THD
OT	120	JEPSON	HOR SLUG CHARACT	MULTI P F CONF 1987
OT	057	KAMATH	VIRT MASS DRAG COEF	I J MULT F 1984
OT	059	MATSUMOTO	FLUCT FROTH PRESS	I J MULT F 1984
OT	005	SMITH	GASONTSNAPPING	FT-TN-THD
PSM	008	ALFORD	DEV,EVAL PSM	J PETR TECHN 78
PSM	007	PATTERSON	PSM	SPE-AIME, 1976
ST	066	AKAGAWA	PRESS FLUCT SLUG	JSME 1971
ST	049	DAVIS	LARGE STRUCT G-L FL	I J MULT F 1984
ST	107	DELHAYE	AVER OP TPF MONITOR	SYM AS MECH ENG 1977
ST	126	ECN	NOISE ANALYSIS	ECN-BROCHURE 1987
ST	015	JAIN	STOCH. FRACT&PRESS	I J MULT F 1983
ST	034	SAMI	SPECTR PRESS FLUCT	ACOUST SOC AM 1986
ST MA	119	ANNUNZIATO	STAT RECOGN FLOW PAT	MULT P F CONF 1987
ST MA	050	DALLMAN	ENTRAINM HOR ANNULAR	I J MULT F 1984
ST MA	105	JONES	VOID FRACT/F-PATTERN	I J MULT F 1975
ST MA	117	LINGA	TERRAIN SLUGGING	MULT-P F CONF 1987
ST MA	058	SPEDDING	HOLDUP TP FLOW	I J MULT F 1984
ST MA	010	TUTU	PRESS FLUCT BS TRANS	I.J.MULT.F. 1984
TH	039	ABRIOLA	SURFACE EFFECTS	I J MULT F 1985
TH	062	BLAKE	FLOW SOUND&VIBR	ACADEMIC PRESS 1986
TH	024	CHESTERS	SWD III	DICT TH DELFT
TH	036	CORCOS	RESOLUTION TURB PRES	ACOUST SOC AM 1963
TH	035	DOWLING	SOURCES OF SOUND	JOHN WILEY
TH	109	ELMENDORP	POLYMER BLENDING	PHD THESIS TUD 1986
TH	111	HENRY	PRES PROP TPF	ARGONNE NAT LAB 1971
TH	028	HINZE	TURBULENCE	MCGRAW HILL 1975
TH	113	LEVICH	PHYSICOHEM HYDRODAN	PRENTICE HALL 1962
TH	013	MAKHOUL	LIN PREDICTION	PROC IEEE 1975
TH	022	NGUYEN	TWO PHASE SON VEL	I J MULT FLOW 1981
TH	090	NISHIHARA	CORRELATION TECHN	PR NUCL EN 1977
TH	054	PROSPEREETI	PRESS FORCE DISPERSE	I J MULT F 1984
TH	046	THORLEY	VIRTUEL MASS-MF FLOW	I J MULT F 1985

9. SYMBOLS

A_b	amplification of turbulent pressure by a bubble	-
a	diameter of gas bubble	m
a_{cr}	critical bubble diameter	m
c	speed of sound	m/s
D_i	internal pipe diameter	m
f_0	bubble resonant frequency	1/s
f_{slug}	slug frequency	1/s
$f(t)$	fast RMS value of the flow-noise	V
g	gravitational constant	m/s ²
K	empirical constant in formula 5.8.	-
L	scale of turbulence	m
P	instantaneous pressure	N/m ²
P_a	average pressure	N/m ²
p	instantaneous variation of pressure	N/m ²
p_g	pressure in gas bubble	N/m ²
p_l	line pressure	N/m ²
p_0	average pressure in liquid	N/m ²
p'	root mean square value of p	N/m ²
Q	volume rate	m ³ /s
Re	Reynolds number	-
S_i	i^{th} statistical variable	various
T	numerical averaging time constant	-
U	instantaneous fluid velocity	m/s
U_a	average fluid velocity	m/s
U_{ns}	no-slip velocity	m/s
U_{sg}	superficial gas velocity	m/s
U_{sl}	superficial liquid velocity	m/s
u	instantaneous variation of fluid velocity	m/s
u'	root mean square value of u	m/s
V_{slug}	slug velocity	m/s

ΔP	pressure drop over ΔL	N/m^2
ΔL	length of pipe-line	m
γ	ratio of principle specific heats	-
ϵ	power consumption in turbulent flow per unit mass	J/s kg
η	dynamic viscosity	kg/ms
λ_k	Kolmogoroff length scale	m
ρ	fluid density	kg/m^3
ρ_g	gas density	kg/m^3
ρ_l	liquid density	kg/m^3
ρ_0	average liquid density	kg/m^3
σ_0	interfacial tension	N/m
ω	angular frequency of turbulence	1/s
ω_0	resonant angular frequency of bubble	1/s

CMC carboxy methyl cellulose

COPS clamp-on production surveillance monitor

PSD power spectral density

PSM production surveillance monitor

RMS root mean square

ACKNOWLEDGEMENT

The author would like to express his gratitude to all the people who have been supporting this project in a material, practical, mental, or any other way. The members of the section Measurement and Control for their hospitality and assistance. Jan de Bruin, Piet de Graaf, and Dennis van Berkum for the modifications of the test-loops, Sarah Ashby, and Cock Schimmel for searching for literature, and Max Colon for measuring viscosities and theoretical part of the work. Finally the author would like to thank the Wolga and the Donau for their everlasting stimulating flow-noise.

